1

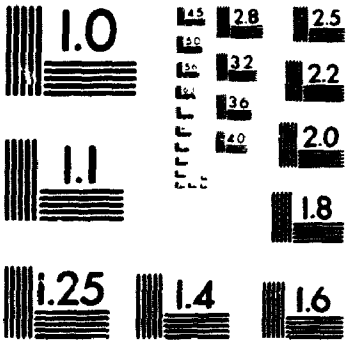

MICROCOPY RESOLUTION TEST CHART
NATIONAL BUREAU OF STANDARDS
STANDARD REFERENCE MATERIAL 1010a
(ANSI and ISO TEST CHART No. 2)

Stratigraphy, Structural Geology, and Structural Controls of Ore Distribution of the Lyon Lake Massive Sulphide Deposit, Sturgeon Lake, Ontario

by

Elizabeth Rosina Koopman, B.Sc.

A thesis submitted to
the Faculty of Graduate Studies and Research
in partial fulfillment of
the requirements for the degree of

Master of Science

Department of Earth Sciences

Carleton University
Ottawa, Ontario
date

ISBN 0-315-89834-8

Name ELIZABETH [illegible]

Dissertation Abstracts International is arranged by broad, general subject categories. Please select the one subject which most nearly describes the content of your dissertation. Enter the corresponding four-digit code in the spaces provided.

EARTH SCIENCES [illegible] — SUBJECT TERM

0372 — SUBJECT CODE

U·M·I

Subject Categories

THE HUMANITIES AND SOCIAL SCIENCES

COMMUNICATIONS AND THE ARTS

Architecture	0729
Art History	0377
Cinema	0900
Dance	0378
Fine Arts	0357
Information Science	0723
Journalism	0391
Library Science	0399
Mass Communications	0708
Music	0413
Speech Communication	0459
Theater	0465

EDUCATION

General	0515
Administration	0514
Adult and Continuing	0516
Agricultural	0517
Art	0273
Bilingual and Multicultural	0282
Business	0688
Community College	0275
Curriculum and Instruction	0727
Early Childhood	0518
Elementary	0524
Finance	0277
Guidance and Counseling	0519
Health	0680
Higher	0745
History of	0520
Home Economics	0278
Industrial	0521
Language and Literature	0279
Mathematics	0280
Music	0522
Philosophy of	0998
Physical	0523
Psychology	0525
Reading	0535
Religious	0527
Sciences	0714
Secondary	0533
Social Sciences	0534
Sociology of	0340
Special	0529
Teacher Training	0530
Technology	0710
Tests and Measurements	0288
Vocational	0747

LANGUAGE, LITERATURE AND LINGUISTICS

Language	
General	0679
Ancient	0289
Linguistics	0290
Modern	0291
Literature	
General	0401
Classical	0294
Comparative	0295
Medieval	0297
Modern	0298
African	0316
American	0591
Asian	0305
Canadian (English)	0352
Canadian (French)	0355
English	0593
Germanic	0311
Latin American	0312
Middle Eastern	0315
Romance	0313
Slavic and East European	0314

PHILOSOPHY, RELIGION AND THEOLOGY

Philosophy	0422
Religion	
General	0318
Biblical Studies	0321
Clergy	0319
History of	0320
Philosophy of	0322
Theology	0469

SOCIAL SCIENCES

American Studies	0323
Anthropology	
Archaeology	0324
Cultural	0326
Physical	0327
Business Administration	
General	0310
Accounting	0272
Banking	0770
Management	0454
Marketing	0338
Canadian Studies	0385
Economics	
General	0501
Agricultural	0503
Commerce-Business	0505
Finance	0508
History	0509
Labor	0510
Theory	0511
Folklore	0358
Geography	0366
Gerontology	0351
History	
General	0578
Ancient	0579
Medieval	0581
Modern	0582
Black	0328
African	0331
Asia, Australia and Oceania	0332
Canadian	0334
European	0335
Latin American	0336
Middle Eastern	0333
United States	0337
History of Science	0585
Law	0398
Political Science	
General	0615
International Law and Relations	0616
Public Administration	0617
Recreation	0814
Social Work	0452
Sociology	
General	0626
Criminology and Penology	0627
Demography	0938
Ethnic and Racial Studies	0631
Individual and Family Studies	0628
Industrial and Labor Relations	0629
Public and Social Welfare	0630
Social Structure and Development	0700
Theory and Methods	0344
Transportation	0709
Urban and Regional Planning	0999
Women's Studies	0453

THE SCIENCES AND ENGINEERING

BIOLOGICAL SCIENCES

Agriculture	
General	0473
Agronomy	0285
Animal Culture and Nutrition	0475
Animal Pathology	0476
Food Science and Technology	0359
Forestry and Wildlife	0478
Plant Culture	0479
Plant Pathology	0480
Plant Physiology	0817
Range Management	0777
Wood Technology	0746
Biology	
General	0306
Anatomy	0287
Biostatistics	0308
Botany	0309
Cell	0379
Ecology	0329
Entomology	0353
Genetics	0369
Limnology	0793
Microbiology	0410
Molecular	0307
Neuroscience	0317
Oceanography	0416
Physiology	0433
Radiation	0821
Veterinary Science	0778
Zoology	0472
Biophysics	
General	0786
Medical	0760

EARTH SCIENCES

Biogeochemistry	0425
Geochemistry	0996
Geodesy	0370
Geology	0372
Geophysics	0373
Hydrology	0388
Mineralogy	0411
Paleobotany	0345
Paleoecology	0426
Paleontology	0418
Paleozoology	0985
Palynology	0427
Physical Geography	0368
Physical Oceanography	0415

HEALTH AND ENVIRONMENTAL SCIENCES

Environmental Sciences	0768
Health Sciences	
General	0566
Audiology	0300
Chemotherapy	0992
Dentistry	0567
Education	0350
Hospital Management	0769
Human Development	0758
Immunology	0982
Medicine and Surgery	0564
Mental Health	0347
Nursing	0569
Nutrition	0570
Obstetrics and Gynecology	0380
Occupational Health and Therapy	0354
Ophthalmology	0381
Pathology	0571
Pharmacology	0419
Pharmacy	0572
Physical Therapy	0382
Public Health	0573
Radiology	0574
Recreation	0575
Speech Pathology	0460
Toxicology	0383
Home Economics	0386

PHYSICAL SCIENCES

Pure Sciences

Chemistry	
General	0485
Agricultural	0749
Analytical	0486
Biochemistry	0487
Inorganic	0488
Nuclear	0738
Organic	0490
Pharmaceutical	0491
Physical	0494
Polymer	0495
Radiation	0754
Mathematics	0405
Physics	
General	0605
Acoustics	0986
Astronomy and Astrophysics	0606
Atmospheric Science	0608
Atomic	0748
Electronics and Electricity	0607
Elementary Particles and High Energy	0798
Fluid and Plasma	0759
Molecular	0609
Nuclear	0610
Optics	0752
Radiation	0756
Solid State	0611
Statistics	0463

Applied Sciences

Applied Mechanics	0346
Computer Science	0984
Engineering	
General	0537
Aerospace	0538
Agricultural	0539
Automotive	0540
Biomedical	0541
Chemical	0542
Civil	0543
Electronics and Electrical	0544
Heat and Thermodynamics	0348
Hydraulic	0545
Industrial	0546
Marine	0547
Materials Science	0794
Mechanical	0548
Metallurgy	0743
Mining	0551
Nuclear	0552
Packaging	0549
Petroleum	0765
Sanitary and Municipal	0554
System Science	0790
Geotechnology	0428
Operations Research	0796
Plastics Technology	0795
Textile Technology	0994

PSYCHOLOGY

General	0621
Behavioral	0384
Clinical	0622
Developmental	0620
Experimental	0623
Industrial	0624
Personality	0625
Physiological	0989
Psychobiology	0349
Psychometrics	0632
Social	0451

The undersigned recommend to the Faculty of Graduate Studies

and Research acceptance of the thesis

Stratigraphy, Structural Geology, and Structural Controls of Ore Distribution of

the Lyon Lake Massive Sulphide Deposit, Sturgeon Lake, Ontario

submitted by Elizabeth Rosina Koopman, B.Sc.

in partial fulfilment of the requirements for
the degree of Master of Science

Thesis Supervisor

Chair, Department of Earth Sciences

Carleton University

Date: August 31, 1993

ABSTRACT

The Lyon Lake deposit is a typical Zn-Cu-Pb-Ag volcanogenic massive sulphide deposit located in the Sturgeon Lake area of the Wabigoon volcano-sedimentary Subprovince of the Archean Superior Province. The stratiform deposit is hosted by a quartz crystal- rich fragmental rhyolite and its hanging wall is the basal mafic member of the overlying volcanic cycle. The footwall to the ore horizon consists of an upper rhyolitic unit composed of interbedded ash and lapilli tuff, immediately underlain by a lower rhyolitic unit of coarse fragmental rock. Underlying the rhyolite, a fining- upward sequence of sedimentary rocks is comprised of greywacke, quartzose siltstone, graphitic shale, massive po-py bands, and a laterally extensive banded iron formation. The occurrence of a banded iron formation underlying the massive sulphide horizon indicates that low temperature hydrothermal venting occurred prior to sulphide deposition. Several lenses of massive sulphide are comprised of discontinuous and contorted bands of coarse- grained sphalerite and pyrite. All stratigraphic units, as well as dykes, and ore, are folded. The dominant structural feature controlling ore distribution is a major open fold characterized by a hinge line trending east-southeast. Hinge lines of mesoscopic folds, foliation, and striations measured on bedding, foliation, and fault planes are all subparallel to the hinge line of the major fold and indicate a direction of stretching parallel to the fold axis. Observed faults have limited control on ore distribution because there is no significant stratigraphic or ore displacement related to them. However, faulting is consistent with the style of folding. The contact between the hanging wall mafic unit and footwall rhyolite is characterized by a high strain zone, possibly a fault. Mineral lineations and striations on foliation planes are subparallel to the mesoscopic folds, and suggest that this high strain zone may be related to folding. A structural

contour map of the hanging wall-footwall contact indicates that the dip of this contact is shallowing in an eastward direction reflecting the plunge effect of the major open fold. The deformation at Lyon Lake has resulted in the re-orientation of portions of orebodies into attitudes that are much shallower than the steep regional dip. Structural analysis has assisted in the increased effectiveness of developing and mining these flatter orebodies.

ACKNOWLEDGEMENTS

The writer gratefully acknowledges the Geological Survey of Canada for funding of field work and subsequent research time, and also for analytical, photographic, and drafting services; and Carleton University for the use of their facilities and for granting me a teaching assistantship.

Sincere gratitude is extended, in particular, to Dr. J.M. Franklin and Dr. K.H. Poulsen of the Geological Survey of Canada, who initiated and developed this thesis project, and Dr. D.H. Watkinson of Carleton University for their guidance and support.

The author would also like to thank M. Patterson - Chief Geologist, and C. Imrie - Supervisor of Engineering/Geology of Noranda Mines Limited, Lyon Lake Division and the mine geologists for allowing access to the Lyon Lake deposit, their generous assistance, informative discussions, and permission to publish.

Thanks are also expressed to geologists of the University of Minnesota-Duluth for stimulating discussions in the field; and to numerous geologists at the Geological Survey of Canada, the Ontario Geological Survey, and Carleton University, with whom I had many interesting and informative discussions about the geology of the Sturgeon Lake area.

Lastly, I would like to extend my appreciation to all my friends for their patience in this effort; and especially to my parents for their unending support, patience, and encouragement throughout this endeavor.

TABLE OF CONTENTS

LIST OF FIGURES

LIST OF PLATES

CHAPTER 1

INTRODUCTION

1.0 Introduction

1.0.1 Statement of problem

Previously, the distribution of massive sulphide at the Lyon Lake mine was interpreted to consist of a series of primary planar sheets or lenses grouped together in an *en echelon* stacked pattern (Harvey and Hinzer, 1981). As mining progressed to greater depths however, tracing the massive sulphide units as a sequence of continuous planar sheets became more difficult. Structural complexities within the ore zones became more evident, necessitating an alternate hypothesis to interpret the massive sulphide distribution. Geological cross- sections (Noranda Mines Limited) showed that the massive sulphide in the upper part of the mine is not continuous with the massive sulphide, as delineated at depth in the mine. The principal focus of the present research is to establish the structural and stratigraphic relationships between the various ore lenses of the Lyon Lake mine. If the massive sulphide unit is not a continuous planar sheet, then what are the possible reasons for its apparent discontinuity?

Several hypotheses exist: Hypothesis 1: several lenses of massive sulphide may be present. In areas of high- temperature hydrothermal venting, massive sulphides were deposited on the seafloor as chimneys. Several chimneys in an area coalesced to form a mound of massive sulphides. Adjacent to any single mound, but separated by sedimentary or volcanic rocks, several other mounds may have developed. Sulphide mounds may form a series of discontinuous mounds or lenses. Hypothesis 2: the discontinuity of the ore lenses is the result of faulting, and either the ore lenses have been relatively displaced, or a single lens has been disrupted by faulting. Hypothesis 3: a single massive sulphide lens has

been folded, resulting in its reorientation, and creating an apparent discontinuity in the single lens if viewed in vertical section, but not if viewed in true section.

1.0.2 OBJECTIVES

The main objectives of this study are 1) to assess the amount to which the recognized eastward plunging linear orientation of the ore bodies is the result of primary disposition or subsequent deformation 2) to document the lithostratigraphic units and geological structures of the Lyon Lake Mine, 3) to determine the structural style that controls the ore distribution at the Lyon Lake Mine in the south Sturgeon Lake volcanic belt, 4) to determine the significance of local structural features as controls on ore distribution, and 5) to establish the nature and significance of the contact between the hanging wall basalt and footwall rhyolite.

1.0.3 METHODS USED TO MEET THE OBJECTIVES

Mine plans, sections, and diamond drill hole data were compiled and reviewed to determine which data could be used to outline the problem, and to determine what additional information is required to solve the problem of tracing the discontinuous massive sulphide units. Ore contacts and the contact between the hanging wall basalt and footwall rhyolite are the only source of information that could reliably be obtained from the mine data. On first examination of the geology and the underground workings, several observations were made; 1) the vertical mine sections show that the ore lens, basalt hanging wall, footwall rhyolite and sedimentary rocks appear to be discontinuous, 2) banded iron formation in the sedimentary sequence is isoclinally folded, and 3) the contact between the hanging wall basalt and footwall rhyolite is marked by a high strain zone. This information was used to select areas of the mine to map at a scale of 1:240. Lithological descriptions, structural measurements, and samples were collected at each

selected area. For each area, the information was compiled and plotted on maps of a common scale, and the structural information plotted on stereograms. Five months of underground mapping, together with core logging, provided an opportunity to establish a broad structural framework for the deposit. From underground and diamond drill core samples, thin sections and polished thin sections were made and analyzed petrographically for primary textures, mineral assemblages, alteration mineralogy, and deformation textures. Selected samples were analyzed for whole-rock major oxides and trace elements by X-Ray Fluorescent Spectroscopy (data on file at the Geological Survey of Canada) and X-Ray Diffractometry (Philips PW 1820 Diffractometer; Ni filtered, Cu radiation) to aid in identifying the lithostratigraphic units, primarily for identifying the origin of ambiguous units.

1.0.4 LOCATION, ACCESS, AND PHYSIOGRAPHY

The Lyon Lake Mine is located in the eastern part of the Sturgeon Lake mining camp of northwestern Ontario, located approximately 200 kilometers northwest of Thunder Bay, Ontario, and approximately 90 kilometers north of Ignace, Ontario. The Lyon Lake Mine is relatively easily accessed by Highway 17, the Trans-Canada Highway, from Thunder Bay, to Ignace, approximately 250 kilometers, and then north by Ontario Highway 599 from Ignace for 72 kilometers, then east on the mine access road for 25 kilometers (Figure 1).

The surficial terrain of the Lyon Lake Mine property is characterized by a flat, gravely and sandy site. To the north of the shaft, the terrain is characterized by spruce and cedar swamps. Outcrop exposure is extremely limited, except at the portal of the underground access ramp. The data base for this study is exclusively from 2 summer's underground mapping, with the exception of several drill holes transecting the hanging wall footwall contact, and the limited outcroppings at the portal.

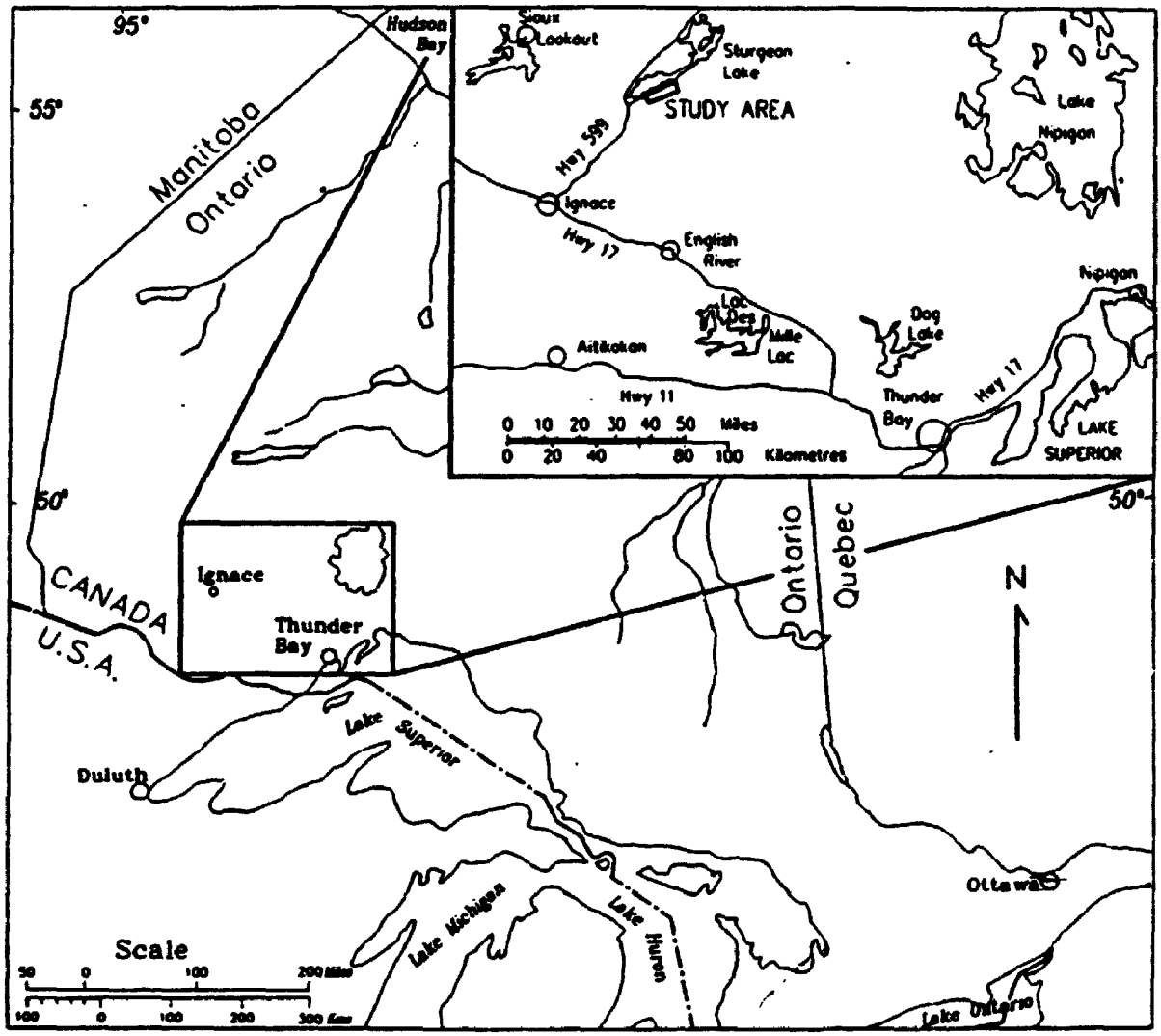

Figure 1: Location of the south Sturgeon Lake area (from Morton et al., 1990).

1.0.5 HISTORY

The Lyon Lake massive sulphide deposit is the second largest volcanogenic massive sulphide deposit in the South Sturgeon Lake district. It has many of the characteristics typical of volcanogenic massive sulphide deposits (Franklin et al., 1977), but lacks a conspicuous alteration zone, and has some unusual stratigraphic relationships, with iron formation in the structural footwall.

A combined air-borne magnetometer and electromagnetic survey was flown over the Sturgeon Lake area for Mattagami Lake Mines Ltd. in March 1969. Ground geophysical follow-up of strong 6 channel anomalies led to the drilling which intersected the footwall iron formation and sedimentary rocks.

Exploration diamond drilling along the geological contact at the Sturgeon Lake mine deposit led to the discovery of the Lyon Lake massive sulphide deposit in October 1971. The Creek Zone, half way between the Lyon Lake and Sturgeon Lake deposits was discovered in February 1972. Deep diamond drill testing for a proposed shaft site late in 1974 discovered a fourth ore zone, the Sub-Creek, at a vertical depth of 500 m.

The area has been previously studied on a regional scale by Franklin et al., (1977), and by Trowell (1974, 1983) and on a local scale by Hinzer (1977), Harvey and Hinzer (1981), Roberts (1981), Friske (1983), and Mumin (1988). Geologists from University of Minnesota-Duluth are at present undertaking a regional stratigraphic and volcanologic study for the Geological Survey of Canada as part of the Sturgeon Lake Project under the Canada-Ontario Mineral Development Agreement.

1.0.6 MINING

Production mining at the Lyon Lake mine commenced in November 1980, with total production of 3,172,540 tons at a grade of 8.67% Zn, 1.26% Cu, 4.50 oz/ton Ag,

and 0.99% Pb (to December 31, 1989). Mining was carried out at a rate of 32,000 tons per month with reserves sufficient to maintain production until December 1991.

The principal mining method was longhole open stoping utilizing trackless equipment; however, a significant amount of 'jumbo mining' was carried out in the flat-lying ore zones. The limited size of the individual ore lenses required intensive development. Production muck was moved to 1 of 5 ore passes which fed the 1800 foot level. This tracked level was the main tramming horizon where 10 ton battery locomotives moved the ore to a single set of passes which fed the 2700 level crusher station at the shaft. The 3 compartment shaft was originally sunk to a depth of 1347 feet, but was deepened in 1982 to its current depth of 2950 feet. Most ore was skipped from the 2800 level and skipping from the 1200 level was used for any ore mined above the 1000 level. Additional access to the underground for human resources and materials was gained via a ramp which extends from surface to the 1900 foot level. Ore was trucked 5 miles west to the Mattabi concentrator for custom milling. The Lyon Lake Mine closed on May 22, 1991.

CHAPTER 2

GEOLOGICAL SETTING

2.0 Regional geology

The Lyon Lake deposit is a stratiform Zn-Cu-Pb-Ag volcanogenic massive sulphide deposit located in the South Sturgeon Lake area in the central part of the Wabigoon volcano-sedimentary subprovince of the Archean Superior Province of the Canadian Shield (Goodwin et al., 1972). The Wabigoon subprovince is bounded to the north by the English River Gneiss Belt and to the south by the Quetico Gneiss Belt. The area of study is in the Sturgeon-Savant Lake crescentic greenstone belt, a typical greenstone belt in the Wabigoon subprovince. The latter is moderately deformed with steeply dipping felsic to mafic volcanic rocks and sedimentary rocks, bounded by granitic batholiths, and intruded by subvolcanic to syntectonic felsic intrusions. The South Sturgeon Lake area is in the south central part of the Sturgeon-Savant Lake belt and is conventionally determined to comprise a simple homoclinal sequence of north- facing, north- dipping volcanic and sedimentary rocks, consisting of several cycles, each representing a major volcanic episode (Trowell, 1974, 1983). Recently, however, several studies have indicated that interpretation as a single homocline may be an over - simplification of the structure. The volcanic and sedimentary rocks have been subjected to greenschist- facies metamorphism and almandine-amphibolite assemblages towards the south and east (Trowell, 1974, 1983). The South Sturgeon Lake sequence strikes west-northwest, dips steeply (65° - 75°), faces north, and forms the southern limb of a syncline with an axis centered through Sturgeon Lake (Trowell, 1983). The volcanic sequence exceeds a total apparent thickness of 9000 meters (Franklin et al., 1977, Trowell, 1974, 1983). The sequence comprises three volcanic cycles generally having basal mafic flows overlain by intermediate to felsic massive and pyroclastic flows locally intercalated with

volcaniclastic sediments near the top of each cycle (Franklin et al., 1977). Trace element and rare earth analyses (Davis et al., 1985) indicate that the lower three cycles have a similar petrogenetic history and are cogenetic with the subvolcanic Beidelman Bay trondjhemite sill which intrudes the base of the lower cycle (Poulsen and Franklin, 1981).

The middle and upper felsic unit of the lowermost cycle is the host to five known Zn-Cu-Ag-Pb volcanogenic massive sulphide deposits. The Mattabi and F-Zone deposits are hosted near the middle, whereas the Lyon Lake Zone, Creek Zone, and Sturgeon Lake Mine deposits occur at or near the top of the felsic unit, spatially above the sedimentary strata.

The South Sturgeon Lake area is recognized and described as a well- preserved Archean submarine caldera complex (Figure 2). This complex is approximately 30 km in strike length and contains up to 4500 m of caldera fill material (Morton et al., 1990). The principal members, include 1) a basal sequence of massive sheet flows, mafic scoria cone deposits and minor aphyric felsic ash flows, with epiclastic beds prominent near its top; 2) a large, sill-like subvolcanic intrusion of trondjhemite, intrusive into the basal sequence; 3) the caldera complex; and 4) a post-caldera sequence of massive beds of pyroclastic ash, dacitic and basaltic flows, and graphitic shale.

Precaldera volcanic rocks, referred to as the Darkwater Succession, represent part of a large subaerial to subaqueous shield-type volcano composed of a thick sequence of basalt lava flows, scoria-tuff cone deposits and debris flows, with minor amounts of interlayered rhyolitic lava flows and pyroclastic fall deposits.

The Caldera sequence has been subdivided into five members (Morton et al., 1990). 1) Jackpot Lake Succession: aphyric pyroclastic ash flow and fall deposits overlie the precaldera volcanic rocks, and possibly represent the initial pyroclastic eruptions that led to the first caldera collapse event. These deposits thin eastward and locally are separated by thin debris flow units. 2) High Level Lake Succession: mafic mesobreccia,

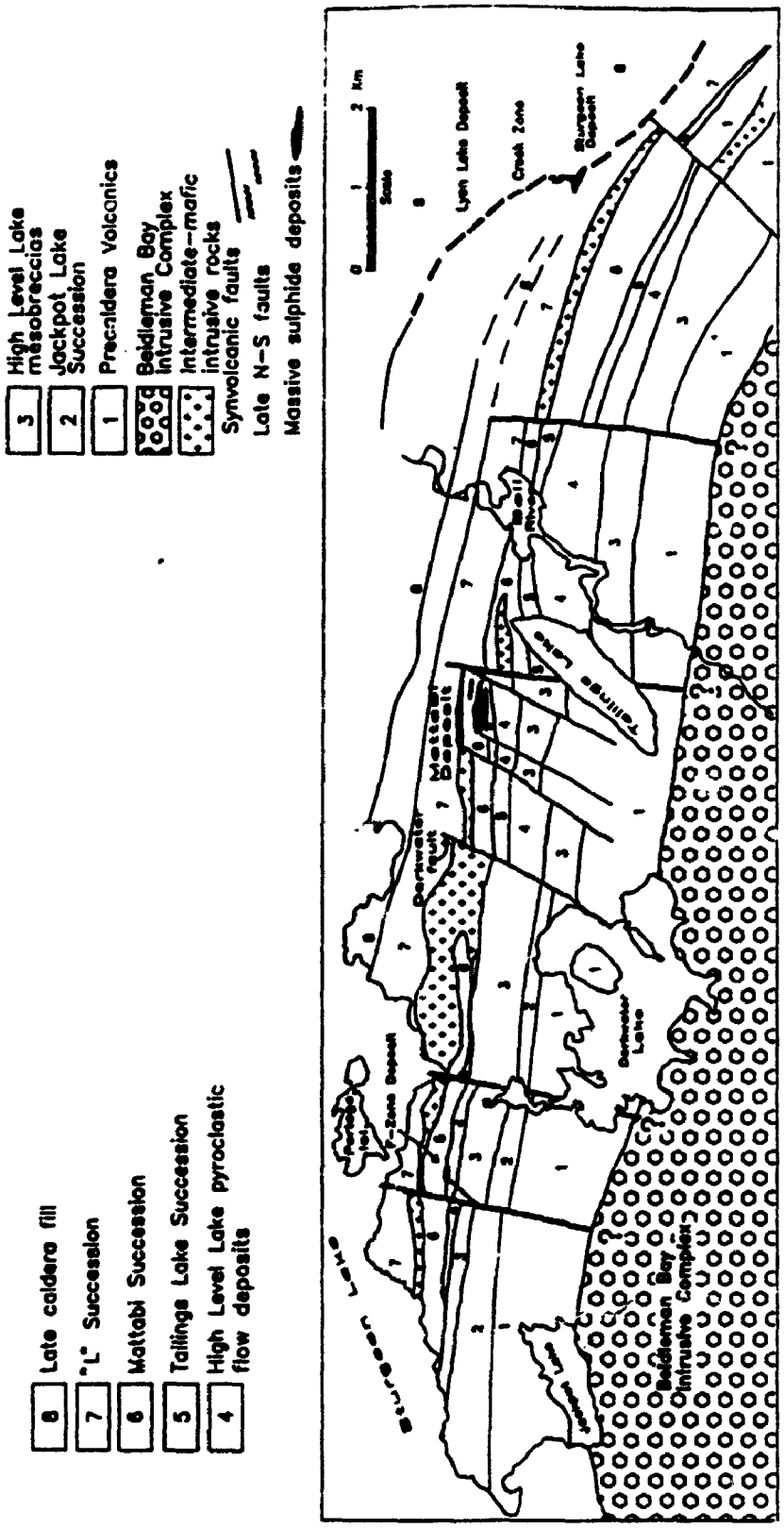

Figure 2: Simplified geological map of the Sturgeon Lake Caldera Complex (from Morton et al., 1990).

extending across the area, immediately overlies the precaldera volcanic rocks and Jackpot Lake Succession and are believed to represent debris derived from caldera walls as collapse occurred. Clasts and debris are mineralogically and chemically similar to the precaldera volcanic rocks and the Jackpot Lake pyroclastic unit. Collapse and breccia formation were simultaneous with eruption and deposition of the High Level Lake quartz crystal ash flow tuff.

Post caldera volcanic rocks consist of pillowed and massive basaltic flows. These mafic flows are in fault contact with the underlying caldera fill sequence. Above these mafic strata are felsic pyroclastic rocks, overlain by hundreds of meters of quartz-phyric ash flow tuff.

2.1. Lyon Lake Mine Geology

The Lyon Lake deposit occurs at the top of the caldera sequence. Figure 3 is a schematic stratigraphic column of the mine lithological units at the Lyon Lake Mine. From the present study, the mafic unit of the overlying cycle is in apparent fault contact with the top of the lowermost cycle and forms the structural hanging wall to the Lyon Lake, Creek Zone, Sub-Creek Zone and Sturgeon Lake Mine. The stratiform Lyon Lake deposit occurs in blue quartz-phyric fragmental rhyolite. The footwall to the ore consists of an upper rhyolitic unit composed of interbedded ash and lapilli tuff, immediately underlain by a lower rhyolitic unit of coarse fragmental rock. A sequence of sedimentary rocks composed of graphitic shale, massive pyrrhotite-pyrite bodies, greywacke, quartzose pelite, siltstone, and banded iron formation, occurs below the footwall rhyolite. Banded iron formation occurs at the base of the sedimentary sequence and provides a stratigraphic marker horizon. In the lower parts of the mine, locally developed heterolithic breccia is spatially related to the ore horizon as host, footwall and hanging wall rocks to the ore. The sedimentary sequence overlies, and is possibly in fault contact with the underlying

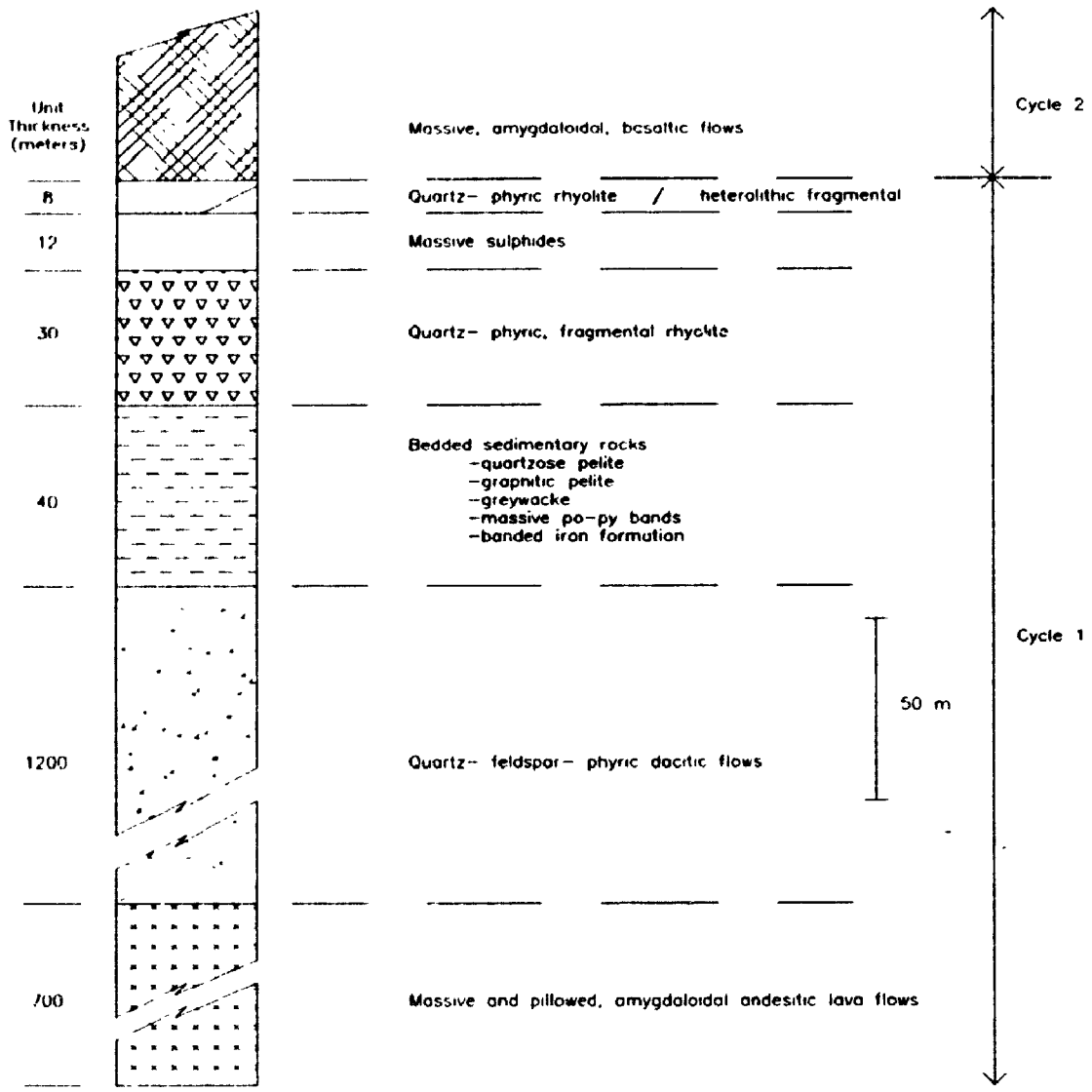

Figure 3: **Stratigraphic section of the Lyon Lake mine area.**

quartz- feldspar- phyric dacitic flows. Massive sulphides form several stacked or en echelon lenses, and are composed of discontinuous and contorted bands of coarse- grained sphalerite and pyrite. Locally centimeter- scale lenses of galena occur within sphalerite bands.

The following section summarizes the mineralogical and textural characteristics of each of the lithological units. Appendix A contains specific detailed maps, observations, and petrographic descriptions of the units for each area mapped.

2.1.1 Quartz- feldspar- phyric dacitic flow

This unit forms the lowermost rock type observed in the underground workings, and is exposed only at one locality in the mine (Appendix A-xxix; 2600 level east end). The apparent thickness observed underground is 70 m, and the total thickness is up to 1200 m based on drill core information (Morton et al., 1990).

Quartz- feldspar- phyric dacite underlies the iron formation. The contact between the quartz- feldspar- phyric dacite and the oxide iron formation is marked by a mafic dyke. The contacts between the dyke, dacite, and iron formation are sharp, and dip subvertically to the north.

The quartz- feldspar- phyric dacite is light to medium gray, massive, fine- grained, and contains ash- to block- size fragments. Blue quartz eyes are 1 to 2 mm in diameter, and comprise 2% of the unit, and locally up to 30%. One to 3 mm wide euhedral to subhedral feldspar phenocrysts comprise 20 to 30%, and locally up to 60% of the unit. Quartz and feldspar phenocrysts are homogeneously distributed in a granular, siliceous and sericitic groundmass.

Monolithic, subrounded to subangular quartz- and feldspar- phyric siliceous fragments up to 15 cm in width occur near the top contact of the quartz- feldspar- phyric dacitic flow. Locally, these fragments have chloritic rims. The fragments near the top

contact of the flow are similar in composition to the massive parts. The compositional and textural similarity suggests that the fragmental part of this unit is a flow- top breccia.

Several 1- to 3- cm- thick, quartz- tourmaline veins occur within this unit. Massive tourmaline generally occurs at the margins of the quartz veins, but also occurs disseminated throughout the vein. Locally, several quartz- tourmaline veins are offset by subhorizontal fractures.

The metamorphic mineral assemblage consists of sericite, quartz, chlorite, +/- biotite. Siliceous bands are common, chlorite alteration is locally intense, and biotite occurs locally with chlorite. Sericite, chlorite and biotite define the foliation, and occur as irregular fracture filling minerals, in quartz- tourmaline veins. Tabular white feldspar laths are partially or completely altered to sericite and carbonate. Fragments are preferentially altered to sericite.

Quartz- feldspar- phyric dacite is pervasively altered to sericite and chlorite. Alteration produces a banded or pseudobanded appearance. Locally, alteration bands are distinctive, varying from very pale green, to medium green, and pink, to pale purple. Sericite and chlorite are abundant, particularly along cleavage planes. Locally, this unit contains up to 3% disseminated and patchy zones of pyrite.

The contact with the overlying sedimentary rocks was observed in one locality (Appendix A-xxix; 2600 level east end). This contact is a tectonized zone characterized by a 50 m- thick contact zone of highly strained rock. The strained contact zone is characterized by strongly foliated millimeter to centimeter scale alternating bands of sericitic and chloritic felsic flow. Also, the basal 10 to 15 meters of the iron formation is disrupted; broken segments of iron formation are oriented parallel to the foliation. These observations suggest that this contact is a possible fault contact. This high strain zone is oriented subparallel to the contact between the hanging wall basalt and the footwall rhyolite that occurs higher in the stratigraphic sequence.

2.1.2 Sedimentary strata

A sequence of sedimentary rocks including banded iron formation, graphitic shale, massive pyrrhotite - pyrite lenses, greywacke, and quartz-rich pelite occurs 15 to 60 meters below the ore horizon. The sedimentary rocks were observed and mapped in numerous areas of the mine, because the best development of primary bedded features occurs in the these rocks. The sedimentary rocks were mapped on the 525, 600, 1000, 1480 - 1580 ramp, 1580, 1800, and 2600 levels. Most of the deformation structures observed at the mine are evident in these sedimentary rocks. The banded iron formation and the ore horizon are the most strongly deformed rocks observed in the mine. The sedimentary unit ranges in apparent thickness from 20 to 60 meters, and may be thicker since the lower sedimentary contact was observed at only one locality (Appendix A-xxix; 2600 level east end) in the underground workings.

The sedimentary rocks consist of a basal iron- oxide or iron- carbonate banded iron formation in possible fault contact (described above) with the underlying felsic flows. The iron formation is overlain by interbedded greywacke, medium- grained felsic quartzose pelite, and graphitic pelite. Locally, massive pyrrhotite - pyrite lensoid bodies occur stratigraphically above the banded iron formation. Beds of sedimentary rock intercalated with iron formation are on average 15 to 45 cm thick.

Quartzose pelite is best exposed along the 1480 to 1580 ramp (Appendix A-xxi; 1450 to 1580 ramp). The unit is massive, medium- grained, pale yellow to light beige or gray, and pink. Commonly, quartz- +/- albite- rich beds alternate with chlorite-rich and sericite-rich beds. Beds vary from 10 to 25 cm in thickness. The presence of minerals such as sericite, chlorite or pink feldspar imparts the colour to the beds. Quartzose pelite typically contains 1 to 5 mm chloritic and pyritic ovoid blebs. These blebs are oriented parallel to the foliation. Locally, quartzose pelite grades into siltstone (Appendix A-xxii; 1580 ramp and level intersection).

Petrographic studies indicate that quartzose pelite is composed of moderately sorted, subrounded to subangular, silt- to sand- size quartz grains and up to 10% feldspar grains. Clastic grains are well packed and comprise 80% of the unit. Quartz grains are clear, and feldspar grains are 'frosted' due to alteration to sericite. The matrix is composed of clay size quartz, sericite, and biotite. Chlorite is locally present, as an alteration product of biotite. Calcite occurs as a pervasive overprint on the pelitic rocks (Appendix B).

Graphitic pelite occurs as very fine- grained, massive, dark gray to black beds, interbedded with iron formation (Appendix A-xxi; 1480 to 1580 ramp, A-xxviii; 1800 level, and A-xxix; 2600 level east). Locally, graphitic pelite is intercalated with greywacke and quartzose pelite (Appendix A-viii; 600 level ore pass, A-xxi; 1480 to 1580 ramp, and A-xxix; 2600 level east end), and massive sulphides (Appendix A-vii; 600 level fuel station). Individual beds of graphitic pelite are 30 to 60 cm- thick, and locally, up to 2 m-thick. Pyrrhotite comprises 5 to 8% of the unit, and commonly occurs as ovoid blebs up to a centimeter in diameter, evenly distributed throughout the bed, and as fine laminations along slaty cleavage planes.

In thin section, graphitic pelite consists of laminations composed of 50% polygonal quartz, 15% chlorite, 10% graphite, and 5% white mica. Trace subhedral pyrrhotite is randomly oriented, and disseminated evenly throughout. Carbonate occurs as a pervasive overprint. Randomly oriented 1 to 2 mm equant carbonate porphyroblasts comprise up to 10% of the rock.

2.2.3 Banded iron formation

Iron-carbonate, -silicate, -oxide, and/or -sulphide banded iron formation forms the basal member of the sedimentary strata in the mine workings, and from drill core intersections, extends laterally along strike 2 kilometers east and west of the mine. The unit has not been observed in outcrop. Based on underground mapping and drill core

information, banded iron formation occurs from near - surface through to the 2600 level, and probably continues at depth as a continuous stratigraphic marker horizon. It is typically thin-banded and laminated, with discreet beds containing pyrite or magnetite laminations. Thin bands and laminations of iron formation associated with greywacke and volcanic rocks, indicate that this banded iron formation is a typical Algoma Type iron formation (Gross, 1965). Compositional variation is observed from level to level, but in general, carbonate iron formation occurs in the upper (surface to 1000 levels: Appendix A-ii, iii, iv, v, viii, ix, x, and xi) and lower mine levels (1700 to 1800 levels: Appendix A-xxviii), and oxide iron formation is developed in the middle levels (1000 to 1700 levels: Appendix A-x, xi, xxi, xxii,), and deepest level of the mine (2600 level; Appendix A-xxxi). The compositional variation represents lateral facies changes, and not the presence of more than one iron formation, because the iron formation can be traced from one level to the next.

From the 525 level to the 1000 level, iron- carbonate iron formation occurs (Plate 1). Iron- carbonate iron formation consists of interlayered beds of iron- carbonate (siderite), chert, and iron- silicate (chlorite). Iron- carbonate beds are composed of quartz and siderite, and iron- silicate beds are composed of quartz and chlorite. Carbonate beds commonly contain laminations of magnetite (Appendix A-x; 1000 level conveyor belt, A-xi; 1000 level crusher area). Locally, iron- carbonate beds contain laminations of pyrrhotite (Appendix A-viii; 600 level ore pass). The individual beds vary in thickness from 1 to 15 cm. Stringers and veinlets of pyrrhotite and pyrite are developed at the margins of iron- silicate beds, parallel to bedding, and in fractures oriented subparallel to the foliation, cross cutting the iron- carbonate and chert beds. From 525 to 1000 levels, the banded iron formation is intercalated with greywacke and felsic volcanic flows.

A lateral facies change occurs from iron- carbonate iron formation observed in the upper levels of the mine, to iron- oxide iron formation observed from the 1000 to 1700

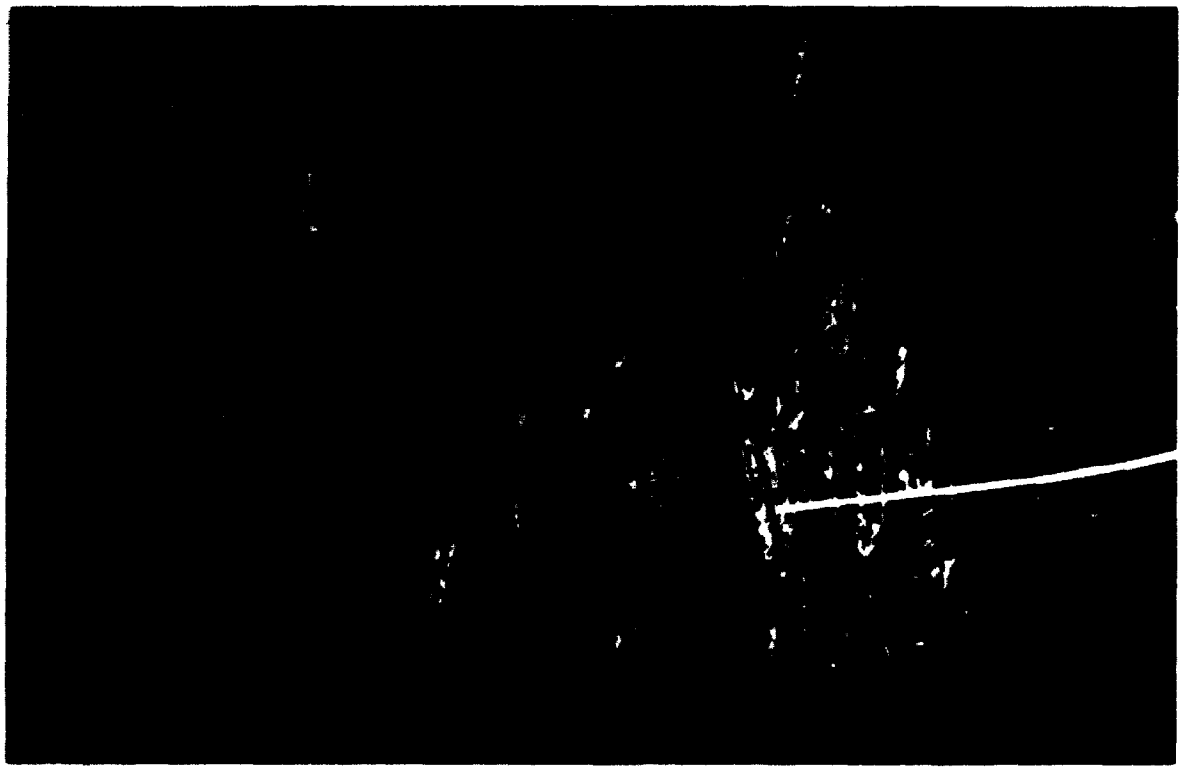

Plate 1: Banded iron formation. Steep, isoclinally folded iron- carbonate iron formation (600 level). Field of view is 2 meters.

levels. Banded iron formation is composed of iron- oxide beds interlayered with beds of chert, iron- silicate, and iron- carbonate. Iron- oxide beds are composed of magnetite + quartz, +/- carbonate. Iron- silicate beds are composed of chlorite + biotite, and iron-carbonate beds are composed of quartz and siderite. Laminations of strongly magnetic pyrrhotite occur in the iron- carbonate beds, and locally in the iron- silicate beds. Magnetite occurs as 2 to 3 cm- thick, monomineralic beds, interlayered with beds of chert and iron- carbonate. Magnetite also occurs as fine laminations in iron- carbonate and chert beds.

On the 1000 level iron formation has an apparent thickness of 200 m, and is characterized by magnetite- and pyrrhotite- bearing cherty beds alternating with iron-silicate beds. Chert, iron- carbonate, and iron- silicate beds are 5 to 8 cm- thick, and locally chert beds are up to 15 cm- thick. Magnetite occurs within iron- carbonate- rich cherty beds, as delicate laminations, which are evenly spaced throughout the bed. Locally, pyrite - pyrrhotite veinlets occur in the iron- silicate beds parallel to bedding. Pyrrhotite is weakly magnetic.

Petrographic studies indicate that the iron- oxide iron formation typically consists of alternating beds of; 1) chlorite, biotite, and magnetite; 2) quartz, and minor carbonate; 3) quartz, chlorite, biotite, carbonate, and magnetite; and, 4) quartz, carbonate, anthophyllite, magnetite and minor chlorite.

Anthophyllite occurs as radiating fibrous, and feathery- textured grains at the margins of the beds, adjacent to the chlorite - biotite beds. Anthophyllite is associated with coarse- grained skeletal euhedral to subhedral magnetite in carbonate altered beds. Locally, magnetite is corroded. Magnetite, anthophyllite, and carbonate bearing beds are intercalated with beds of clean, fine- grained polygonal quartz with minor interstitial carbonate. Other intercalated beds are composed of quartz, carbonate and chlorite.

On the 1000 level, sedimentary rocks other than the iron formation are less abundant and the iron formation is associated with quartz-phyric felsic flows (Plate 2).

On the 1480 to 1580 level ramp (Appendix A-xxi), the banded iron formation is composed of 1 to 2 cm-thick magnetite beds interbedded with 1 to 2 cm-thick gray and black chert (Plates 3 and 4). The gray chert and iron- silicate beds commonly contain fine laminations of magnetite and iron- carbonate. Cherty beds up to 30 cm- thick contain thin beds and laminations of magnetite, 3 to 10 mm- thick. Between these cherty beds, 2.5 to 15 cm-thick argillite and chlorite beds occur. Commonly, cherty beds are fractured perpendicular to bedding. On this level, banded iron formation is interbedded with graphite and quartzose pelite, and beds of massive pyrrhotite and pyrite.

From the 1580 to 1700 levels, the banded iron formation is basal to, and intercalated with an apparent 100 m- thick zone of the complete sedimentary section described above.

On the 1800 level (Appendix A-xxviii), banded iron formation is compositionally similar to that observed on the 600 and 1000 levels (Appendix A-viii; 600 level ore pass, Plate 1, Appendix A-x; 1000 level conveyor belt, and Appendix A-xi; 1000 level crusher area). Banded iron formation on this level is composed of beds of iron- carbonate, chert, iron- silicate, +/- iron- oxide. Beds average 5 to 8 cm- thick. Locally, 2.5 to 5 cm- thick magnetitic beds are intercalated with cherty beds. The latter contain laminations of magnetite. Iron formation on this level is associated with graphitic pelite and siltstone.

On the 2600 level, banded iron formation consists of intercalated beds of chert, iron- silicate, and iron- oxide beds. Beds vary from 0.5 to 5 cm- thick. Locally, chert beds are up to 10 cm- thick, and contain laminations of magnetite + anthophyllite. Iron-silicate beds are dark green, composed of chlorite and biotite, and locally contain 1to

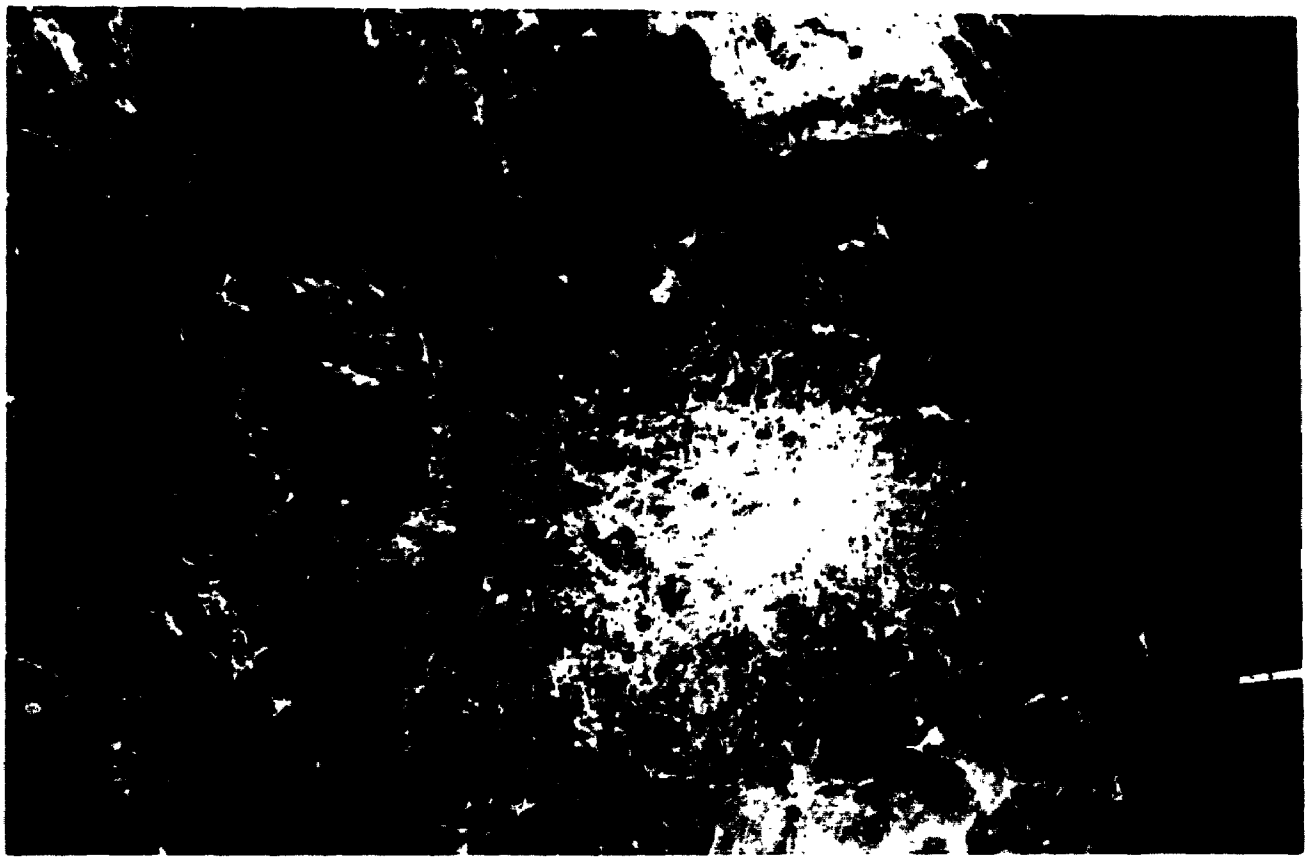

Plate 2: Banded iron formation (upper part of photo) in contact with quartz- phyric rhyolite (lower part of photo; 1000 level conveyor belt area). Field of view is 3.5 meters.

Plate 3: Centimeter scale bands of magnetite and chert, plus iron silicate (1480 to 1580 ramp). Field of view is 4 meters.

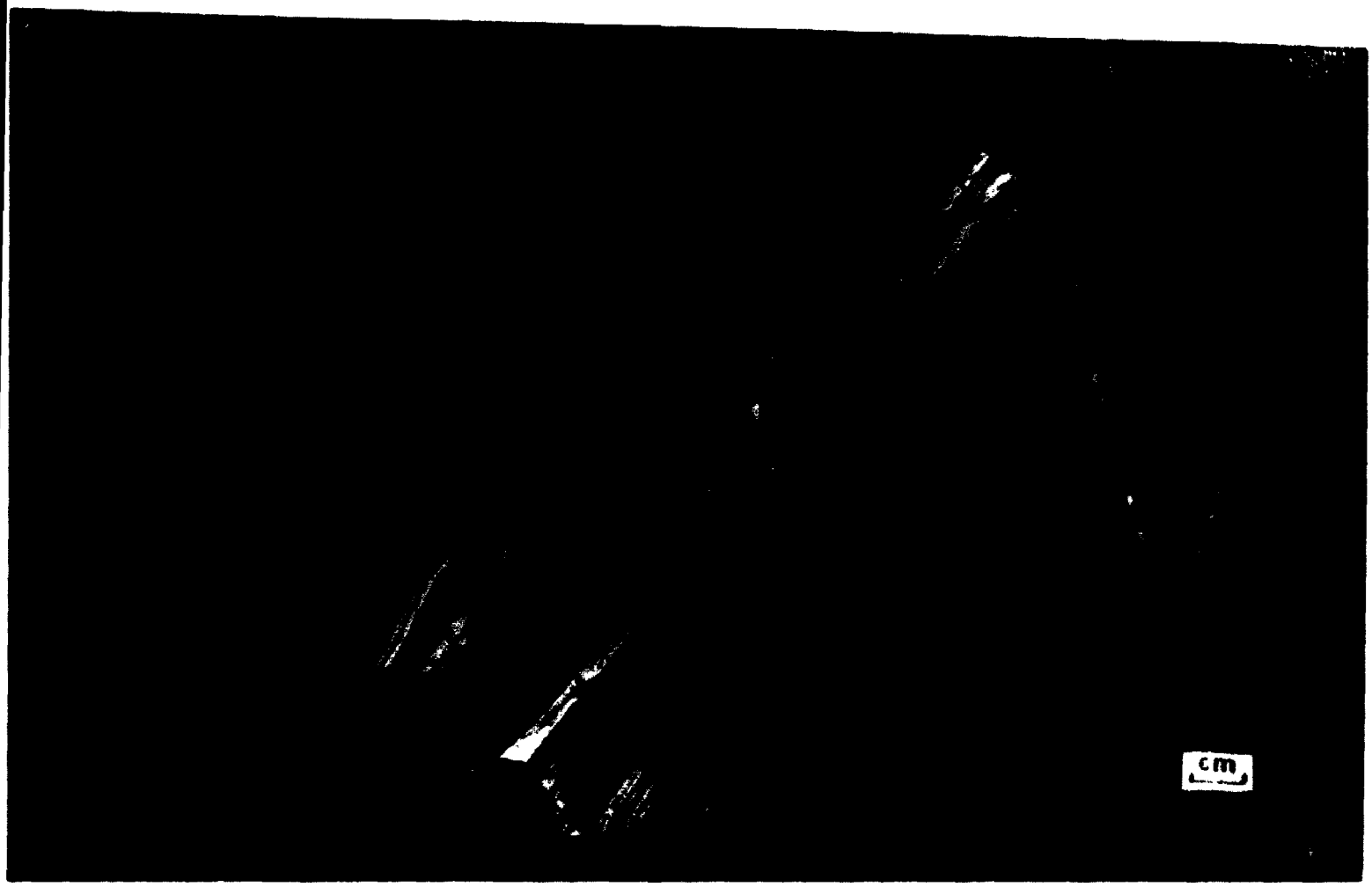

Plate 4: Sample from location in Plate 3. Fine laminations of magnetite (light gray, intercalated with cloudy, gray and black chert (1480 to 1580 ramp).

3%, 1 to 3 mm garnets.

Locally, near the contact with the underlying quartz-feldspar-phyric felsic flows, the iron formation is fragmented and individual fragmented beds are hosted in a graphitic pelite matrix.

A moderate schistosity is developed in the iron- silicate beds of the iron formation, and is oriented parallel to bedding. Late quartz- filled fractures oriented perpendicular to bedding occur in the chert beds. Locally, deformation has caused boudinage and fracturing of iron- carbonate and cherty beds, and attenuation in the iron- silicate beds (Appendix A-viii; 600 level ore pass and Appendix A-xxix; 2600 level east end).

Iron formation is isoclinally folded, and locally, chert and iron- carbonate beds are disrupted, boudinaged, and fractured.

2.1.4 Heterolithic fragmental unit

This unit is spatially associated with the ore, forming its footwall, host, and/or hanging wall, from the 1640 level to the 1850 level. This unit does not occur in the upper levels of the mine. The thickest part of this unit, approximately 40 meters, was observed on the 1640 to 1700 levels (Appendix A-xxv; 1640 level north access drift). The unit is composed of angular fragments of varying composition, in an aphanitic dark green to black matrix. Siliceous, felsic lithic, chloritic, sulphidic, argillic, and quartz-phyric rhyolitic fragments are supported in a very fine- grained, dark green to black, locally pyritic and garnetiferous matrix. White siliceous fragments are the largest, 5 to 15 cm in diameter, and the most abundant, comprising 40 to 50% of the rock (Plate 5). One millimeter to [illegible] cm. argillic, graphitic, and sulphidic fragments are less obvious in the dark matrix, and comprise up to 10% of the unit.

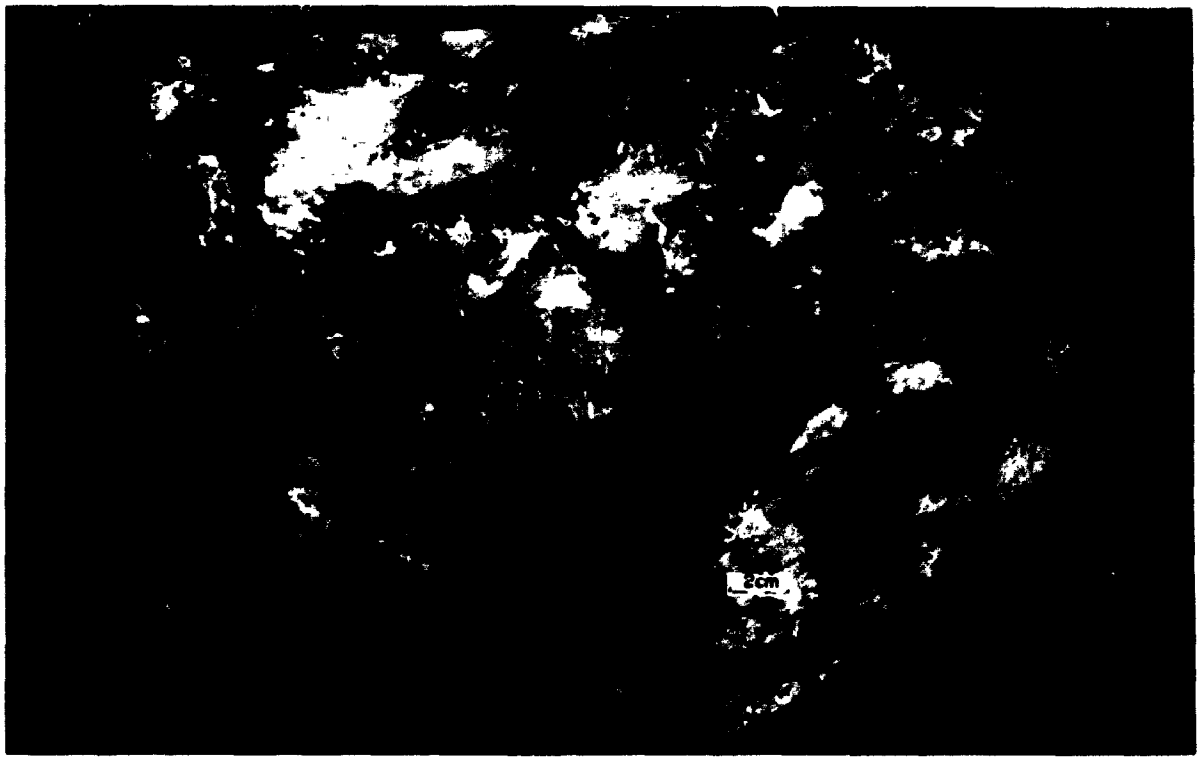

Plate 5: Heterolithic fragmental. Dominantly angular white siliceous fragments, plus felsic lithic and sulphidic fragments in an aphanitic dark green to black matrix.

Petrographic studies indicate that the matrix is composed of polygonal quartz, plagioclase, sericite, chlorite and carbonaceous material. Rhyolitic and cherty fragments are distinguished from the matrix by the fine- grain size of recrystallized quartz, and pervasive sericitic alteration in the fragments. Locally, blue and gray quartz phenocrysts vary from 0.5 to 2 mm in diameter, and comprise < 1% of the matrix.

The matrix is also chloritic, and contains up to 10% chloritoid porphyroblasts. Chloritoid porphyroblasts are 0.5 to 2 mm in size, randomly oriented, evenly distributed, and locally in clusters. Chloritoid grains are twinned and skeletal.

A very strong schistosity is developed in the unit, defined by sericite and chlorite in the matrix. The fragments are oriented parallel to the foliation and have aspect ratios of 2:1 to 10:1. In zones of intense deformation, aspect ratios of fragments may be as high as 20:1.

The heterogeneity, angularity of the fragments, geometry, and the local distribution of this unit suggests this deposit is a debris flow, or talus slope deposit. The white siliceous, argillic, chloritic, and sulphidic fragments observed in this unit bear a strong resemblance to the composition of beds in the iron formation. The source of these fragments is likely from the underlying lithological units which include the iron formation and sedimentary rocks.

2.1.5 Rhyolite

The sedimentary sequence is overlain by a fine- grained quartz- phyric rhyolite, which forms the immediate host and footwall to the massive sulphide lenses.

In general, the sequence of pyroclastic flows consists of block sized fragments at the base, grading stratigraphically upwards with increasing abundance of lapilli- sized fragments, overlain by quartz- phyric ash flow, overlain by aphyric ash beds. Overlying the ash beds, an additional coarse fragmental unit occurs, representing the base of a

subsequent pyroclastic flow. Up to two flows within the rhyolite sequence were identified on the 525 level 1116 cross cut (Appendix A-ii) and the 1260 sub-level (Appendix A-xiii).

Contacts between pyroclastic flows are very diffuse and may be distinguished by the presence of block size fragments overlying aphyric ash.

The lower contact of the rhyolite with the underlying sedimentary rocks is irregular and diffuse, overprinted by iron- carbonate- filled micro- fractures in the graphitic pelite and iron- carbonate and sericite alteration in the rhyolite (Appendix A-xxii; 1580 ramp and level intersection). Locally, this contact is sharp (Appendix A-ix; 600 level 1082 cross cut), or occupied by an intermediate dyke (Appendix A- ii; 525 ore pass and 1116 cross cut).

The rhyolite unit is light gray to beige, varies from massive to lithic fragmental in texture. It is characterized by blue, and less commonly, gray and black euhedral quartz phenocrysts ranging in size from 1 to 3 mm. The abundance of quartz phenocrysts shows a gradational variation from 1 to 20% stratigraphically upwards and proximal to the massive sulphide. Typically, blue and gray quartz eyes are more abundant and larger (3 mm) proximal to the massive sulphide body, whereas deeper in the footwall, quartz phenocrysts are less abundant, smaller (1 mm), and gray and black. One to two percent pyrite is disseminated throughout the rock.

Fragmental rhyolite varies from coarse volcanic breccia at the base to interbedded felsic ash and lapilli tuff towards the top. Fragmental rhyolite is composed of 20 to 30%, subangular, monolithic, siliceous quartz- phyric fragments in a quartz- phyric, chlorite, carbonate, and sericite- bearing matrix. Locally, fragments contain 1 to 2 mm size pyrite and chlorite- filled amygdules. Fragments are typically 1 to 15 cm in diameter (Appendix A-xviii; 1480-1235 stope), and may be up to 45 cm in diameter in the upper parts of the mine (Appendix A-ii; 525 ore pass and 1116 cross cut), and up to 1 m in diameter in the

lower parts of the mine (Appendix A-xviii; 1480-1235 stope). Fragments more commonly vary in size from 1 to 5 cm, averaging 2 cm in diameter (Appendix A-xiii; 1260 sub-level).

On the 1480 level (Appendix A-xv), the immediate footwall to the ore is characterized by a 30 to 60 cm- thick zone of banded siliceous ash, underlain by quartz-phyric fragmental rhyolite. This is atypical in comparison to other areas mapped in the mine; more commonly, blue quartz-phyric rhyolite tuff hosts the massive sulphides. In this area, the banded siliceous horizon is composed of 5 to 10% disseminated, 1 to 2 mm euhedral pyrite, and locally contains discontinuous veinlets of sphalerite which are parallel to bedding. The typical quartz-phyric fragmental rhyolite underlies this siliceous banded horizon.

Typically, the rhyolite contains abundant quartz- and iron- carbonate- filled microfractures and minor 1 to 5 mm- thick pyritic filled stringers and microfractures.

Fragments are pervasively overprinted by carbonate. The immediate footwall to the ore, the quartz-phyric rhyolite lapilli unit is pervasively altered to chlorite, whereas, deeper in the footwall, sericite alteration is pervasive (Appendix A-ii; 525 ore pass and 1116 cross cut, Appendix A-xiii; 1260 sub-level, and Appendix A-xxiv; 1640 west sill). The distribution of chlorite and sericite alteration zones is semi- conformable to the main ore body. Garnets are pervasive, vary in size from 0.5 to 3 mm, and comprise 3 to 5% of the unit (Appendix A-xiv; 1300-1269 cross cut, Appendix A-xviii; 1480-1235 stope, and Appendix A-xxiv; 1640 west sill). Locally, garnets comprise 10% of the unit, proximal to the ore zone (Appendix A-xiii; 1260 sub-level).

The quartz-phyric fragmental rhyolite has a very well defined, moderate to strong foliation (Plate 6) striking northwest, and dipping steeply to the north. Cleavage is evenly spaced at 1 cm, defined by sericite and chlorite. Fragments have aspect ratios of 2:1 to 5:1; long axes are oriented parallel to the foliation. Locally, 5 to 8 cm- thick pyrrhotite bearing quartz veinlets occur parallel to the foliation (Appendix A-x; 1000 level conveyor

Plate 6: Strongly foliated quartz- phyric rhyolite footwall (1260 level). The penetrative fabric presents an evenly spaced fracture cleavage. The scale bar is divided into one inch divisions.

belt). Overall, the rhyolite is most intensely deformed near the contact with the massive sulphides and the hanging wall basalt.

2.1.6 Sulphides

The Lyon Lake volcanogenic massive sulphide deposit consists of at least three zones, the Lyon Lake , Creek, and Sub Creek Zones. All three zones occur in the blue quartz-phyric rhyolite at the top of the caldera complex.

The sulphides described by Harvey and Hinzer, (1981) occur in several stacked or en echelon concordant, massive sulphide lenses. The sulphide lenses comprise discontinuous and contorted bands of coarse- grained sphalerite and pyrite (Plate 7), varying from fine laminations to massive bands up to 3 m- thick. Pyrrhotite and chalcopyrite are present locally as thin beds or stringers. Locally, gross zonation of sulphides occurs where bands of sphalerite are predominant at the margins and pyrite bands are most abundant in the core of the lens. Banding is generally subparallel to bedding.

Ore lenses within the Lyon Lake Mine are relatively small, irregular massive sulphide lenses averaging approximately 15,000 to 20,000 tons each. The Lyon Lake, Creek and Sub Creek Zones are not single ore lenses, but groupings of spatially related smaller ore zones.

The ore lenses consist of massive to banded fine- grained sulphides with variable amounts of gangue. The principal sulphides are pyrite, sphalerite, chalcopyrite, galena, and pyrrhotite with minor amounts of tetrahedrite, arsenopyrite, and tennantite. Gangue to the ore consists of aggregates of quartz and carbonate and inclusions of sheared wall rock and boudinaged dykes. Quartz is the most abundant gangue mineral, followed by carbonate, with minor chlorite, muscovite, rare phlogopite and possible clinozoisite.

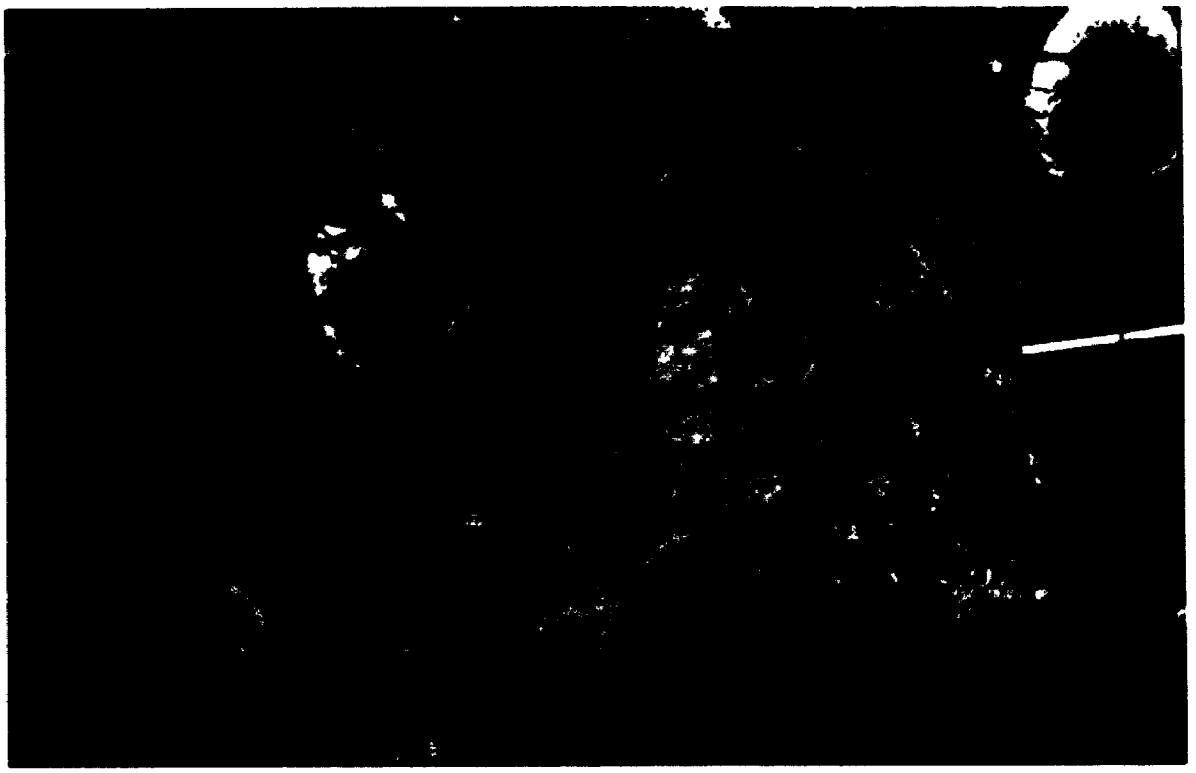

Plate 7: Banded massive sulphide. Coarse- grained massive sphalerite and pyrite. Black bands are massive sphalerite and the light gray bands are pyrite. Note the contorted sphalerite bands at the top, left of center of the photograph. Field of view is 1.5 meters.

2.1.7 Basalt

The basal mafic member of the "post caldera" sequence (Morton et al., 1990) forms the hanging wall to the massive sulphide horizon. This unit outcrops to the east between the Lyon Lake Mine and Sturgeon Lake Mine. It is compositionally basalt (Franklin et al., 1977). The basalt (Plate 8) is dark green, fine- grained, moderately to strongly foliated, and consists of feldspar-phyric massive to amygdaloidal sheet-flows and debris flows. Subhedral feldspar phenocrysts are 1 mm in diameter, and comprise 2 to 3% of the unit. Amygdules comprise up to 5% of the unit. Spherical and elongate amygdules are quartz and carbonate filled, and vary in size from 2 to 20 mm, locally, up to 4 cm (Appendix A-xii; 1000 level exploration access drift). In the strongly schistose basalt, amygdules have aspect ratios up to 5:1. The long axes of the amygdules are oriented parallel to the foliation. Locally, 1 to 2%, 1 mm size disseminated magnetite grains (Appendix A-i; 200 level #1 crosscut), and 2 to 3% disseminated 0.5 to 1 mm size euhedral pyrite (Appendix A-ii; 525 ore pass and 525-1116 crosscut) occur in this unit. One- to ten mm- thick, irregularly distributed quartz and iron- carbonate stringers and fractures occur parallel to the foliation. Carbonate stringers are more abundant at the highly strained base of the basaltic flow unit, proximal to the contact with the footwall rhyolite. Locally, minor stringers of pyrrhotite and pyrite occur sub-parallel to foliation (Appendix A-ii; 525 ore pass and 525-1116 crosscut).

A felsic to intermediate dyke occurs near the base of the basaltic flow (less than 1 m from the contact), or at the contact between the basaltic flow and the footwall rhyolite. This relationship was observed at every exposure of the contact between the hanging wall basalt and the footwall rhyolite.

Wherever the contact between the hanging wall and footwall rocks was observed underground, the base of the mafic unit is strongly schistose, and the top of the footwall rhyolite is strongly cleaved. Based on underground mapping and drill core logging, this

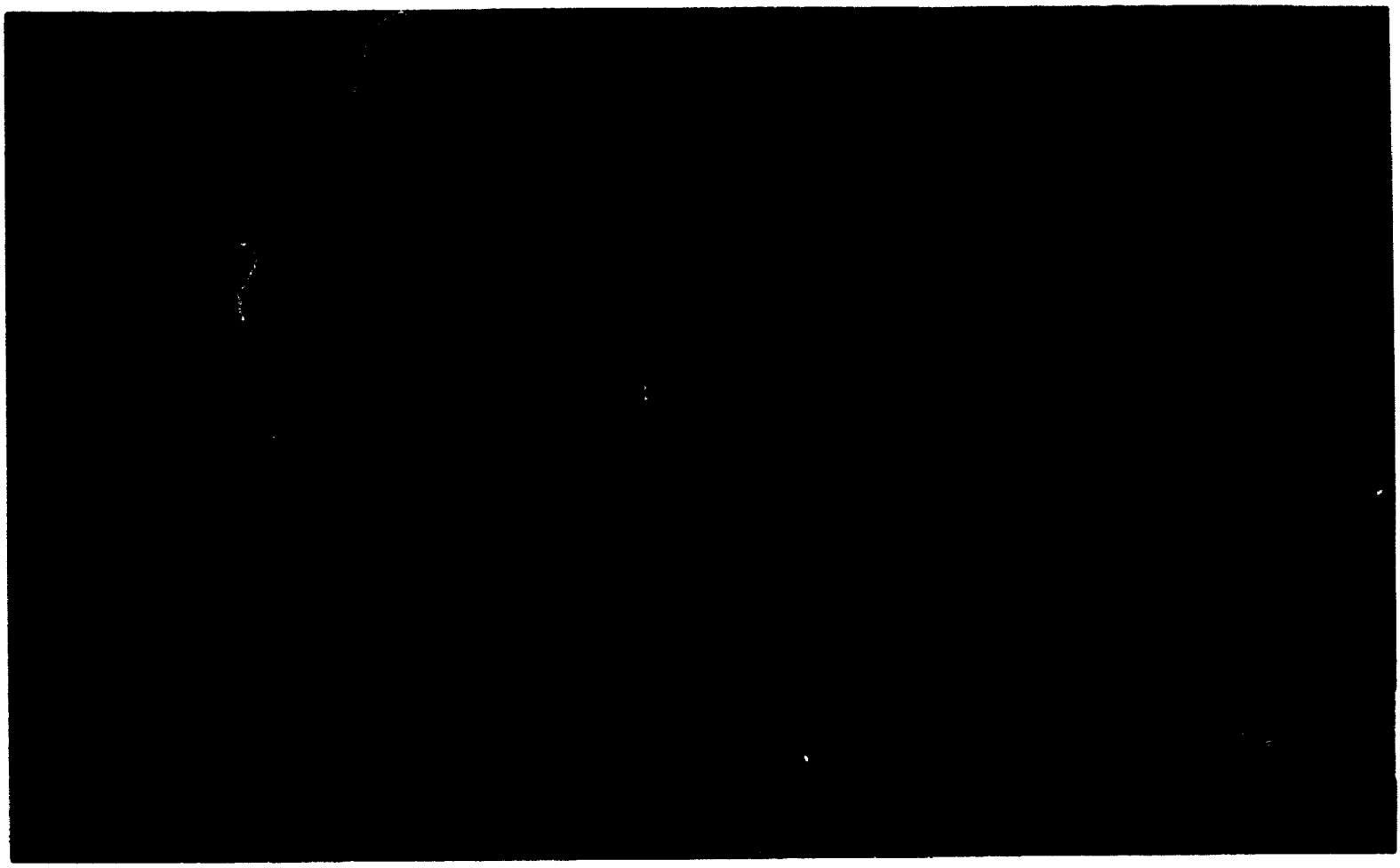

Plate 8: Strongly foliated hanging wall basalt. Quartz- carbonate filled amygdules (white) are elongate, and quartz- carbonate stringers (orange-beige wisps) are oriented parallel to the foliation.

basalt truncates the host rhyolite, ore, and footwall sedimentary sequence (Appendix A-ii; 525 ore pass and 525-1116 cross cut). Locally, in undeformed areas, centimeter- thick chloritic layers were observed which may represent sheet-flow contacts, defining 20 to 30 cm- thick sheet-flows (Appendix A-vi; 600 level garage). In strongly schistose zones, proximal to the contact with the footwall rhyolite, the schistosity produces a metamorphic layering of alternating green and white bands (Appendix A-i; 200 level #1 crosscut). Several 15- to 20- cm- thick subhorizontal pyrite- bearing quartz veins, 6 to 8 m in length were observed in highly strained basalt on the 600 level (Appendix A-vi; 600 level garage). Pillows were not observed underground or in outcrop in the mine area.

Petrographic study indicates that basaltic flows are composed of 10 percent twinned, oligoclase phenocrysts, up to 1 mm in size. Oligoclase phenocrysts are locally altered to sericite. Ovoid amygdules up to 1 mm in diameter, make up to 5 percent of the rock, and are filled with polygonal grains of clear quartz, plus carbonate. The matrix is composed of 0.2 mm laths of albite, equant quartz, and wispy and granular chlorite interwoven with flakes of biotite. Plagioclase, chlorite and biotite are preferentially oriented, defining the foliation. Less than 1% relict hornblende grains were observed. Carbonate occurs pervasively, in microfractures and locally with quartz in microfractures. Microcrystalline pyrite occurs as randomly oriented euhedral grains associated with the chlorite in the matrix. This unit varies from massive to strongly foliated, locally exhibiting protomylonitic texture.

CHAPTER 3

STRUCTURAL GEOLOGY

3.0 Introduction

Structural complexities within the ore zones at the Lyon Lake Mine became more evident as mining progressed. These complexities required detailed structural mapping as an aid to projecting the stratigraphic and structural control of the orebodies to greater depth within the mine area.

Detailed structural observations were made to 1) assess the amount to which the recognized eastward plunging linear orientation of the ore bodies is the result of primary disposition or subsequent deformation, 2) to determine the structural style that affects the ore distribution at the Lyon Lake Mine in the south Sturgeon Lake volcanic belt, and 3) to determine the significance of local structural features as controls on ore distribution. These observations were made through detailed examination of selected areas underground.

Each mapped area was selected for the purpose of working towards solving specific problems. Stratigraphic and structural observations and measurements were made at each location, and statistically compiled using equal area stereographic projections. Bedding measurements and relationships were taken to establish a primary reference frame. The spatial distribution of bedding will define major fold or fault structures within the area. Cleavage and schistosity measurements were recorded in all lithological units. A spaced cleavage occurs in more competent rocks such as rhyolite, sedimentary rocks, and chert beds in the iron formation, where typically sericite or chlorite defines cleavage planes. In the cherty beds of the iron formation, commonly quartz plus magnetite defines a pressure solution cleavage. Less competent rocks such as the basalt and silicate beds in the iron formation exhibit a schistosity defined by the segregation of chlorite into bands parallel with the foliation. Linear fabrics observed on bedding, foliation, fold, and fault

surfaces, and the intersection lineation of bedding/cleavage, fold axes, mineral stretching lineations, and slickensides were measured to aid in identifying areas of structural homogeneity, and the kinematics of deformation. Fold geometries, descriptions and measurements were taken as these features of folded surfaces provide information on the geometry, style, and mechanism of folding. Vergence relationships of asymmetric folds (Bell, 1981) were recorded to locate major fold axial surfaces. The vergence of minor folds changes across the surface of a major fold.

3.1 Structural observations at Lyon Lake

3.1.1 Bedding

Detailed structural observations are generally limited to sedimentary rocks, rhyolite, and massive sulphide. The contact between the hanging wall basalt and the footwall rhyolite is interpreted to be a fault contact (see below), and therefore, not included as a conformable bedding feature.

Bedding (S_0), is well preserved in the strata of the sedimentary sequence, including the banded iron formation (Plate 9), graphitic pelite and quartzose pelite of the sedimentary sequence. Locally, the contact between the aphyric or quartz-phyric ash flow top, and the base of the overlying fragmental rhyolite all give information on bedding attitudes.

In the South Sturgeon Lake belt, bedding generally strikes west northwest (290°), and steeply dips to the north (60 to 70°). However, within the mine, from west to east, bedding attitudes vary from west northwest, steeply dipping north, to northwest, shallowly dipping east, to west northwest, steeply dipping north.

3.1.2 Cleavage

Plate 9: Bedding is best preserved in the banded iron formation. Fold wavelength is approximately 10 meters. Field of view is approximately 4 to 5 meters.

A penetrative cleavage (S_1) is developed in the felsic volcanic (Plate 6) and sedimentary rocks. Cleavage strikes parallel to bedding, but dips more steeply than bedding (Figure 4). The orientation of the cleavage is 309°/76°.

The cleavage is defined by the parallel alignment of mica and chlorite, of quartz-, carbonate-, pyrite-, and pyrrhotite- stringers and veinlets, and the elongation of fragments, in the felsic volcanic rocks. Cleavage tends to be evenly spaced on a centimeter scale in these competent units.

3.1.3 Schistosity

A penetrative schistosity (S_1) is well developed in the basalt (Plate 8), the heterolithic breccia, and the silicate beds of the iron formation. Locally, the graphitic pelite (Appendix A-xxviii; 1800 level) exhibits a strong schistosity. The schistosity is defined by the parallel alignment of chlorite in the basalt and iron- silicate beds, and in the matrix of the heterolithic breccia. The schistosity is also defined by the elongation or flattening of amygdules, fragments, and quartz-carbonate stringers in the various rock types. Schistosity is also observed in the felsic and intermediate dykes defined by the alignment of chlorite. Refraction of the foliation in the dykes is common, where competency differs from the more ductile basalt. Figure 5 illustrates the pole distribution of dykes and shows that they are statistically oriented parallel to the schistosity and cleavage (Figure 4), at the mine.

The average measured orientation of this foliation is 309°/76°, to which all lithological contacts have parallel strike orientations. In most localities underground, the foliation is bedding-parallel, but dips more steeply than the envelope of bedding (Figure 6). This angular relationship confirms that the area is on the south limb of a major syncline.

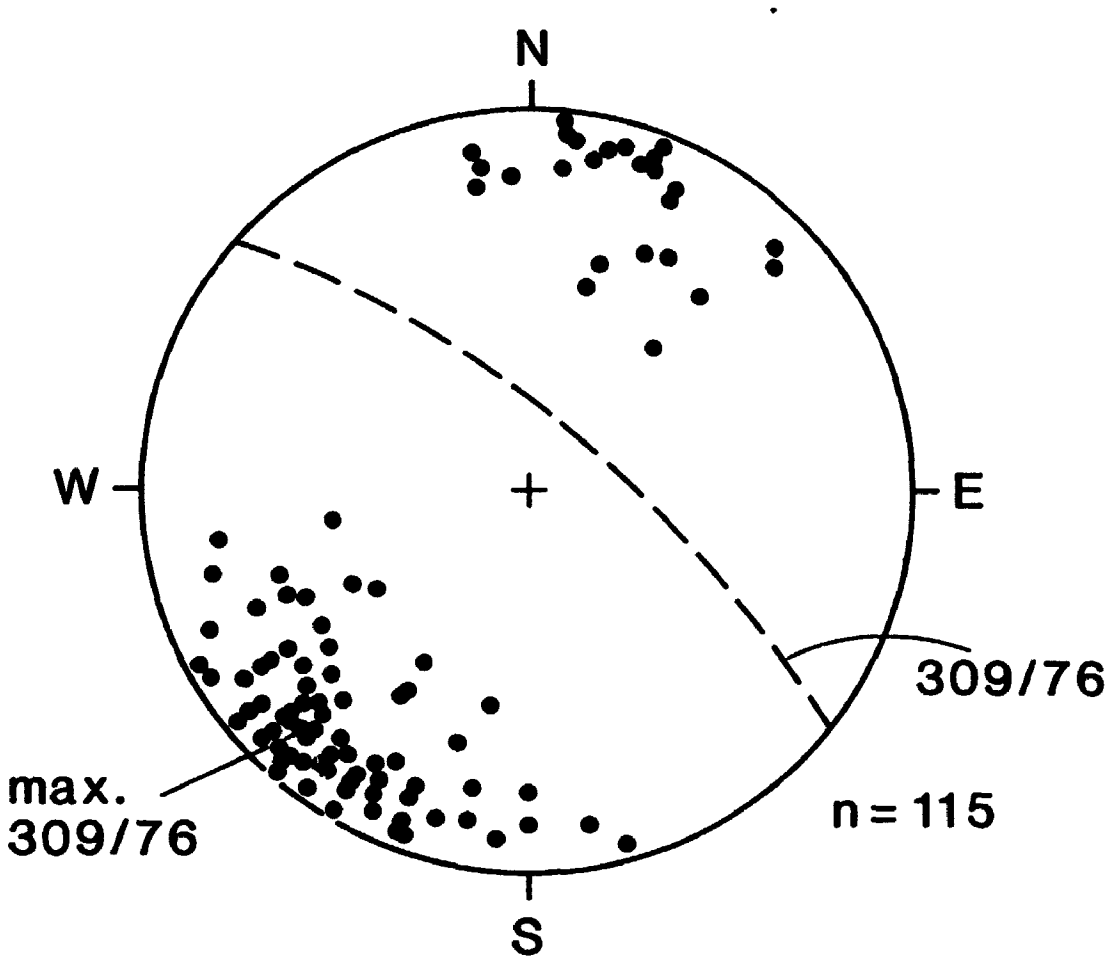

Figure 4: Equal-area stereographic projection of the poles to schistosity and cleavage. The dashed plane represents the mean orientation of foliation.

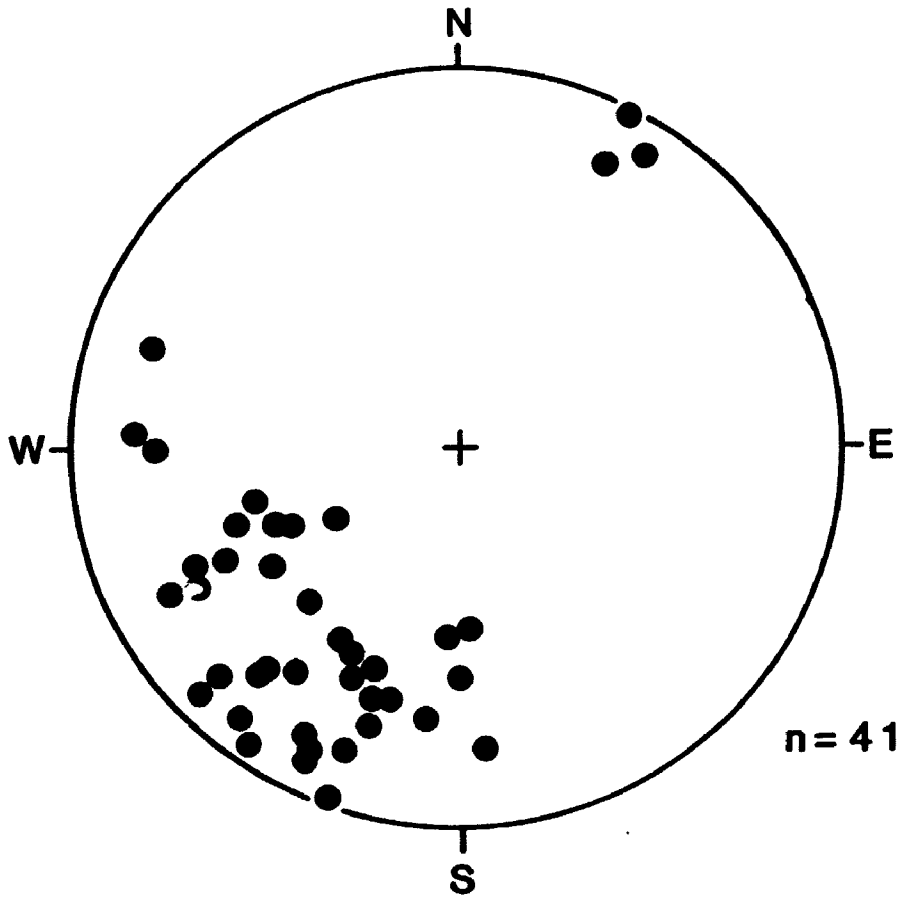

Figure 5: Equal-area stereographic projection of the poles to dykes.

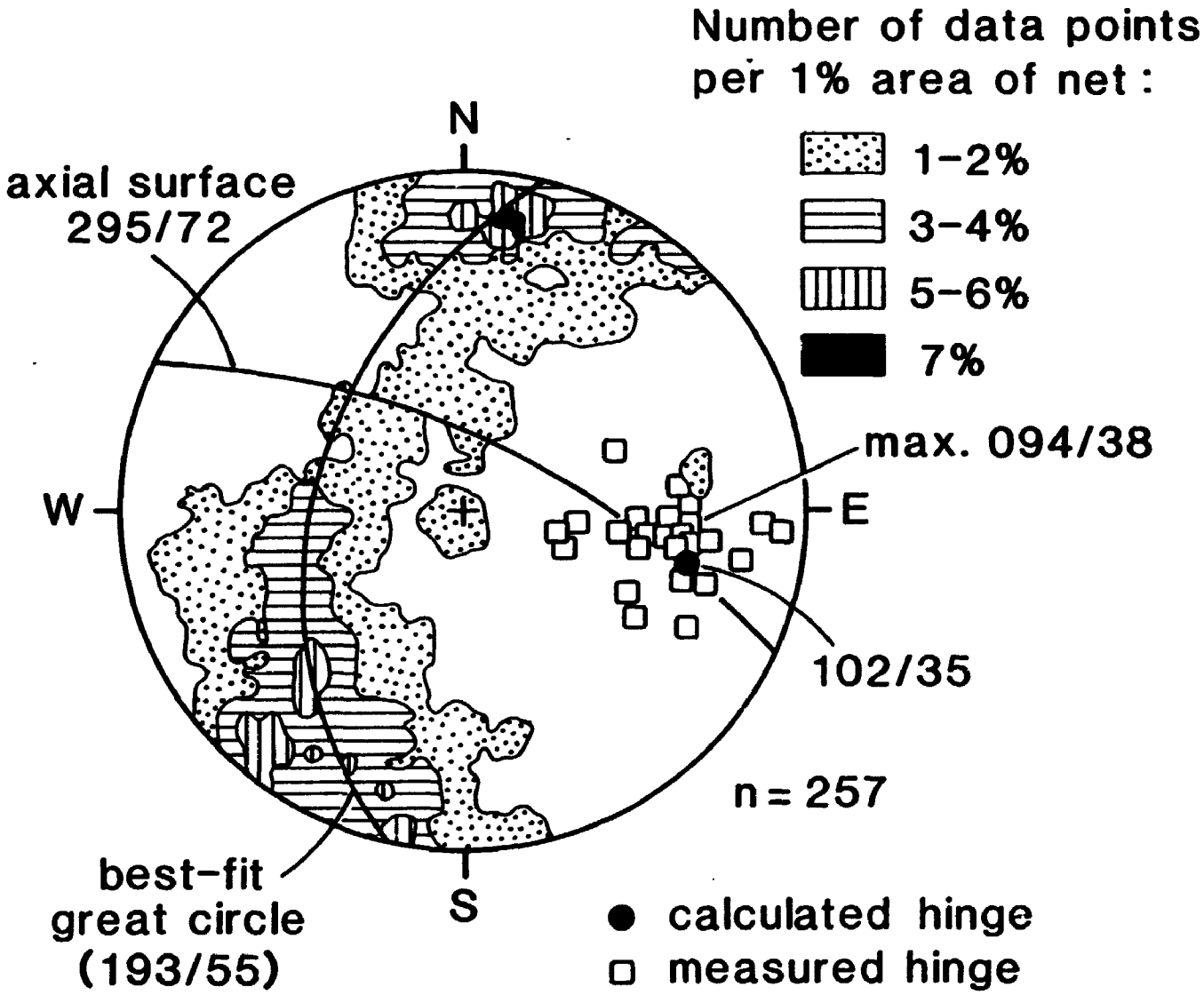

Figure 6: Equal-area stereographic projection of the poles to bedding and measured hinge lines. The data for bedding poles are contoured using the Schmidt method. The pole to the estimated best-fit great circle through the poles to bedding yields the calculated hinge assuming cylindrical folding.

Locally, the penetrative foliation is so intense that a tectonically induced layering of alternating chlorite- rich and quartz- carbonate- rich bands is observed in the basalt.

3.1.4 Lineations

Striations on bedding and schistosity - cleavage planes have been observed locally. The striations generally have a shallow plunge to the east (Figures 7 and 8).

3.1.5 Folds

3.1.5.1 Description of mesoscopic folds

Two scales of folding are apparent at the Lyon Lake mine. Mesoscopic isoclinal folds are developed in the banded iron formation (Plate 10), the massive sulphide body, and locally, intrusive rocks. The folds are isoclinal and asymmetric, with hinge lines trending east southeast, parallel to the strike of the strata.

Asymmetrically tight to isoclinally folded ore, iron formation, and sedimentary strata, with wavelengths of up to 10 meters are abundant on all levels of the mine (Plates 3 and 9). Many dykes are asymmetrically and tightly folded at the drift scale. Figure 6 illustrates the distribution of poles to bedding and the hinge lines measured on mesoscopic folds in the mine. The pole distribution defines a near - cylindrical fold characterized by a calculated hinge line trending 102° and plunging 35° east. This orientation is very close to the average measured hinge lines trending 094° and moderately plunging 38° east. The axial surface related to this fold is oriented at 295°/72° (Figure 6), which is subparallel to the regional foliation.

The types of folds observed in the banded iron formation closely resemble the geometry of Class 1B parallel, Class 1C, and Class 2 similar folds (Ramsay, 1967). Folds are of equal thickness in the hinge and the limbs (Class 1B), or the folds tend to be thickened in the hinge area, and thinned on the limbs (Class 1C, 2). The shape of the folds

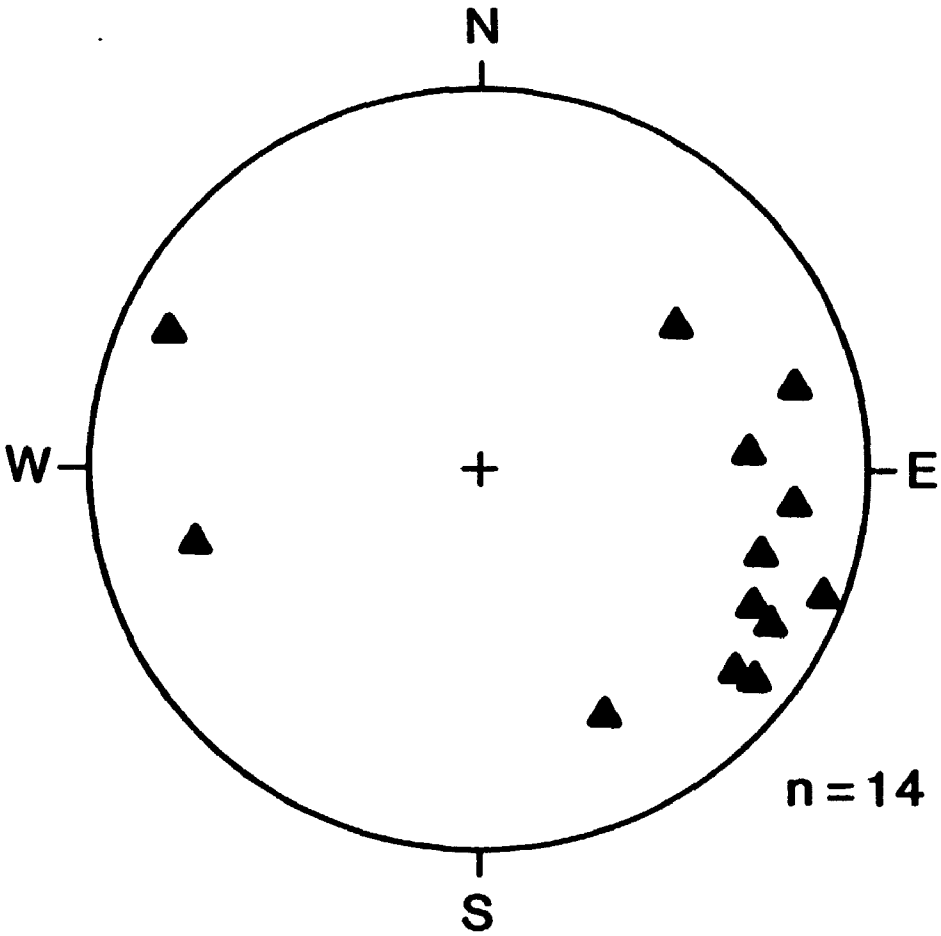

Figure 7: Equal-area stereographic projection of striations measured on bedding surfaces.

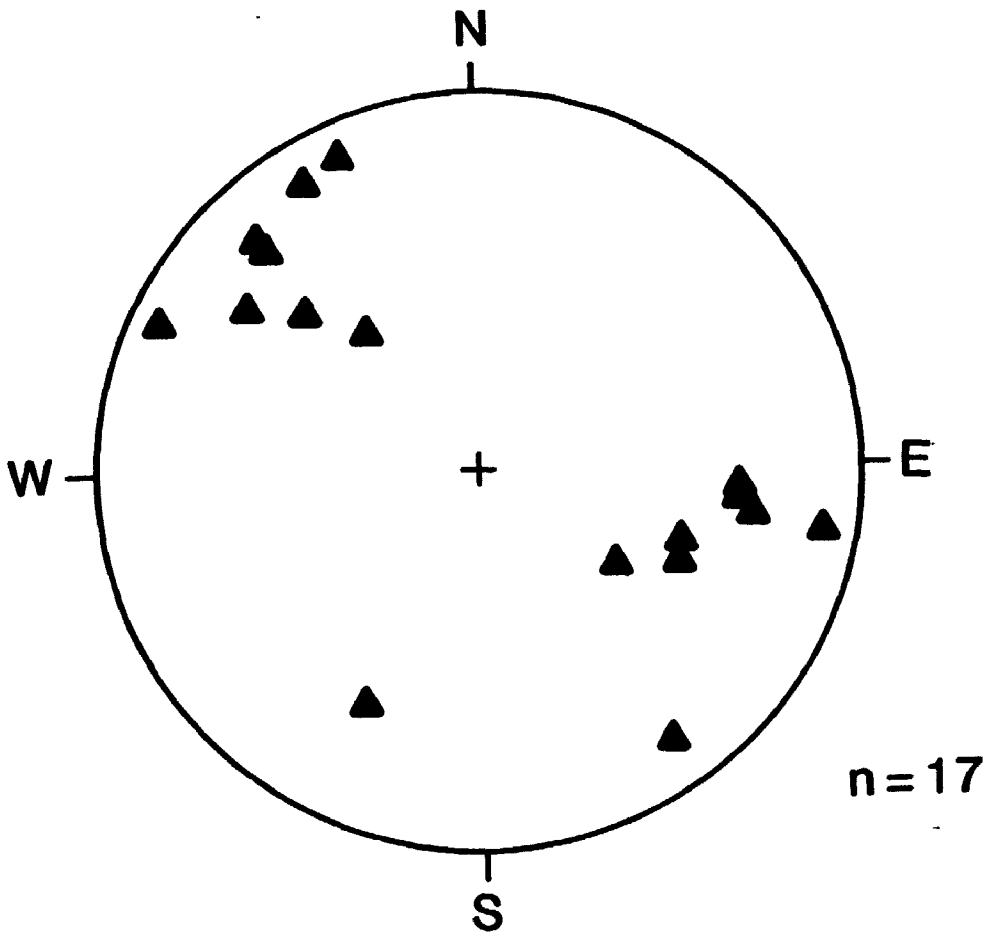

Figure 8: Equal-area stereographic projection of striations measured on schistosity and cleavage planes.

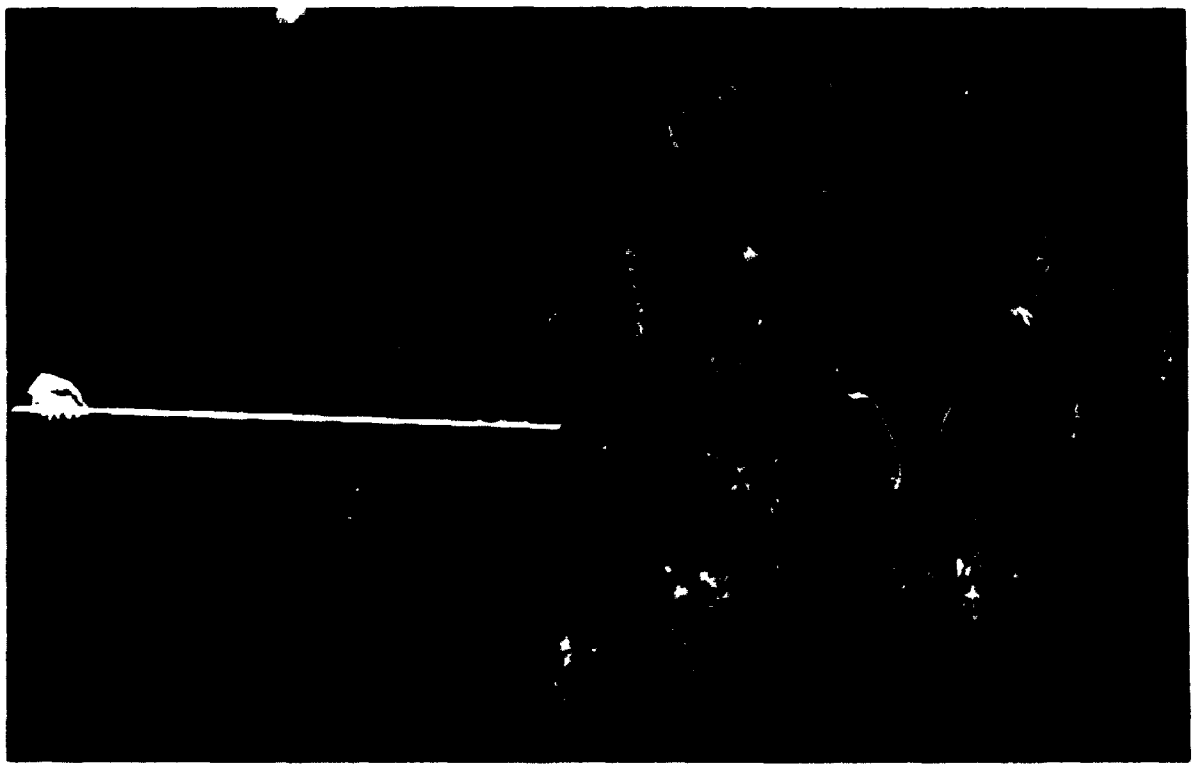

Plate 10: Mesoscopic isoclinal folds in the banded iron formation (600 level). Fold wavelengths are 30 to 40 centimeters. Cross section viewed to the west.

is repeated from one layer to the next. Class 1 folds are defined by Ramsay (1967) as having converging dip isogons, i.e. "the curvature of the surfaces of the layers are not equal, in that, the inner arc curvature exceeds that of the outer arc", and Class 1B, parallel folds, where "the dip isogons are perpendicular to layering in both the hinge area and the limbs". Similar folds tend to be thickened in the hinge zone and thinned on the limbs. Similar folds are defined by Ramsay (1967) as having parallel dip isogons, i.e. "the changes of curvature of the surfaces of the layers are the same throughout the fold, the variation in the dip of the surfaces is the same, and the geometrical form of the sides of the layers are identical".

The mechanism of folding in the iron formation and the sedimentary strata is flexural. This type of folding may reflect the influence of layering and the high ductility contrast between the layers, particularly in the iron formation where chert and/or carbonate layers alternate with chlorite- and/or magnetite- rich layers. Ramsay (1967) states that because the displacements in flexural folds are always parallel to the bedding or lamination surfaces there is no tendency for the orthogonal thickness across the layering to change; the folds therefore always show a parallel (Class 1B) form.

Class 1B folds or buckle folds are formed by a compressive stress acting along the length of the layers. In the rocks with strong competency contrasts, the more competent layers tend to buckle, while the less competent layers develop into similar folds. Folds that nucleate as class 1B folds develop into class 1C folds with an additional homogeneous strain (Ramsay, 1967). Many fold forms at the Lyon Lake Mine are intermediate between buckle and similar folds, suggesting that the similar folds in the iron formation may have been formed by a progressive flattening of what were initially buckle folds.

Many of the folds in the iron formation exhibit extreme attenuation of the limbs, to the point where discontinuities commonly developed parallel to the layering in the limbs of the folds. The development of discontinuities also occur parallel to the axial surfaces of

the folds. Slip along these surfaces is common and displaces fold hinges. Other folds have boudinaged limbs and fold closures of competent layers. Carbonate- and oxide- iron formation, and intrusive rocks typically exhibit slip along axial surfaces, and boudinaged fold closures and limbs, whereas silicate- iron formation typically exhibits attenuated limbs and dismembered fold closures.

3.1.5.2 Description of major fold

The dominant structural feature controlling ore distribution is a (major) open fold characterized by a shallow hinge line trending east-southeast (Figure 9, Koopman et al., 1989; Dube et al., 1989). Although the rocks generally strike east-west, face and dip 65°-75° north, detailed structural underground mapping and drill hole information indicate that all stratigraphic units are folded in the mine area, and this deformation extends southeasterly to the Sturgeon Lake Mine area. Figure 9 is a cross section through the central part of the mine at 12,200 E. The flexure is located at the 1480 level and has a wavelength of up to 100 meters, and an amplitude of up to 30 meters. Mesoscopic folds described above have a southward vergence on north- dipping limbs and a northward vergence on south dipping limbs of the larger asymmetric z - shaped fold. In contrast to the upper and lower levels of the mine, all the lithologic units within the flexure are thickened and subhorizontal, shallowly dipping northeast or southeast. The sphalerite content relative to the pyrite has increased in these flat zones (M. Patterson, Noranda Mines Ltd., pers. comm.). Detailed mapping on the 1480 level at section 12,200 E (Appendix A-xvii; 1480-1230 sill drift/1235 stope) illustrates the geometric configuration of the fold pattern, and the structural style of folding. This area represents the nose of the major fold, where the ore is shallowly dipping 15° to 20° east. Figure 10 shows the pole distribution of the contact between the ore and the surrounding rocks, measured on all levels of the mine. The pole distribution defines a great circle oriented at 210°/74° and

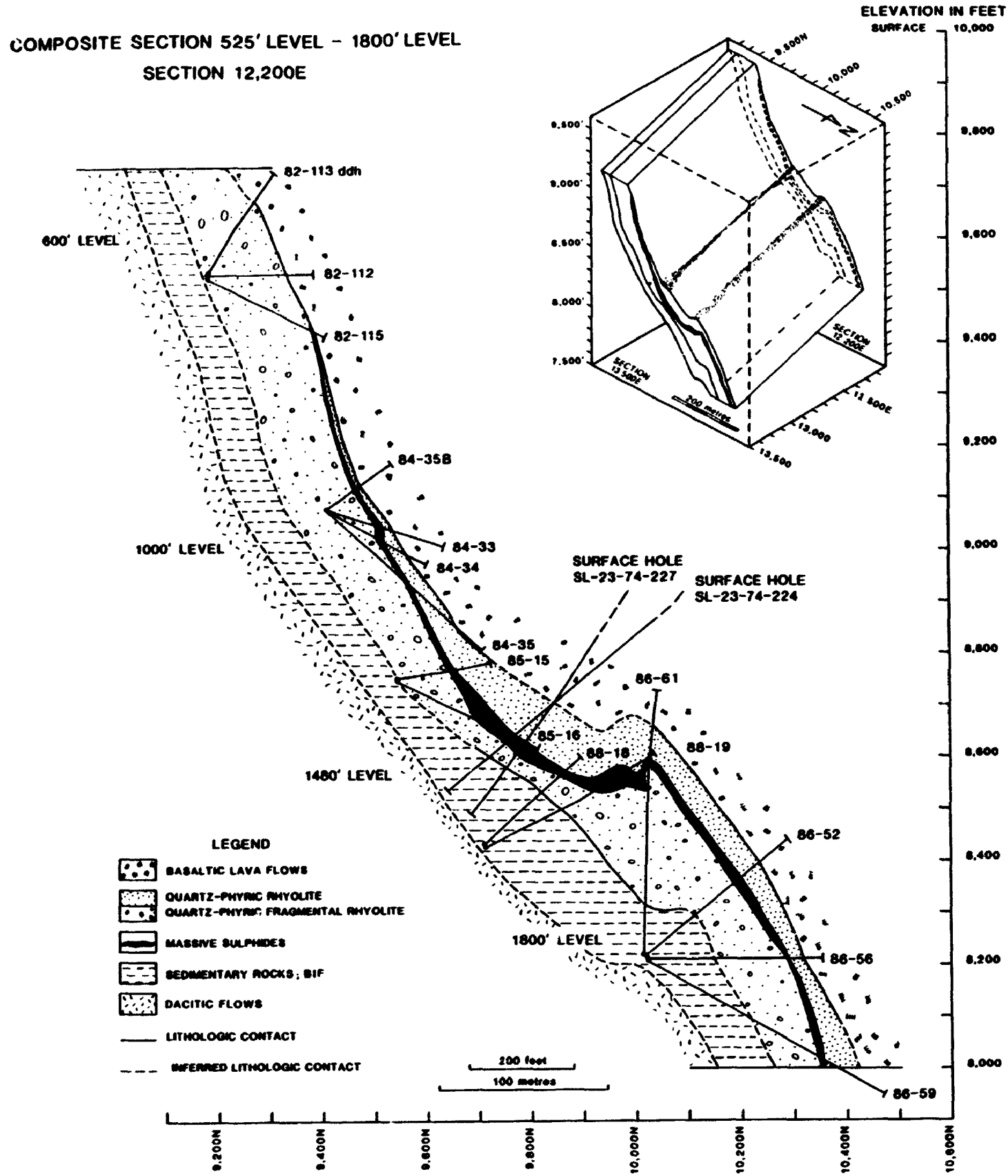

Figure 9: Composite cross section (12,200E) of the Sub Creek Zone. Inset: isometric projection of the deposit showing the plunge of the major flexure. North arrow indicates Mine North which is 40° east of true north. (Note: Section 13,500E is a projection of Section 12,200E).

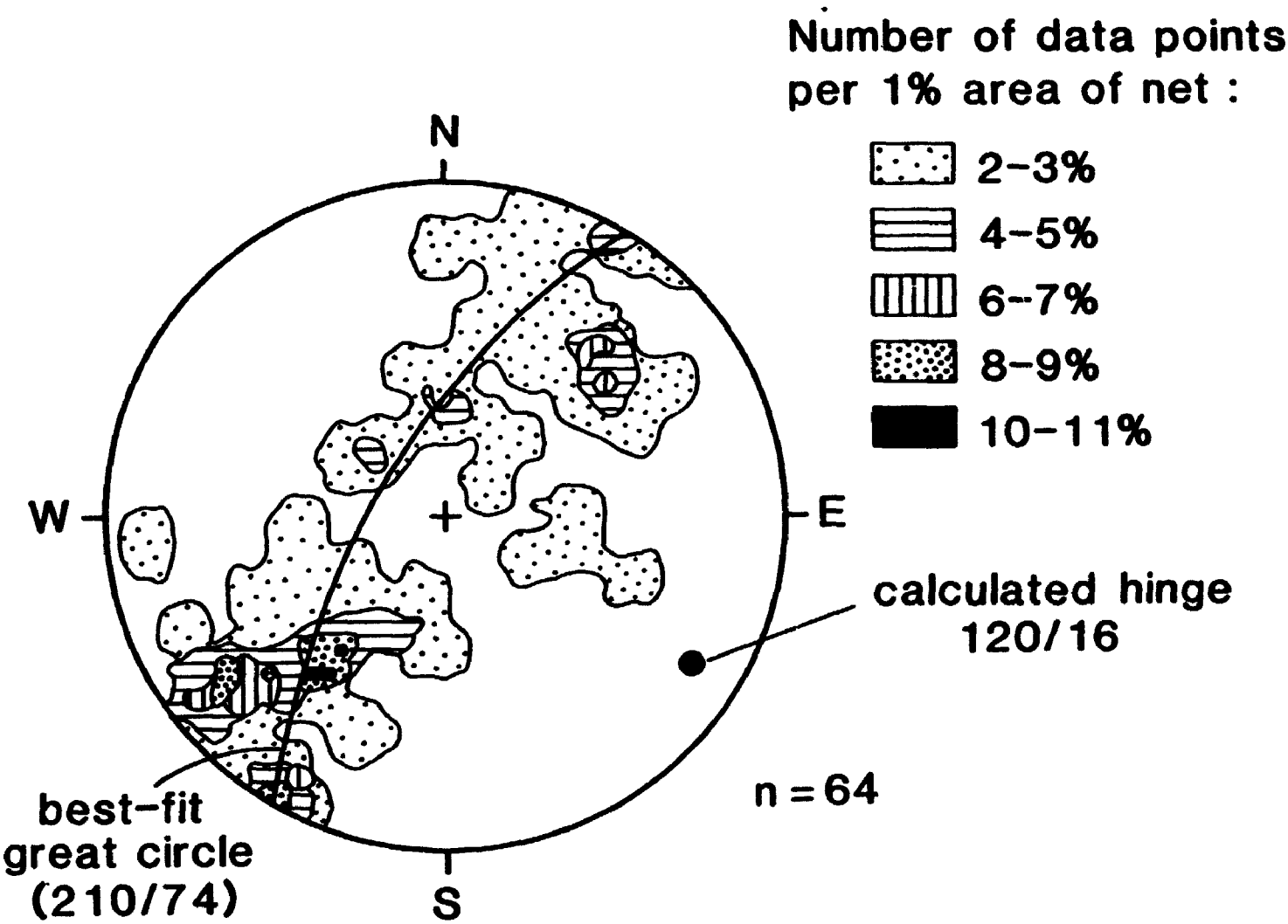

Figure 10: Equal-area stereographic projection of poles to the contact between the ore and enclosing rocks. The data are contoured using the Schmidt method and the best-fit great circle is located by visual estimate.

with a calculated hinge line oriented at 120°/16°, coincident with the plunge of the mesoscopic fold axes. The plunge of the hinge line of the major fold is shallower than that of the mesoscopic folding (35° - 40°) as defined in Figure 6.

The difference in plunge of these folds may be attributed to several possibilities. The plunge difference may be 1) a reflection of the primary orientation, or the more irregular orientation and thickness of the ore lenses in contrast to the surrounding strata; 2) a result of the major fold being the enclosing fold envelope of the tight to isoclinal, moderately plunging mesoscopic folds; or 3) attributed to the fact that the large fold is non-cylindrical.

The attitude of the S_1 foliation is 309°/76° (Figure 4), which is axial planar to the F_1 large and small folds (Figure 6). The foliation strikes parallel to, but dips more steeply than the envelope of bedding. This angular relationship confirms that the area is on the south limb of a major syncline.

Striations on bedding and foliation planes generally have a shallow plunge to the east (Figure 7 and 8), subparallel to the measured fold hinge. The striations may have resulted from oblique stretching of the fold.

Evidence of earlier (F_0) isoclinal and refolded folds has been observed on the limbs of larger folds in the iron formation on the 1000 level and 1580 ramp (Appendix A-x; 1000 level conveyor belt, Appendix A-xxi; 1480 - 1580 ramp). In the 1480 - 1580 ramp, subhorizontal axial planes of F_0 folds may be related to an earlier folding event; however, distribution of poles to bedding planes of these refolded folds is consistent with that of the whole mine (Figure 11). Therefore, fold axes of F_0 earlier folds and the F_1 major flexure are probably coaxial. Alternatively, because iron formation is easily deformed, these earlier folds may have a primary soft-sedimentary origin, later reoriented by the D_1 event that established the fold pattern of the mine area.

All types of dykes have been folded and show vergence relationships similar to

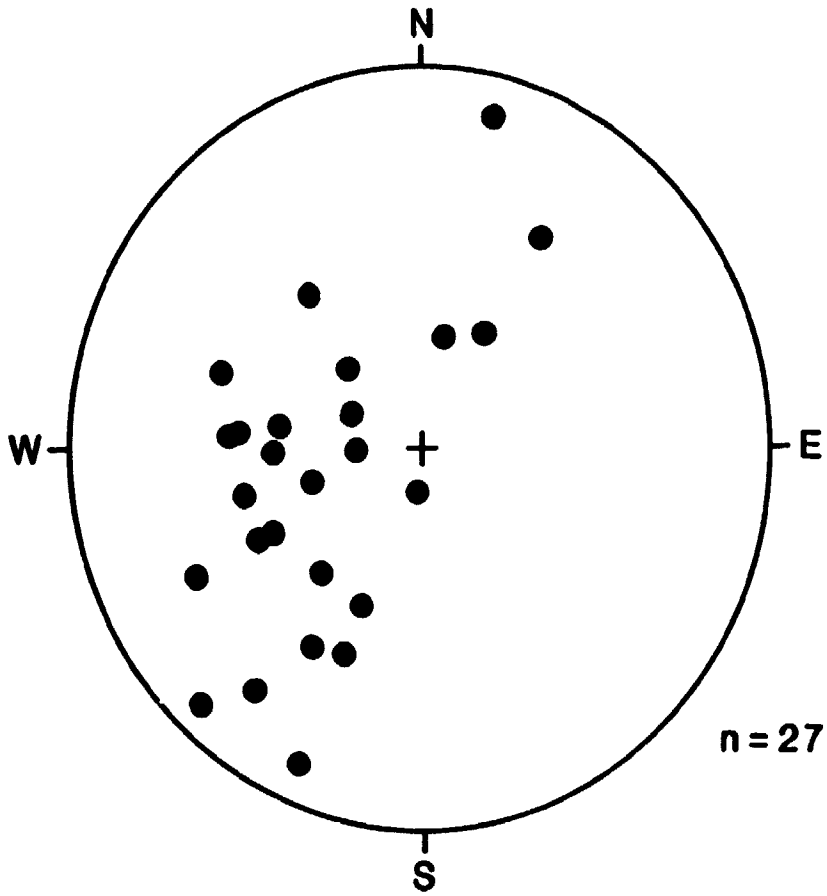

Figure 11: Equal-area stereographic projection of poles to bedding measured on bedding surfaces of early folds.

bedding planes; that is, the dykes show southward vergence of folds in north- dipping dykes and northward vergence of folds in south- dipping dykes. Figure 5 illustrates pole distribution of dykes and shows that they are statistically parallel to schistosity and cleavage (Figure 4). Folded felsic dykes are common in the footwall rhyolite (Plate 11, Appendix A-xiii; 1260 sub-level, Appendix A-x; 1000 conveyor belt, Appendix A-xix; 1480 manway drift, and Appendix A-xxvii; 1720 sub-level). Fold hinges measured on the dykes in the footwall rhyolite are oriented parallel to the hinge lines of the mesoscopic folds, and therefore have been affected by the same folding event. Locally, apparent non-folded dykes cross-cut highly deformed iron formation (Appendix A-viii; 600 ore pass, Appendix A-x; 1000 conveyor belt, and Appendix A-xxi; 1480 - 1580 ramp), whereas in other areas, dykes of similar composition may be strongly folded. The contrast in rheological properties between the iron formation and the dykes possibly affected the wavelength and amplitude of the folds resulting in disharmonic fold patterns. The original orientation of these dykes is a major constraint; any dyke having a primary orientation parallel to the axial surface will not be folded, but will have a discontinuity at its contact, whereas dykes contained within the fold axis and perpendicular to the axial surface will show maximum folding. Consequently, the various primary orientations of the dykes and the disharmonic type of folding could explain the apparent local nonfolded character of some dykes. Alternatively, a post F_2 generation of dykes cross- cuts the folded iron formation. Evidence of dykes intruding folded iron formation and separating fold hinges from limbs was not observed.

3.1.6 Veins

Subhorizontal quartz veins and en echelon patterns of quartz veins are common throughout the mine in zones of moderately to strongly foliated basalt, felsic rocks, and the heterolithic fragmental unit, and locally, as ladder veins in felsic dykes. The average

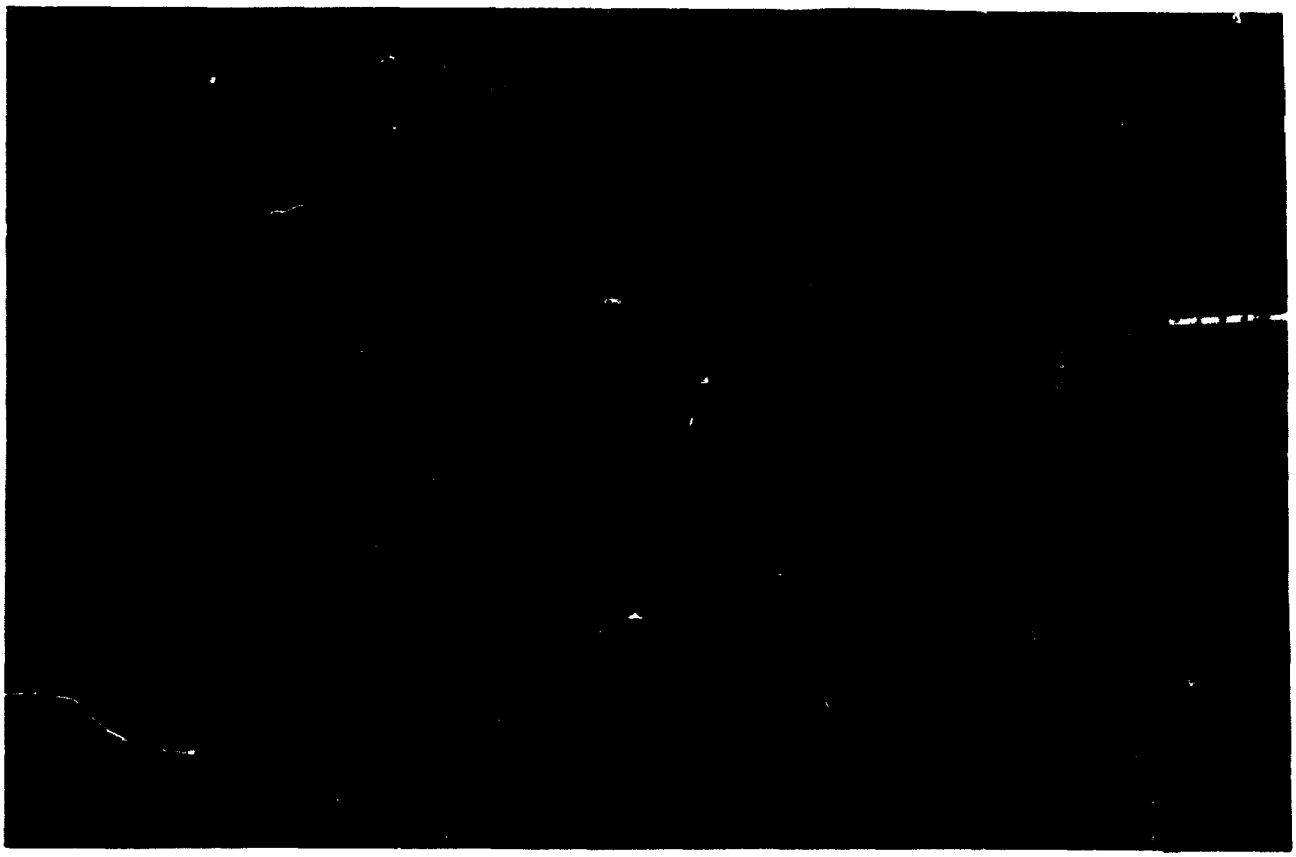

Plate 11: Folded felsic dyke in footwall rhyolite (100 level conveyor belt area). Cross section viewed to the east. Field of view is 1.5 meters.

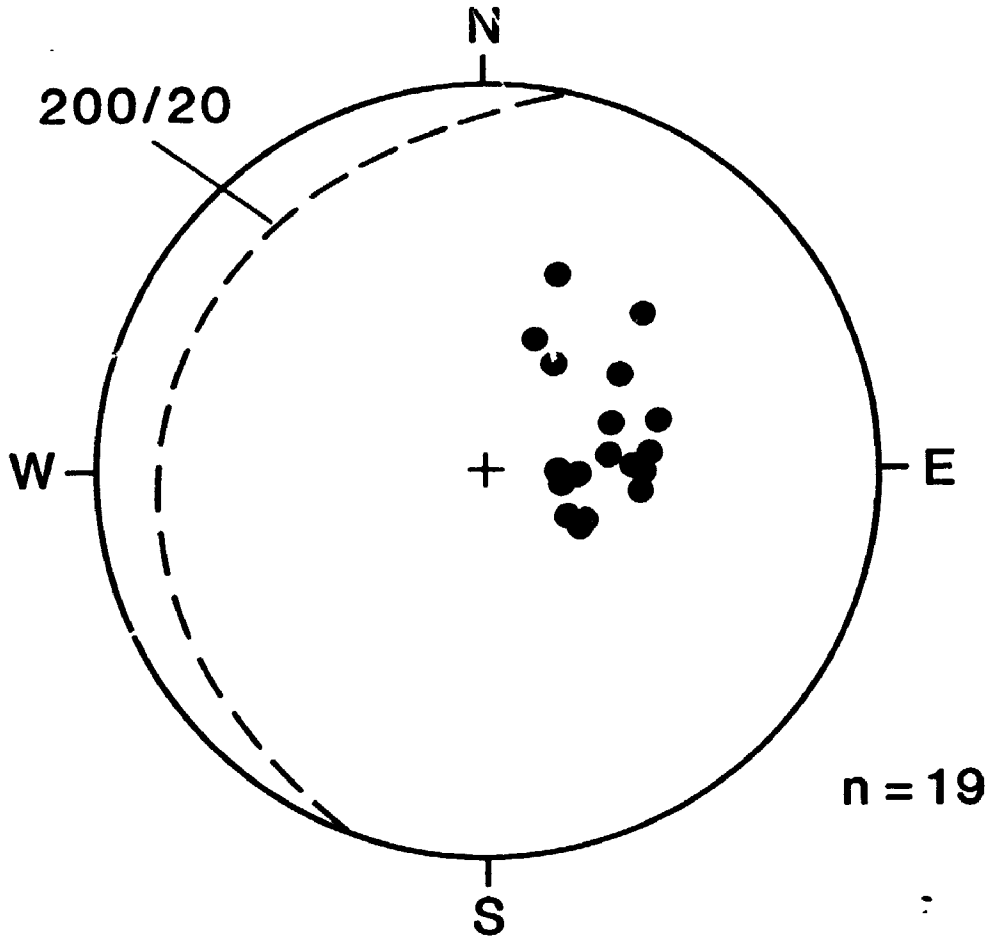

Figure 12: Equal-area stereographic projection of poles to sub- horizontal quartz veins. The dashed subhorizontal plane depicts the estimated mean orientation of the veins.

orientation of these veins is 200°/20° (Figure 12), which is statistically sub-perpendicular to the axial plane cleavage (Figure 4). This angular relationship suggests that these quartz veins are related to the folding event and indicate the direction of stretching of the mine strata.

3.1.7 Faults

3.1.7.1 Description of brittle faults

Faults are not a common structural feature in the mine sequence with the exception of the contact between the hanging wall basalt and the footwall rhyolite, which is discussed below. Faults are typically brittle and are characterized by a sharp planar discontinuity. Deformation of the enclosing wall rocks associated with faulting is not evident. These fault planes are filled with fault breccia cemented with quartz and carbonate. Locally, fault breccias contain up to 40 percent sulphides (Appendix A-xiii; 1260 sub-level, Appendix A-xx; 1480 cross cut north of manway). Faults dip steeply to the north (306°/78°) and strike subparallel to the overall strike of the strata (Figure 3.9). Slickenlines on different fault planes plunge east, subparallel to the fold axes, and according to the steps, the latest movement was oblique and dextral (Figure 3.10). Displacement along these faults (Appendix A-xvii; 1480 - 1230 sill drift/1235 stope, Appendix A-xxi; 1480 - 1580 ramp) is very small, in the order of 1 to 5 m. These faults are discordant to bedding, and locally overprint F_1 folds (Appendix A-xxi; 1480 - 1580 level ramp). The faults may represent shear surfaces, syn- to post F_1 folding and may be related to stretching parallel to the fold axis.

3.1.7.2 Description of breccia faults

Irregular, discontinuous lenticular zones of quartz-breccia occur at or near the contact between the ore and its footwall or hanging wall rocks. They occur subparallel to

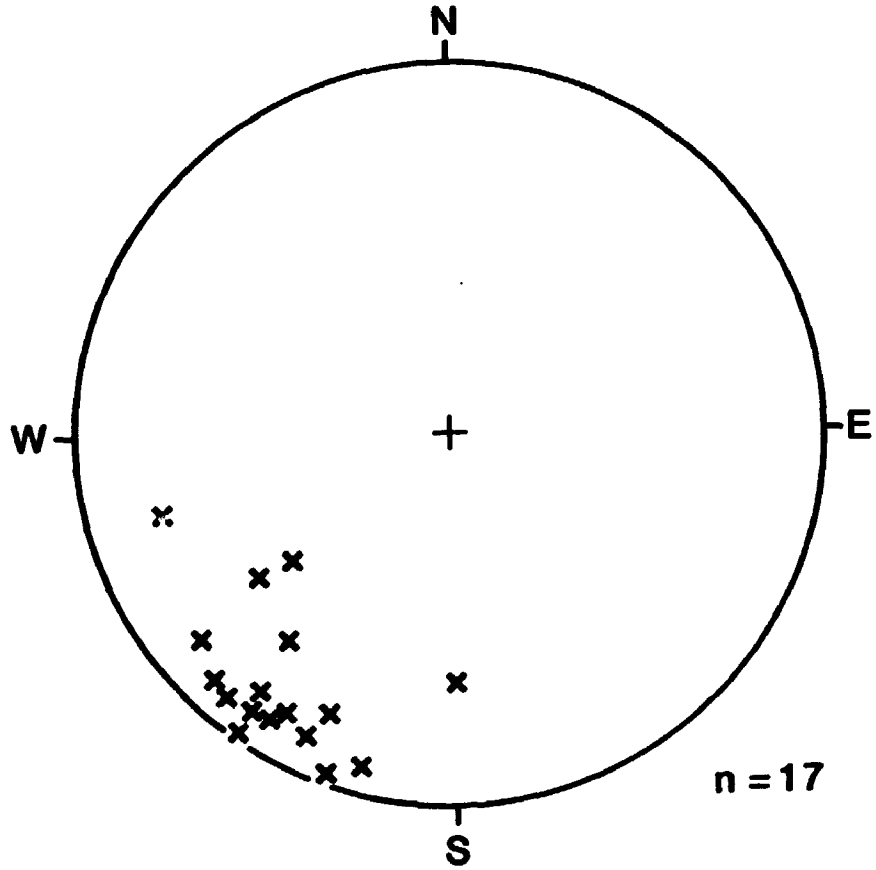

Figure 13: Equal-area stereographic projection of poles to faults.

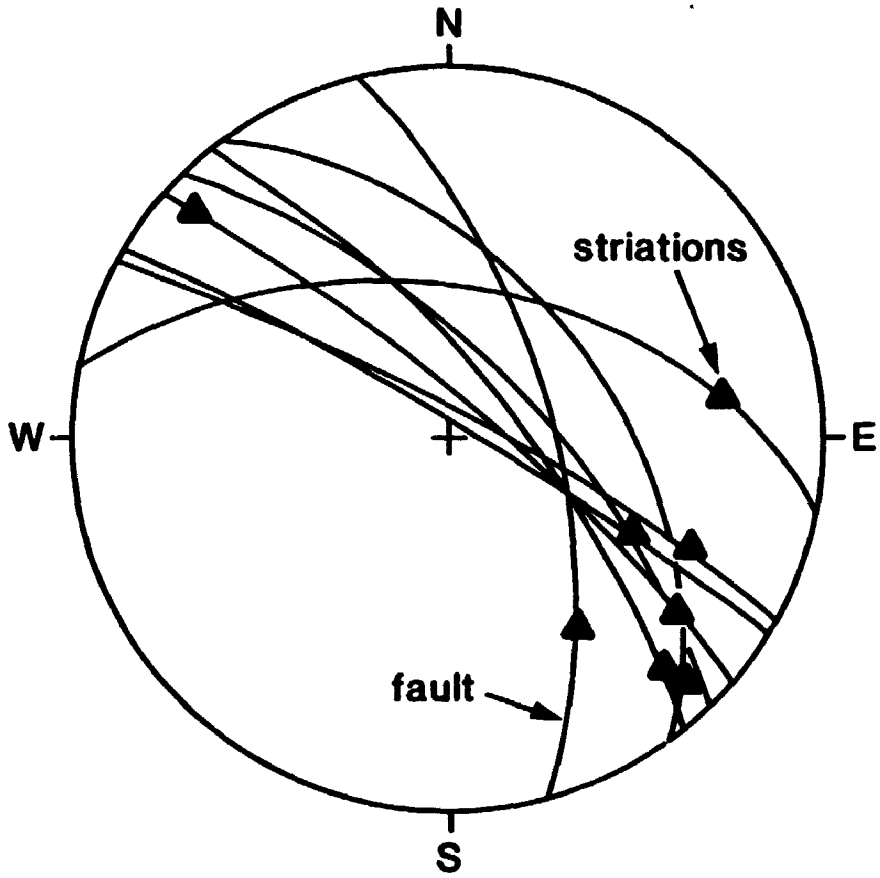

Figure 14: Equal-area stereographic projection of striations measured on faults.

these contacts. Quartz-breccias typically contain iron- carbonate and sulphides. Up to 40% sulphides consisting of pyrite, sphalerite, chalcopyrite, and galena occur in fractures within quartz. These lenticular zones of quartz-breccia are particularly abundant on the 1480 level (Appendix A-xvii; 1480 - 1230 sill drift/1235 stope), where the ore is located in the nose of the major fold (Plate 12). These zones of quartz-breccia are concordant with the strata, and are not associated with a significant displacement of the ore. Slickenlines observed in one of these quartz- breccia zones are oriented $127^{o}/15^{o}$, indicating that the latest movement was slightly oblique, similar to movement on the brittle faults. On the 1260 sub-level, a zone of breccia in the hanging wall to the ore is associated with ductile shear related to the hanging wall fault. The shear zone contains steeply dipping, en echelon tension gashes (Appendix A-xiii; 1260 sublevel).

The spatial association of these breccias with the ore, primarily in the hinge area of the major fold, suggests that these breccia units originated in dilatant zones formed during folding.

3.2 Hanging wall - Footwall Contact

3.2.0 Introduction

The orientation of the contact between the hanging wall basalt and footwall quartz-phyric rhyolite varies from easterly, north of the Mattabi Mine area, to northwest in the Lyon Lake and Sturgeon Lake Mines area, to more easterly again, west of the Lyon Lake Mine area (Figure 2). This contact truncates several graphitic argillite units in the footwall (Franklin, 1977), and is close to the ore horizon at Lyon Lake. Franklin et al. (1977) suggested that the deposits may have formed on a local intravolcanic unconformity surface. Mumin (1988), described the area as having been an oceanic rift environment, with mineralization localized along the rift axis at varying stratigraphic intervals. Morton et al. (1990) suggested that the hanging wall basaltic rocks are the final episode of caldera

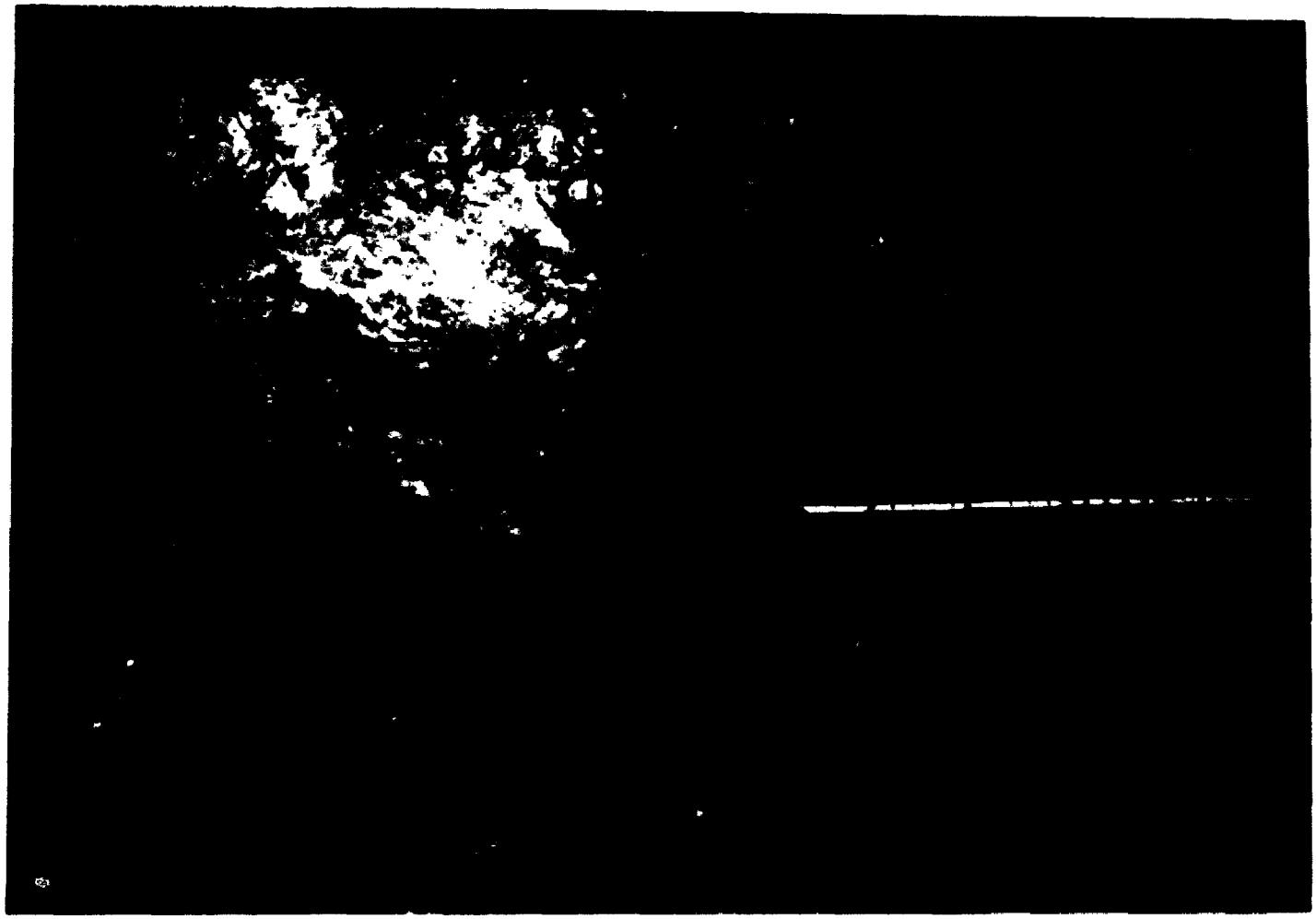

Plate 12: Quartz breccia fault. These breccia zones are typically subhorizontal, and most abundant in contact with the massive sulphide in the fold hinges of the ore zone (1480 level 1230 stope). Field of view is 1.5 meters.

fill, that represent the end of caldera pyroclastic activity and the start of a new, more quiescent cycle of volcanism. Detailed underground mapping, core logging, and surface mapping for this study indicate that this contact is characterized by a high strain zone which truncates several units. This unit was emplaced in its present position by faulting, (pre-F1 folding), and is stratigraphically unrelated to the underlying caldera sequence which hosts the massive sulphide deposits in the camp.

3.2.1 Description of the hanging wall fault

Detailed mapping on the 200-, 525-, 600-, 1000- levels, and surface outcrops reveal that the contact is a high strain zone. This high strain zone has been observed to be 7 m, 16 m, 30 m, (Appendix A-i; 200 #1 crosscut, Appendix A-iii; 525 - 1116 crosscut, Appendix A-xii; 1000 exploration drift, respectively), and more than 100 m wide on the 600 level (Appendix A-vi; 600 level garage). Most of the deformation seems to be evident in the more ductile hanging wall basalt. Within this high strain zone, basalt typically exhibits a strong schistosity, and the more competent rhyolite exhibits a well- defined cleavage. Deformation in the basalt is characterized by an intense, pervasive schistosity defined by the parallel alignment of chlorite, elongate amygdules with aspect ratios up to 5:1, and 1- to 10- mm- thick quartz- carbonate stringers. The long axes of the amygdules and quartz-carbonate stringers are oriented parallel to the schistosity. Locally, deformation in the basalt is so intense that a metamorphic layering of siliceous and chloritic bands occurs (Appendix A-i; 200 level #1 crosscut and Appendix A-vii; 600 level fuel station). Deformation related to this fault in the rhyolite attains a thickness of 15 m (Appendix A-vii; 600 level fuel station), and is characterized by a well- defined, evenly-spaced fracture cleavage. Rhyolite is typically intensely fractured, siliceous, with sericite or chlorite developed along cleavage planes. Locally (Appendix A-ii; 525-1116 crosscut extension), the hanging wall basalt is in contact with the massive sulphides. At this

locality, the massive sulphides are reoriented and 'smeared' along the contact between the hanging wall basalt and the underlying felsic dyke. Massive sulphides locally exhibit mullion structures. In other areas, the contact is marked by a sheared felsic dyke; elsewhere, the dyke is not sheared, discordant and intrudes the basalt (Appendix A-v; 525 fuel bay and training drift and Appendix A-vii; 600 level fuel station). Several 15- to 20-cm- thick subhorizontal quartz veins 6.5- to 8- m in length occur in this high strain contact zone.

This fault strikes 286°, and has a variable north dip from subvertical farthest into the hanging wall, to 50° to 70° near the contact with the footwall (Figure 15). The orientation of this fault is subparallel to bedding and the regional foliation. Mineral lineations or striations are not present on the schistosity planes in the basalt, but striations measured on cleavage surfaces in the rhyolite are oriented subparallel to hinge lines of mesoscopic F_1 folds. Striations and mineral lineations measured on foliation and bedding planes, striations on cleavage planes related to the hanging wall fault, and the orientation of hinge lines, are all subparallel to each other, suggesting that the folding and faulting are related.

Figure 16 is a contour map of this contact, constructed by the compilation of all drill hole intersections and observed underground contacts. The contours illustrate the variable dip of this contact, indicating a steep zone - flat zone - steep zone in a northward direction reflecting the limb - nose - limb of the major fold. The contours also show that the dip of this contact is shallowing in an eastward direction reflecting the plunge effect of the major open fold. The Sturgeon Lake Mine to the east possibly represents the surface expression of the fold nose of a similar major fold.

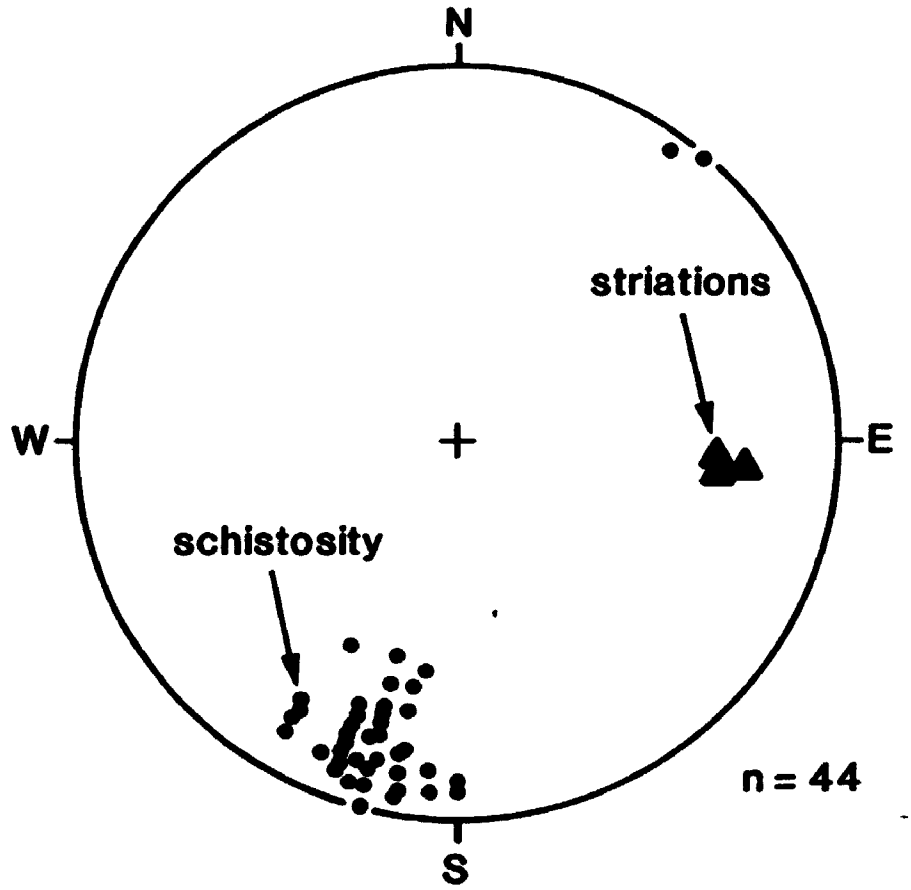

Figure 15: Equal-area stereographic projection of poles to schistosity and cleavage related to the hanging wall fault.

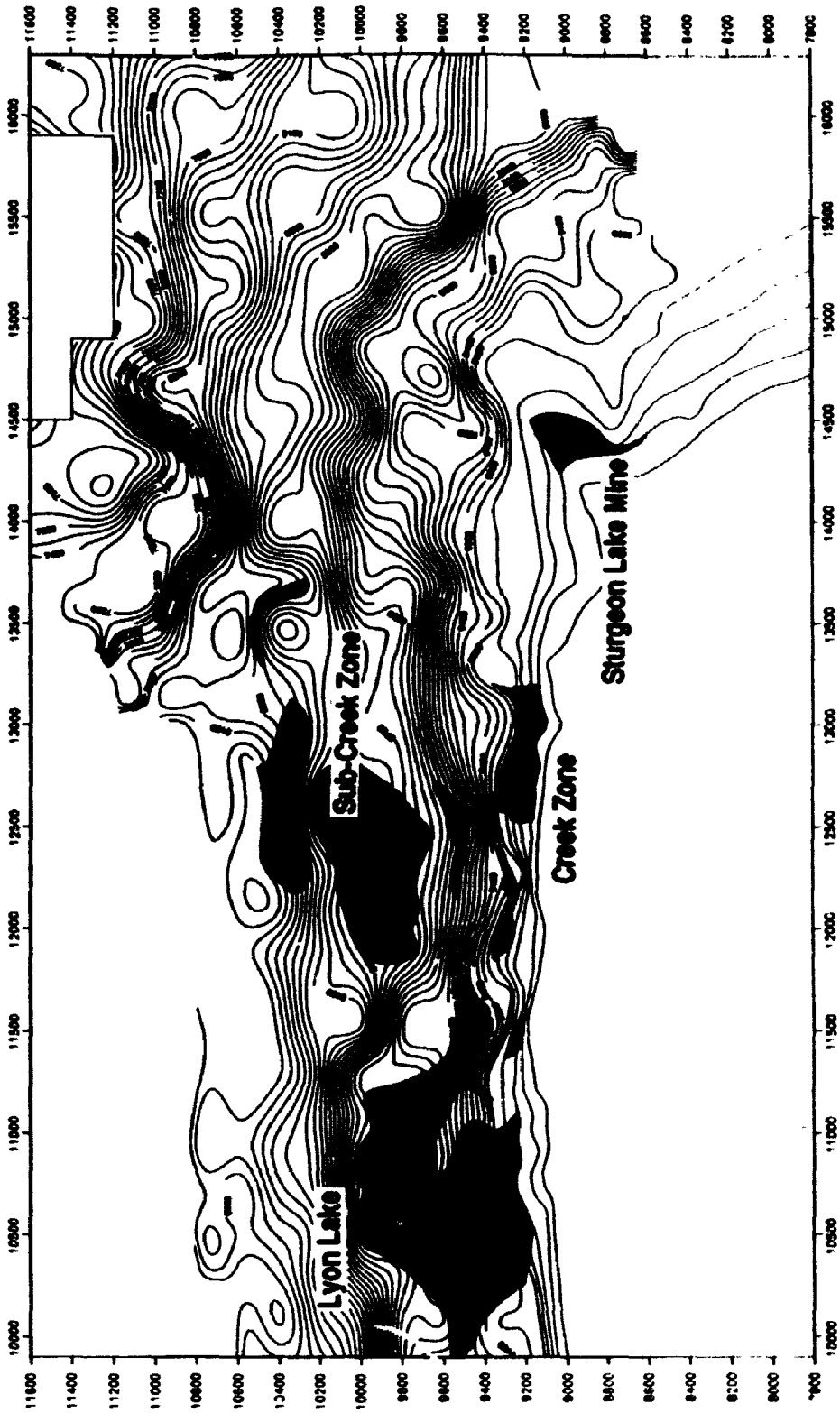

Figure 16: Structural contour map of the contact of the hanging wall basalt and footwall felsic volcanic rocks illustrating that the dip of this contact is shallowing in an eastward direction reflecting the plunge effect of the major open fold. Shaded areas are plan view of stoped ore zones. This contact is projected vertically to plan view (Koopman et al., 1990).

3.2.2 Timing of the hanging wall fault

Figure 9 shows that this contact is folded, and the asymmetry of the fold suggests relative motion in section is reverse. The subhorizontal quartz veins, and also the orientation of stretched amygdules and quartz-carbonate stringers in the sheared basalt also suggest vertical extension. However, the true sense of motion, and the amount of displacement associated with this fault is not constrained. Although this fault truncates all the lithologies, the intersection of the fault with bedding is at a low angle, and much of the movement along this fault is probably layer- parallel slip. The fault is folded, therefore pre- dating the folding event, and the asymmetry of the fold is a geometric consequence only, giving no information about the fault sense. Striations observed on cleavage planes in this fault zone are subparallel to the hinge lines of mesoscopic folds. As a result of folding, it is likely that this fault was reactivated, and the striations observed on cleavage planes in this fault zone are a reflection of tectonic extension related to the folding.

3.3 INTERPRETATION OF STRUCTURAL OBSERVATIONS

3.3.1 Interpretation of folds

Folds are recognized as being the most common and obvious manifestation of ductile deformation of rocks. They are generally found in areas which have been subjected to regional deformation and metamorphism.

Fold types at Lyon Lake include Class 1B, 1C, and 2, as well as intermediate and extreme varieties of the classes (Ramsay, 1967). Folds with parallel form are formed by a compressive stress acting along the length of the layers. In multilayered rocks where ductility and competency ratios are high, the competent layers usually show a nearly perfect parallel fold form, whereas the incompetent layers become preferentially thickened in the hinge zones and thinned in the fold limbs. Ramsay (1967) states that folds which nucleate as class 1B parallel folds develop into intermediate and class 1C folds with

subsequent homogeneous strain. Progressive flattening of the folds occurs by continued compression acting across the layers, or shearing on closely spaced planes oblique to the layer being folded.

The type of folds at Lyon Lake indicates ductile behaviour of the rocks during deformation. The formation of folds, and the consistent east- southeast orientation of fold axes at Lyon Lake is consistent with an approximately north - south maximum compression of the South Sturgeon Lake Belt.

3.3.2 Interpretation of hanging wall fault

The contact between the hanging wall basalt and the footwall rhyolite is interpreted to be a major fault zone. Matching points on either side of the fault plane were not observed. However, dislocative and strain indicators were documented to determine that the nature of this contact is a fault. The features observed include the truncation of all the lithological units observed at Lyon Lake by the hanging wall basalt, and foliation planes within the contact zone contain striations. The fault has a low angle (nearly bedding parallel) and may be a thrust fault, although the sense of motion is not known.

Striations measured on foliation planes in the rhyolite in this fault zone, and the orientation of hinge lines of mesoscopic folds are all subparallel, suggesting the folding and faulting are related. However, this faulted contact is folded, which suggests faulting pre- dates folding. Therefore, at least two possible hypotheses arise to explain the tectonic development of this structural relationship:

Hypothesis 1: If faulting and folding are related; that is, drag along the low- angle fault generated the folding pattern:

In thrust fault regimes (foreland fold and thrust belts), where a thrust sheet moved over a ramp it became folded, forming the characteristic flat - ramp - flat structure (Ramsay, 1967, Suppe, 1985). Folding may be intimately associated with the thrust faulting with the faults cutting folded beds at high angles, and penetrative foliations may have been developed.

Ramsay (1967) stated that the progressive development of hanging wall fold structures is complex, and there are several fold- forming possibilities which depend on the location of the hanging wall with respect to the footwall. Suppe (1985) developed a model in which the footwall is completely inert and remains undeformed. Folds are formed only in the hanging wall as it is forced over the underlying staircase - like steps.

This model (Suppe, 1985) suggests that no folds occur in the footwall block, yet folds are common in the footwall block in the mine. Ramsay (1967) stated that folds can be developed in the footwall by the formation of new thrust planes with ramp - flat geometry in the foot- wall, by the forward propagation of the lower thrust along the incompetent layer. At Lyon Lake, all the lithological units are folded (hanging wall and footwall). A lower thrust in the footwall rocks may exist at the highly strained contact between the quartz- feldspar- phyric dacite and the overlying sedimentary strata. This contact is a tectonized zone characterized by a strong foliation subparallel to the hanging wall fault. The footwall sedimentary rocks, particularly the iron formation and graphitic horizons, represent incompetent units relative to the more massive quartz- feldspar- phyric dacite, and act as glide planes for propagation of a thrust along the incompetent layer. Another possibility for developing folds in both the hanging wall and footwall would be to initiate the thrust after a certain amount of layer buckling of the competent and incompetent strata had taken place.

At Lyon Lake, if the shearing and folding are coeval, i.e., thrust faulting produced the folds, the reverse motion in section, coupled with the oblique orientation of observed

linear structures suggests oblique dextral movement of the contact fault. Local layer-parallel shearing should have developed on the limbs of the fold. Linear features associated with faulting and folding would be developed perpendicular to, or at a high angle to the fold axis, in contrast to the observed parallel fold axis and lineations. Faults should have developed at a high angle to folded beds, and axial planar foliations should have developed at a high angle to the propagating thrust surface. Linear features observed at Lyon Lake are subhorizontal, and the axial planar cleavage is parallel to the fault zone, which is geometrically inconsistent with coeval faulting and folding.

Hypothesis 2: The shear zone is folded by a later deformation event:

Figure 9 illustrates the case where the fault contact is folded. Linear features measured at Lyon Lake on cleavage planes related to this fault are parallel to fold axes, which suggest that this fault has been affected by the folding event. There is no evidence of a preserved cleavage developed during faulting. A cleavage developed during faulting would probably be crenulated by the later cleavage developed during folding. A crenulation cleavage was not observed at Lyon Lake; however, continued deformation could result in complete rotation of an early cleavage into a later cleavage which developed during fold formation. Striations on cleavage planes, which are oriented east-southeast in this fault zone are consistent with the tectonic shortening and extension related to folding.

The author favours the second possibility to explain the observed faulting and folding relationship. As a final point, if the fault was folded by later deformation, then the asymmetry of the fold is a geometric consequence only, and gives no information about the sense of motion on the fault.

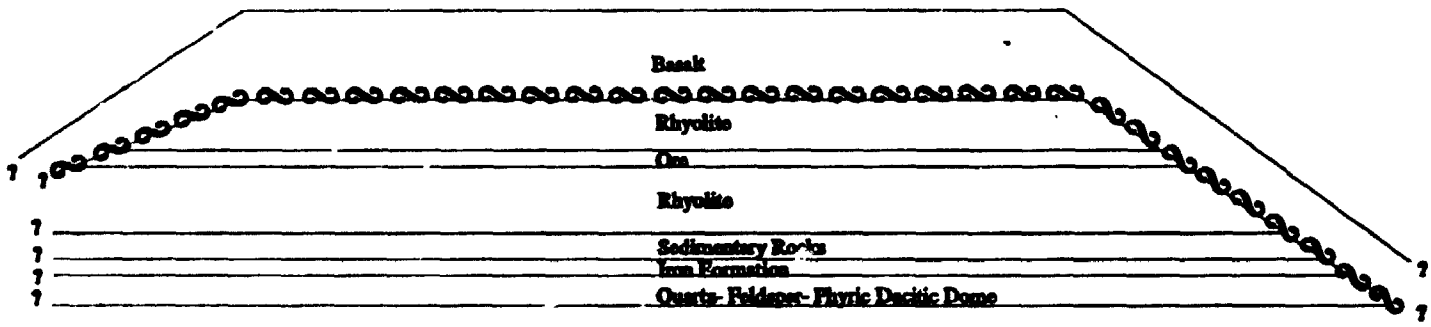

Figure 17: Early Deformation (pre- folding) - thrust faulting of the hanging wall basalt.

3.4 Summary

1. An early deformation is postulated which emplaced the footwall strata and the hanging wall basalt into its pre- folding stratigraphic position by faulting (Figure 17). This fault truncated the underlying strata at a low angle, which suggests thrust faulting as a likely faulting mechanism. Planar and linear features associated with thrust faulting were either not developed, or are not preserved in the rocks. The primary disposition and direction of transport of the hanging wall basalt and its overlying lithological units are not constrained.

2. Isoclinal refolded folds are superposed by mesoscopic folds of a subsequent deformation event. These early folds may be a manifestation of the deformation event associated with faulting, however they are not localized in the zone of faulting.

3. A later deformation event developed asymmetric folding of the strata, forming mesoscopic isoclinal folds on the limbs of this asymmetric fold. Also, during this deformation, a pervasive regional foliation developed axial planar to mesoscopic folds, and the asymmetric fold.

4. Quartz- carbonate veins perpendicular to the axial planar cleavage were formed during, and possibly after the folding event.

5. Discontinuous lenticular quartz-breccia- filled faults developed in dilatant zones that formed during the folding event, as evident by their localization in the hinge zone of the asymmetric major fold.

6. Brittle faults are not affected by folding, and are discordant to the bedding. The latest movement associated with these late faults is oblique and dextral, parallel to the fold axes.

3.5 STRUCTURAL MODEL

The contact between the hanging wall basalt and the footwall rhyolite is a major fault zone in the Sturgeon Lake belt. This fault has been affected by folding and therefore, developed prior to the formation of folds (during regional deformation). The primary disposition of the hanging wall basalt is not constrained; however, it is postulated that the onset of regional north - south compression resulted in the development of thrust faults, and that the hanging wall basalt was emplaced in its present stratigraphic position by thrust faulting.

The north- facing and north- dipping sequence of volcanic and sedimentary rocks in the South Sturgeon Lake belt forms the south limb of a regional east trending syncline (Trowell, 1983). During regional deformation, north - south compressive stress resulted in initial thrust faulting, and caused the sequence to be folded along east - west hinges (Figure 18), accompanied by the development of a regional foliation that is axial planar to the fold. The asymmetrically- folded strata at the Lyon Lake Mine occurs in a parasitic minor fold on the south limb of this regional syncline. The Z - asymmetry of this fold is consistent with the development of parasitic folds on the south limb of an east plunging syncline. Smaller scale mesoscopic folds occur on the limbs of the asymmetric mine- scale fold. The orientation of all fold axes in the mine sequence is consistent with the regional north - south compression, and east - west tectonic extension.

Continued deformation resulted in brittle failure, with the development of late faults with oblique and dextral motion.

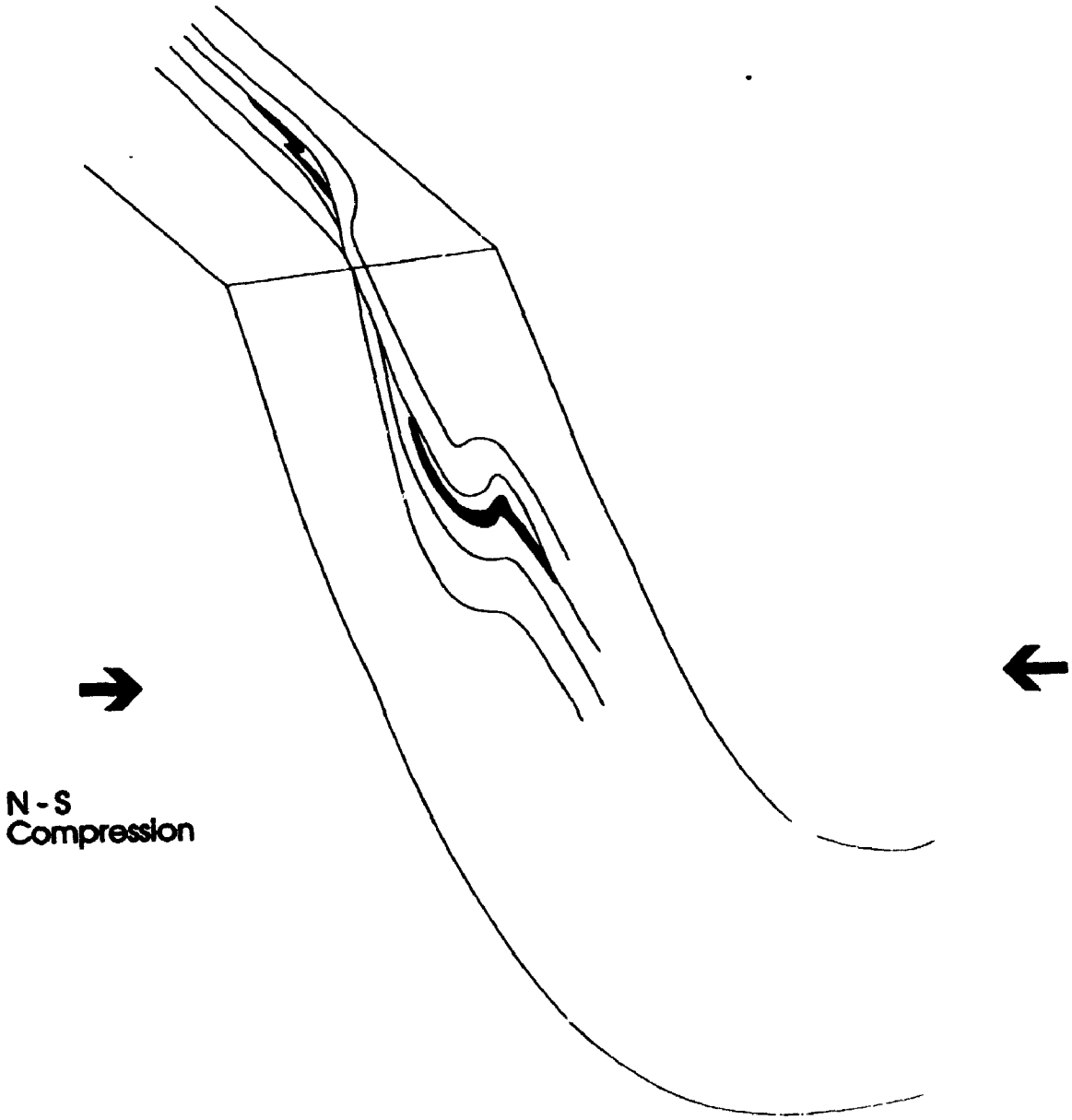

Figure 18: Regional Deformation resulting in fold formation. The Lyon Lake stratigraphic sequence forms a parasitic fold on the limb of the larger regional syncline.

CHAPTER 4

SUMMARY AND DISCUSSION

4.0 Summary of the lithological units and structural components

The Lyon Lake massive sulphide deposit occurs at the top of the Sturgeon Lake Caldera complex in a sequence of volcanic and sedimentary strata. It has many of the typical geological attributes of volcanogenic massive sulphide deposits, but lacks a conspicuous alteration zone. The deposit has an unusual stratigraphic relationship, with iron formation in the footwall.

The succession of the footwall and hanging wall rocks of the Lyon Lake massive sulphide deposit is dominated by volcanic and sedimentary rocks of variable composition and style of deposition. Underground mapping allowed the identification of five distinct units based on stratigraphic position and composition, as well as the identification and documentation of the occurrence of a banded iron formation in the footwall sedimentary sequence, footwall to the massive sulphide horizon.

The lowermost rocks encountered in the footwall are massive quartz- feldspar-phyric felsic flows. This unit was observed in one locality within the mine; the most easterly developed cross cut on the deepest level (2600). The uppermost part of this unit is flow top breccia of the lava dome. These flows are thought to be correlative with feldspar- bearing lava flows and domes which occur close to the caldera margins and are believed to represent the last felsic eruptive products associated with caldera formation (Morton et al. 1990).

A sequence of sedimentary rocks overly these lava flows, separated from the latter by a mafic dyke. The lowermost sedimentary unit is banded iron formation. The contact between banded iron formation and the lava flows is a highly strained zone indicated by a strong schistosity, disrupted beds of iron formation, and emplacement of a mafic dyke.

The orientation of this strained contact is subparallel to sedimentary strata, and also, the fault contact between the hanging wall basalt and the footwall rhyolite. The disrupted beds of iron formation at the contact may be the result of syn- depositional slumping during deposition on an irregular domal surface; however, the highly strained zone and emplaced dyke along this contact could also suggest that this contact is a fault contact. Iron formation lies immediately above this dome and the competency contrast between iron formation and the dome could have served as a slip plane. This contact was observed in only one locality, and other evidence for this contact being a fault is inconclusive. Further studies using drill core that intersects this contact are required to more conclusively determine the nature of this contact. If this lower strained zone is a fault, then the stratigraphic assemblage hosting the Lyon Lake deposit is a wedge bounded by two low angle faults. The strata hosting the deposit could be unrelated to adjacent lithologies.

Bedding is best developed in the metasedimentary rocks. The sequence of metasedimentary rocks consists of banded iron formation, graphitic pelite, greywacke, quartz- rich pelite, and massive pyrrhotite - pyrite lenses. The banded iron formation forms the basal unit of the sedimentary sequence. The iron formation is conformably overlain by interbedded greywacke, medium- grained quartzose pelite, and graphitic pelite. Locally, massive pyrrhotite - pyrite lenses are intercalated with graphitic pelite. The banded iron formation is laterally extensive, and is a useful stratigraphic marker horizon. As the thickest portion of the iron formation and its associated sedimentary strata seem to correspond to the thickest ore section, it is possible that the hydrothermal vents for the both the iron formation and the massive sulphides were coincident structures. Alternatively, both ore and iron formation could have been thickened by subsequent folding. The presence and thickness of Fe - oxide banded iron formation beneath the ore horizon reflects an extensive low temperature hydrothermal event sustained over a period

of time prior to the hydrothermal event related to sulphide deposition. The iron formation and sedimentary rocks represent a hiatus in volcanic activity, and low temperature hydrothermal activity and sedimentation in basins during a period of volcanic quiescence.

If the contact between the sedimentary sequence and the underlying felsic flows is conformable, then the sedimentary rocks are probably dome- derived. In contrast, if this contact is a fault contact, then the source of the sedimentary detritus is indeterminate.

The heterolithic fragmental unit locally forms the host, footwall, and hanging wall rocks to the ore. The heterogeneous nature of fragments and matrix, and the restricted distribution of this unit represents deposition of a local debris flow deposit or talus deposit. The presence of chloritoid and almandine garnet porphyroblasts in the matrix define this as the most hydrothermally altered unit within the mine stratigraphy. This unit could therefore represent a fault- related permeable rock which acted as a conduit for localization of the ore- related hydrothermal fluids.

Felsic pyroclastic flows conformably overly the sequence of sedimentary rocks. The contact is irregular and gradational from quartzose and graphitic pelite to quartz-phyric tuff and lapilli tuff. Locally, this contact is more distinguishable where it is defined by an intermediate dyke. Unlike the contact lower in the stratigraphic sequence (described above) between the quartz- feldspar- phyric flows and the sedimentary rocks, and also, the stratigraphically higher contact between the hanging wall basalt and the footwall rhyolite, this contact shows no evidence of disruption due to tectonism. Structural fabric along this contact is consistent with the fabric in the sedimentary rocks and overlying rhyolite flows. These felsic flows consist of coarse monolithic volcanic breccia at the base to interbedded felsic ash and lapilli tuff towards the top. Contacts between pyroclastic flows are very diffuse, but may be distinguished by the presence of block- sized fragments overlying aphyric ash flows. The uppermost quartz- phyric flow typically forms the host to the ore (except where heterolithic breccia occurs which forms

the zone of fluid localization). These pyroclastic flows probably represent the final eruptive products during caldera formation. The host blue quartz- phyric ash flows formed the seafloor on which massive sulphides were deposited.

The contact between the massive sulphides, footwall rhyolite, and the hanging wall basalt is a fault contact. The contact is characterized by a strong schistosity in the basalt and a cleavage in the footwall rhyolite. The hanging wall basalt truncates the massive sulphide horizon, footwall rhyolite, and the sedimentary sequence towards the east.

Intermediate dykes are the most abundant type of dyke. These dykes occur at the contacts between all lithological units, and cross cut the footwall strata. Fine- grained mafic dykes are most abundant in the deeper parts of the mine and are most commonly observed along the upper ore contact, and within the ore lenses, as irregular deformed intrusive bodies. These mafic dykes were probably feeders to mafic flows, but not likely feeders to the hanging wall basalt, as this mafic unit is not conformable with the underlying stratigraphy, hence unrelated. Mafic and intermediate dykes which cross- cut the footwall strata are commonly folded which indicates that the emplacement of these intrusive rocks post- dates deposition of the footwall rocks, and pre- dates the folding event. Locally, both intermediate and mafic dykes occur at the fault contact between the hanging wall basalt and footwall rhyolite. As highly sheared contacts and lithological contacts may be zones of weakness, the dykes may have been emplaced prior to, or coeval with faulting and subsequently folded.

Prior to initiation of this project, the geologists at the Lyon Lake Mine had recognized an eastward- plunging linear orientation of orebodies in the mine The purpose of this study was to assess the degree to which this linear feature is a result of the primary disposition of the ore as opposed to subsequent deformation. The present study demonstrates that all the stratigraphic units, massive sulphide lenses, and dykes are folded. The dominant structural feature affecting ore distribution is an (major) open fold

characterized by a shallow hinge line trending east - southeast. The present study also shows that axes of minor folds throughout the mine have a relatively consistent orientation subparallel to the long axes of orebodies and therefore folding offers a likely explanation for the linear nature of the ore lenses and for the occurrence of flat zones. Structural thickening of the ore in these flat zones as a result of folding, and also, higher grade ore (pers. comm. Mike Patterson, Noranda Mines Ltd.) in these zones indicates from an economic point of view, the importance of identifying and locating these flat zones as exploration targets for increased ore reserves.

Other minor structures such as extensional veins, schistosity and striated planar surfaces are also consistent with tectonic shortening and extension of the ore bodies and their enclosing rocks. En echelon distribution of ore lenses within the productive horizon, may reflect the deformation of several primary sites of ore deposition but could also be attributable to an en echelon folding pattern (Campbell, 1955). Further study is required to test the viability of the second hypothesis.

Other faults, though common throughout the mine, are late brittle faults and appear to have no control on ore distribution. The maximum observed vertical displacement of ore by these late faults is 50 centimeters (Figure A-39; Appendix A-xvii).

The high strain zone located at the contact between the footwall rhyolite and hanging wall basalt was also observed to the southeast, in the Sturgeon Lake Mine area. The striations observed in the high strain zone are subparallel to the hinge of the folds and suggest that the high strain zone may have formed during folding, or caused intense deformation and possible folding of the strata. The entire footwall stratigraphic succession in the eastern part of the area is truncated by the hanging wall basalt at a low angle, it is probable that this high strain zone corresponds to a major "thrust" fault zone.

All the lithological units are folded, and the faulted contact between hanging wall basalt and the footwall rhyolite is also folded. The fact that this hanging wall fault is

folded indicates that low angle faulting occurred prior to regional tilting and folding of the strata.

4.1 Summary of the history and evolution of the Lyon Lake Deposit

1. Development of felsic lava dome. These domes occur close to the caldera margins and are believed to represent the last felsic eruptive products associated with caldera formation (Morton et al., 1990).

2. The uncertainty of the nature of the contact between the dome and the overlying sediments results in two possible interpretations for the vol nological history and evolution of the Lyon Lake Deposit.

   2a. Low angle fault at the contact between the dome and overlying sedimentary rocks represents a tectonic break in stratigraphy. The sequence of sedimentary rocks and overlying felsic volcanic footwall rocks would be unrelated to the underlying lithological units and caldera development and fill of the Sturgeon Lake Caldera Complex.

   2b. If the contact between the dome and the overlying sedimentary rocks is conformable, dome- derived sediments and low temperature hydrothermal activity resulted in the development of iron formation and sedimentation in basins along the flanks of the dome.

3. Pyroclastic eruption of volcanic breccia, lapilli tuff and ash flows, and local synvolcanic talus / debris flow deposits.

4. Eruption of blue quartz- crystal rich tuff and renewed high temperature hydrothermal activity resulting in the formation of the Lyon Lake Zn, Cu, Ag, Pb Deposit.

5. Time Break - Fault Contact

6. Truncation of the massive sulphide deposit and footwall stratigraphy by the hanging wall basalt, followed by parallel tilting and folding of all the lithological units during regional north - south compression. This resulted in the development of the regional foliation (east - west striking, north- dipping, and north- facing), and the reorientation of the massive sulphide body from a horizontal body into a steeply dipping, gently folded, east- southeast, shallow plunging linear feature.

CHAPTER 5

CONCLUSIONS

1. The dominant structural feature affecting ore distribution is an open fold characterized by a shallow hinge line trending east- southeast.

2. Axes of minor folds throughout the mine have a relatively consistent orientation subparallel to the long axes of the ore bodies, and therefore, folding offers a likely explanation for the linear nature of the ore lenses and for the occurrence of "flat zones".

3. Other structures such as schistosity and striated planar surfaces are also consistent with tectonic shortening and extension of the ore bodies and their enclosing rocks.

4. The entire stratigraphic succession in the eastern part of the area is truncated by the hanging wall basalt. The contact between the hanging wall basalt and the footwall rhyolite corresponds to a major fault zone which predates folding.

5. The deformation has resulted in the re-orientation of portions of ore bodies into thicker and higher grade flat zones.

6. Brittle faults, though common throughout the mine, appear to have limited control on ore distribution. No significant lithological or ore displacement related to the faults was observed. However, faulting is consistent with the observed style of folding.

2 of/de 2

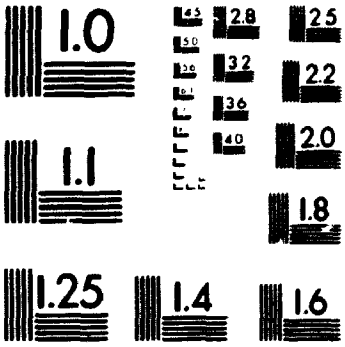

MICROCOPY RESOLUTION TEST CHART
NATIONAL BUREAU OF STANDARDS
STANDARD REFERENCE MATERIAL 1010a
(ANSI and ISO TEST CHART No 2)

7. The geometry of small scale detailed structures observed at the Lyon Lake Mine, reflect the geometry of the larger regional scale.

8. As a result of this study, recognition of flat ore and the plunge of folds is critical in locating the extension of flat zones at depth.

9. The down- plunge extensions of the flat zones of folds at Lyon Lake, are prime exploration targets.

REFERENCES

Bell, A.M. (1981): Vergence: an evaluation; Journal of Structural Geology, v. 3, p. 197-202.

Campbell, J.D. (1955): En echelon folding; Economic Geology, v. 53, p. 448-472.

Davis, D.W., Krogh, T.E., Hinzer, J., and Nakamura, E. (1985): Zircon dating of poly[illegible] volcanism at Sturgeon Lake and implications for base metal mineralization; Economic Geology, v. 80, p. 1942-1952.

Dube, B., Koopman, E.R., Franklin, J.M., Poulsen, K.H., and Patterson, M.R. (1989): Preliminary study of the stratigraphic and structural controls of the Lyon Lake massive sulphide deposit, Wabigoon Subprovince, northwestern Ontario; in Current Research, Part C, Geological Survey of Canada, Paper 89-1C, p. 275-284.

Franklin, J.M., Gibb, W., Poulsen, K.H., and Severin, P. (1977): Archean metallogeny and stratigraphy of the South Sturgeon Lake area; Mattabi field trip: 23rd annual meeting of the Institute of Lake Superior Geology, 75 p.

Friske, P.W.B. (1983): Wall-rock alteration and ore genesis at the Lyon Lake deposits, Northwestern Ontario; University of New Brunswick, Ph.D. thesis.

Goodwin, A.M., Ambrose, J.W., Ayres, L.K., Clifford, P.M., Currie, K.L., Ermanovics, I.M., Fahrig, W.F., Gibb, R.A., Hall, D.H., James, M.J.S., Irvine, T.N.., McLaren, A.S.,

Norris, A.W., Pettijohn, J.F., and Ridler, R.H. (1972): The Superior province; Geological Association of Canada, Special Paper 11, p. 527-624.

Gross, G.A. (1965): Geology of iron deposits in Canada. 1. General geology and evaluation of iron deposits; Geological Survey of Canada Economic Geology Report 22, 181 p.

Groves, D.A. (1984): Stratigraphy and alteration of the footwall volcanic rocks beneath the Archean Mattabi massive sulfide deposit, Sturgeon Lake, Ontario; M.Sc. thesis, University of Minnesota, Duluth, MN.

Harvey, J.D. and Hinzer, J.B. (1981): Geology of the Lyon Lake ore deposits, Noranda Mines Limited, Sturgeon Lake area, Ontario; Canadian Institute of Mining and Metallurgy Bulletin, v. 74, no. 833, p. 77-84.

Hinzer, J.B. (1977): Geology, geochemistry, of the Lyon Lake and Creek ore zones, Sturgeon Lake; Unpublished M.Sc. thesis, University of Western Ontario, London, Ontario.

Koopman, E.R., Dube, B., Franklin, J.M., Poulsen, K.H., and Patterson, M.R. (1989): Deformation of the Lyon Lake massive sulphide deposit, Wabigoon Subprovince, northwestern Ontario, Canada; Institute on Lake Superior Geology, Program with Abstracts, May 1989, Duluth, Minnesota.

Koopman, E.R., Franklin, J.M., and Poulsen, K.H. (1990): Structural and stratigraphic controls of ore distribution of the Lyon Lake Zn-Cu-Pb-Ag deposit, Sturgeon Lake,

Ontario; Geological Survey of Canada Minerals Colloquium, Program with Abstracts, Abstract, January 1990.

Koopman, E.R., Franklin, J.M., and Poulsen, K.H., (1989): Structural and stratigraphic controls of ore distribution in the Lyon Lake Zn-Cu-Pb-Ag deposit, Sturgeon Lake, northwestern Ontario; Ontario Mines and Minerals Symposium Mineral Development and Lands Branch Mineral Development Forum, Abstract, December 1989.

Koopman, E.R., Patterson, M.R., Franklin, J.M., and Poulsen, K.H., (1990): Stratigraphic and structural geology of the Lyon Lake massive sulphide deposit, Sturgeon Lake, Ontario; in Franklin, J.M., Schnieders, B.R., and Koopman, E.R., (eds.), Mineral deposits in the Western Superior Province, Ontario, Field Trip #9, International Association on the Genesis of Ore Deposits, 8th Symposium, Geological Survey of Canada, Open File 2164, p. 95-104.

Morton, R.L., Hudak, G.K., Walker, J.S., and Franklin, J.M., (1990): Physical volcanology and hydrothermal alteration of the Sturgeon Lake Caldera Complex; in Franklin, J.M., Schnieders, B.R., and Koopman, E.R., (eds.), Mineral deposits in the Western Superior Province, Ontario, Field Trip #9, International Association on the Genesis of Ore Deposits, 8th Symposium, Geological Survey of Canada, Open File 2164, p. 74-94.

Mumin, A.H. (1988): Tectonic and structural controls on massive sulfide deposition in the south Sturgeon Lake volcanic pile, Northwestern Ontario and Hydrothermally altered rocks associated with the Lyon Lake Archean, volcanogenic massive sulfide ore deposits, Sturgeon Lake, Northwestern Ontario; M.Sc. thesis, University of Toronto, 138 p.

Poulsen, K.H. and Franklin, J.M. (1981): Copper and hold mineralization in an Archean trondhjemitic intrusion, Sturgeon Lake, Ontario; in Current Research, Part A, Geological Survey of Canada Paper 81-1A, p. 9-14.

Ramsay, J.G. (1967): Folding and fracturing of rocks; McGraw-Hill, New York, 568 p.

Roberts, G.W. (1981): An examination of structural and stratigraphic ore controls, Lyon Lake mine, Ontario; Noranda Mines, internal company report, 13 p.

Suppe, J. (1985): Principles of Structural Geology; Prentice Hall, New Jersey, 537 p.

Trowell, N.F. (1974): Geology of the Bell Lake-Sturgeon Lake area, districts of Thunder Bay and Kenora; Ontario Geological Survey Report 114, 67 p.

Trowell, N.F. (1983): Geology of the Sturgeon Lake area, districts of Thunder Bay and Kenora; Ontario Geological Survey Report 221, 97 p.

Wolfson, I., (1988): Petrographic Report, Lyon Lake ore samples; Unpublished company report.

APPENDIX A - Description of site specific field mapping observations

Introduction

This section includes descriptions of specific areas of the mine which were selected for detailed mapping, in order to examine specific problems. Mine drifts that are perpendicular to the strata were selected to document the lithostratigraphic sequence of the strata. Areas of the mine which exposed major cross sections of the banded iron formation were mapped to establish the lithostratigraphic relationships of the sedimentary rocks; also, structural analysis was undertaken in order to determine the structural style of the mine. Areas of the mine exposing the contact between the hanging wall basalt and footwall rhyolite were selected to establish the nature of this contact. Selected areas were based on the best possible exposures and accessibility.

The detailed descriptions to follow are organized in descending order from the upper to lower parts of the mine. Surface is referred to as 0 Level (arbitrarily given an elevation value of 10,000 feet by Noranda Mines Limited), and subsequent level names represent the approximate depth in feet below surface.

Appendix A-i: 200 LEVEL #1 CROSSCUT

This area was selected to map the contact between the hanging wall basalt and the footwall rhyolite as represented in the upper mine. Outcrop in the mine vicinity is very limited, and a surface expression of this contact was not observed. The 200 level (Figure 19) is the first level extensively developed in the mine workings, and was selected to observe the nature of the contact between the hanging wall basalt and the footwall rhyolite nearest to surface.

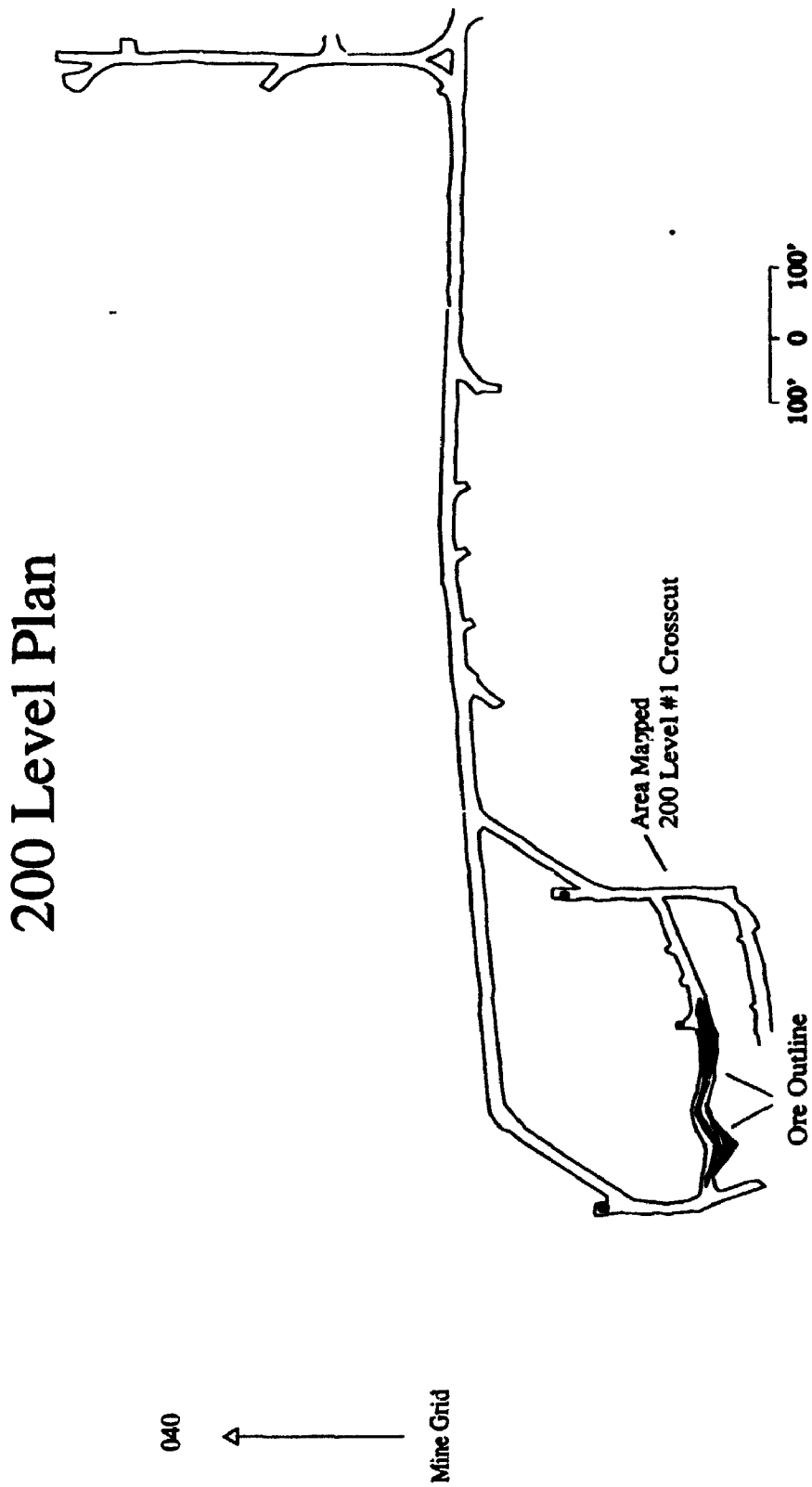

Figure 19: 200 level plan map. Location map of area of detailed mapping.

General observations in this area include steeply dipping north- facing amygdaloidal basalt overlying quartz- phyric rhyolite. The contact between the basalt and the rhyolite is marked by a shear zone.

The amygdaloidal basalt is dark green, fine- grained, and moderately to strongly foliated, intruded by an intermediate dyke near the base. Basalt is composed of 5% rounded to ovoid quartz- carbonate- filled amygdules up to 1 cm in diameter. Other amygdules show aspect ratios of 5:1, elongated parallel to the foliation. Locally, 1 mm size disseminated magnetite grains occur. Deformation increases towards the contact with the underlying rhyolite. Sheared basalt near the contact contains abundant quartz veinlets parallel to foliation, producing metamorphic layering of alternating green and white colouration to the rock. In some places the basalt is so strongly deformed that it crumbles (probably made up mostly of clay minerals).

The rhyolite is light gray, and comprised of 1%, 1 to 2 mm, clear and blue quartz eyes and disseminated pyrite, intercalated with thin lapilli tuff beds, characterized by lapilli- sized cherty and lithic fragments. The rhyolite is slightly to moderately micaceous. Foliation is a steep, north- dipping, moderately well developed cleavage with sericitic halos of 1 to 5 mm- thick along cleavage planes. Sixteen meters south of the basalt contact, quartz- phyric fragmental rhyolite is strongly foliated with veinlets and stringers of quartz and chlorite containing pyrite and chalcopyrite subparallel to foliation. The rhyolite is intruded by a chlorite and carbonate altered intermediate dyke.

The contact between the hanging wall basalt and the footwall rhyolite is marked by a steep, north- dipping, high strain zone approximately 6.5 m wide. At the contact with the hanging wall basalt, the upper 2 m of the rhyolite is silicified and strongly fractured. The fractures contain white micaceous minerals and carbonate. The basalt in this zone is strongly schistose, characterized by stretched amygdules and abundant quartz-carbonate stringers, both trending parallel to the schistosity.

Appendix A-ii: 525 ORE PASS AND 525-1116 CROSSCUT

This area (Figure 20) was selected because it is one of the few accessible places where the entire stratigraphic succession of the Lyon Lake mine is exposed. This area includes the hanging wall basalt, massive sulphides, footwall rhyolite, and below this, sedimentary footwall rocks, including iron formation at the base of the sedimentary rocks.

Basalt is a very fine- grained, dark green, strongly schistose, chloritized and carbonatized rock, containing 2 to 3% disseminated 0.5 to 1 mm size euhedral pyrite. Pervasive quartz-carbonate stringers and minor stringers of pyrrhotite and pyrite occur sub-parallel to foliation. A 2 to 8 cm- thick massive sulphide lenses occurs near the base of this unit, and pinches out at the contact with the footwall rhyolite. Near the contact between ore and rhyolite, the basalt contains 1 to 5 mm- thick stringer veins filled with quartz, carbonate, biotite, and chalcopyrite. Sheared basalt extends 16 m, to the end of the 525-1116 crosscut.

Petrographically, basaltic flows comprise of up to 10 percent twinned, oligoclase phenocrysts up to 1 mm in size are strongly altered to sericite. Ovoid amygdules up to 1 mm in diameter, make up to 5 percent of the rock, and are filled with polygonized clear quartz. The matrix is composed of 0.2 mm laths of albite, quartz, and wispy and granular chlorite interwoven with flakes of biotite. Plagioclase, chlorite and biotite are preferentially oriented defining the foliation. Less than 1% relict hornblende grains were observed. Carbonate occurs pervasively, in microfractures and locally with quartz in microfractures. Microcrystalline pyrite occurs as randomly oriented euhedral grains associated with the chlorite in the matrix. This unit varies from massive to strongly foliated.

The rhyolite immediately below ore is strongly chloritic and sericitic. This unit is fragmental, composed of well packed felsic lithic fragments in a chloritic and carbonatized matrix. Pyrite is often observed in the matrix associated with chlorite. Fragments range

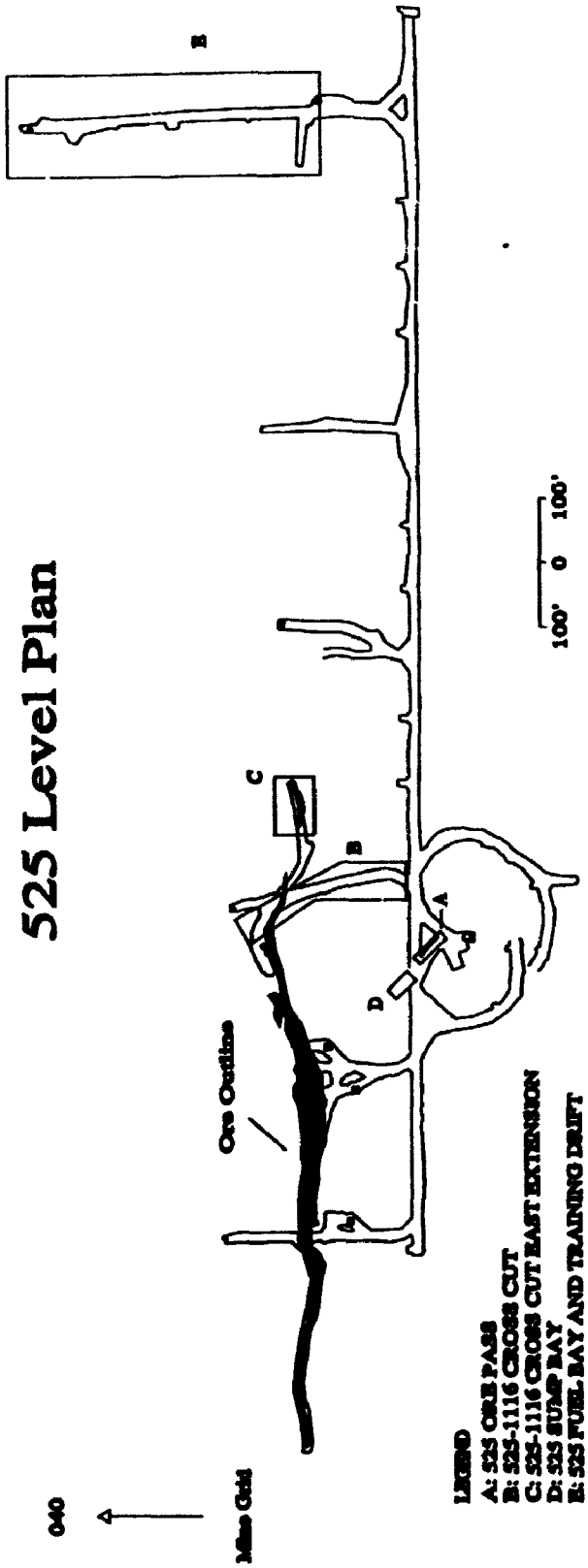

Figure 20: 525 level plan map. Location map of areas of detailed mapping.

from lapilli to block size, up to 45 cm in diameter, stretched parallel to foliation. The aspect ratio of the fragments varies from 2:1 to 5:1. Cherty and lithic fragments are pervasively carbonate- altered and contain 1 to 2 mm- size, ovoid, pyrite filled blebs. Some fragments contain chlorite specks which are probably altered vesicles. The rhyolite contains abundant quartz- and iron- carbonate- filled microfractures and minor pyritic-filled stringers and microfractures. Fracture cleavage is evenly spaced, at about 1 cm. Moving up-section, cherty fragments increase in size and abundance. This sequence of pyroclastic flows consists of block- sized fragments at its base, grading stratigraphically upwards with increasing abundance of lapilli size fragments. The top of this sequence is overlain by quartz- phyric lapilli tuff and aphyric ash beds. Overlying these ash beds, an additional coarse fragmental zone occurs, representing the base of a subsequent pyroclastic flow. Immediately below the contact between the quartz- phyric rhyolite and massive sulphides, rhyolite contains 1% of 1 to 2 mm size blue and gray quartz eyes, and up to 30%, mainly cherty, lapilli size fragments stretched parallel to the foliation, and to the ore contact. Quartz- phyric rhyolite hosts the massive sulphides, and between massive sulphide bands, the rhyolite is strongly deformed, containing abundant fractured quartz veining with pyrrhotite and chalcopyrite, and minor carbonate infilling the fractures, parallel to the foliation.

Quartz veins, typically 30 cm- wide are perpendicular to, and in contact with the ore lens. These quartz veins contain sulphide minerals and biotite. Biotite is abundant at the margins of the quartz veins, and is also disseminated throughout the veins. Biotite increases in abundance closer to the massive sulphide lens, and is the dominant mineral in the matrix of the massive sulphides. Chalcopyrite and pyrrhotite, plus minor pyrite, occurs as disseminated mineralization, and in fractures and veinlets within the quartz veins. Biotite is spatially associated with the sulphides in the quartz vein.

Overall, the rhyolite is most intensely deformed near the contact with the massive sulphides and the hanging wall basalt. Blue and gray quartz eyes are more abundant and larger (up to 3 mm) proximal to the massive sulphide bands than deeper in the rhyolite footwall. Contacts between pyroclastic flows are very diffuse and may be distinguished by the presence of block size fragments overlying aphyric ash. Immediately below the ore, the quartz- phyric unit is strongly deformed and pervasively altered to chlorite, whereas, deeper in the footwall, sericite alteration dominates.

The lower contact of the rhyolite with the underlying sedimentary rocks is irregular and diffuse, overprinted by iron- carbonate micro-fractures in the graphitic shale and iron-carbonate and sericite alteration in the rhyolite. Locally, the contact is occupied by an intermediate dyke.

Appendix A-iii: 525-1116 CROSSCUT-EAST EXTENSION

This drift trends parallel to the strata, and was mapped to examine the contact between the hanging wall basalt and the footwall rhyolite. The stratigraphic units observed in this area include hanging wall basalt, banded massive sulphides, and footwall quartz- phyric lapilli tuff. The contact between the footwall rhyolite and the massive sulphides is marked by a 30 to 60 cm wide, broken and attenuated felsic dyke. All the units are steeply north- dipping, and north- facing. The entire area is intensely sheared, locally exhibiting mullion structures in the massive sulphides. The massive sulphide varies from 7 cm to 60 cm wide, and has been reoriented and 'smeared' along the contact between the footwall rhyolite and felsic dyke, and along the contact between the hanging wall basalt and felsic dyke. Shearing is parallel to bedding.

Locally, a zone of quartz breccia occurs at the contact between the massive sulphide body and the rhyolite unit. This breccia contains approximately 30% sulphides (chalcopyrite and pyrrhotite), and 5 to 10% iron- carbonate in veins and fractures.

Appendix A-iv: 525 SUMP BAY

This area has an excellent exposure of isoclinally- folded iron formation. The iron formation is characterized by iron- carbonate, -oxide, -silicate beds intercalated with beds of chert. Cherty beds vary in thickness from 1 to 5 cm- thick; thickened in nose of folds. These cherty beds contain fine laminations of magnetite. Late quartz- filled fractures occur radially in the chert beds. Iron- silicate beds vary from 1 to 3 cm- thick, and are comprised of massive chlorite.

Appendix A-v: 525 FUEL BAY AND TRAINING DRIFT

This area was mapped to examine the nature of the contact between the hanging basalt, and the footwall rhyolite. The contact between the hanging wall amygdaloidal basalt and the footwall quartz- phyric rhyolite is intensely sheared, similar to the 525 east extension drift described above. Locally, the contact is occupied by a sheared felsic dyke; elsewhere, the dyke is discordant and intrudes the basalt.

Appendix A-vi: 600 LEVEL GARAGE

This area (Figure 21) exposes a 100 meter- thick section of subvertical north-dipping, sheared amygdaloidal basalt. 1 to 2 cm- thick quartz-carbonate veins are pervasive, oriented parallel to schistosity. Locally, elongated amygdules with aspect ratios from 2 : 1 to 3 : 1 also occur parallel to schistosity. Several 15 to 20 cm- thick subhorizontal quartz veins 6.5 to 8 m in length were observed in this shear zone. The quartz veins contain disseminated pyrite. Locally, joints parallel to subhorizontal quartz veins are abundant.

Appendix A-vii: 600 LEVEL FUEL STATION

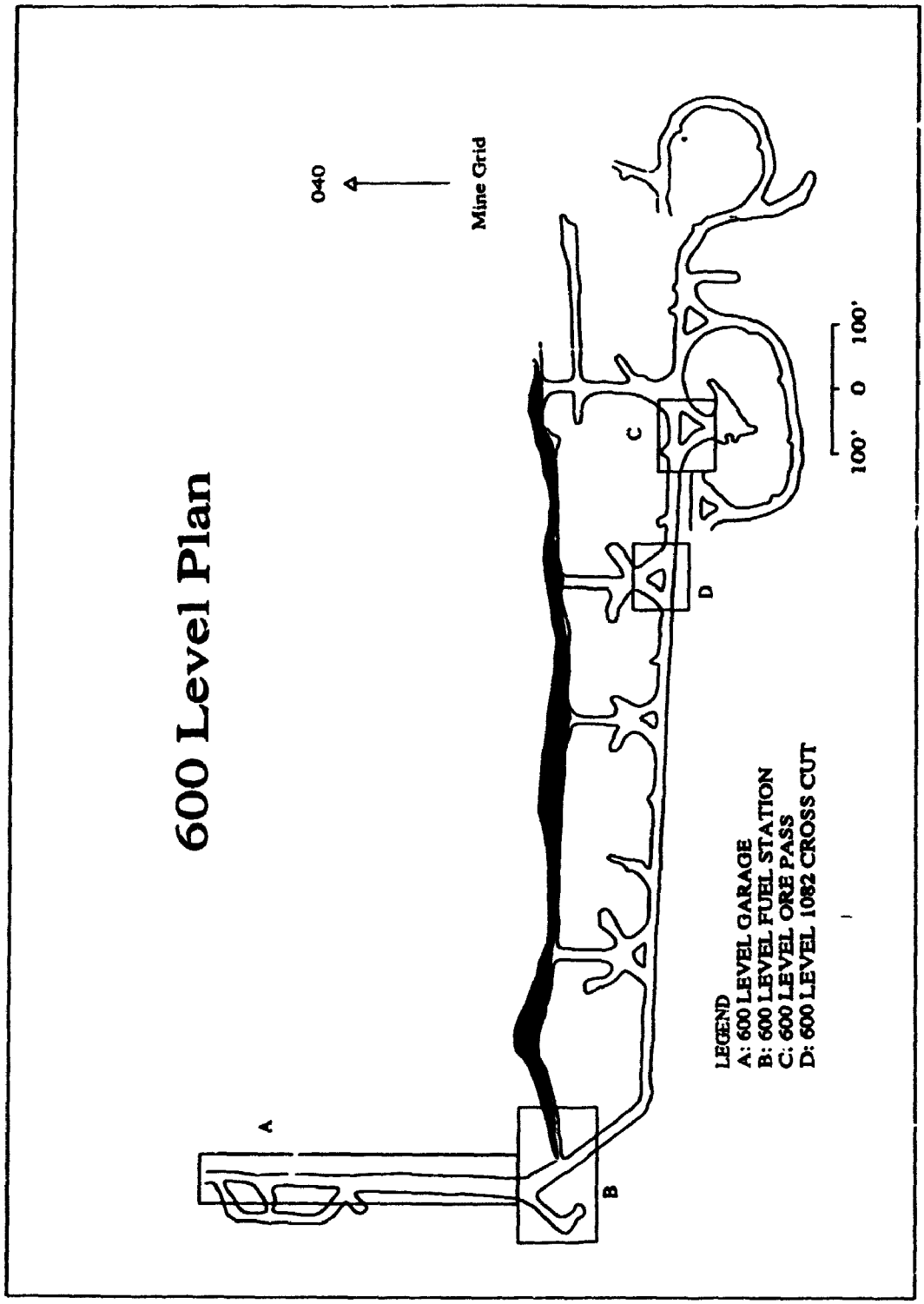

Figure 21: 600 level plan map. Location map of areas of detailed mapping.

This area exposes a cross section from the hanging wall basalt, through the contact zone with the footwall rhyolite, the rhyolite, minor massive sulphides, and minor graphitic sedimentary rocks. The entire area is moderately to strongly deformed; most of the deformation is evident in the more fissile hanging wall basalt, and at the contact between the hanging wall basalt and the footwall rhyolite. Deeper in the footwall rhyolite, a 30 to 60 cm- thick, discontinuous lens of folded massive sulphides occurs parallel to the limb of a folded bed of graphitic shale.

Basalt is very fine- grained, dark green, strongly schistose, chloritized and carbonatized rock, containing 2 to 3%, 1 mm size feldspar phenocrysts, 5% elongated quartz-filled amygdules, and 1 to 2% disseminated 0.5 to 1 mm size euhedral pyrite. Pervasive quartz-carbonate stringers with disseminated pyrite, and minor stringers of pyrrhotite and pyrite occur sub-parallel to the schistosity. Locally. 1 cm- thick bands of chlorite occur parallel to stratigraphy; these may represent contacts between sheet flows. Felsic dykes intrude the basalt, and are oriented subparallel to schistosity. Sub horizontal quartz veins up to 60 cm- thick occur near the contact with the footwall rhyolite, and contain carbonate- and chlorite- filled fractures.

The contact between the hanging wall basalt and footwall rhyolite on this level is strongly sheared. The contact is marked by a felsic dyke and a shear zone up to 100 meters wide. Schistosity in the basalt is parallel to the contact with the dyke. One to 2 cm- wide quartz veinlets with iron- carbonate and disseminated pyrite occur at the contact between basalt and the dyke.

The felsic dyke is rust- coloured, medium- to fine- grained, and contains 2 to 3 mm clots of chlorite oriented parallel to the foliation. Shallow east- dipping 5 to 8 cm- thick quartz- carbonate- tourmaline tension veins containing disseminated pyrite, cross cut the felsic dyke.

The quartz- phyric rhyolite lapilli tuff unit is strongly sheared, and contains quartz fragments 0.5 to 2 cm long, 0.5 cm wide in a foliated chloritic matrix. 1 to 5 mm- thick stringer veinlets of pyrite occur parallel to the foliation.

The area has a well defined strong north- dipping subvertical schistosity, and regular fracture planes parallel to schistosity but dipping more steeply. The intersection between the schistosity and the fracture planes produces a sub-horizontal lineation. Locally, the shearing is so strong that a tectonic layering of alternating chlorite- rich and quartz- carbonate- rich bands is observed in the basalt. The schistosity of the shear zone is less steep approaching the contact between the basalt and the felsic dyke. In fact, the schistosity becomes parallel to this lithological contact. It is very difficult to observe C-S fabric in section. In general, all planar fabrics are parallel or sub-parallel, but in detail, the schistosity dipping less steeply than the fracture cleavage plane. If the fracture plane represents the shear plane, and the schistosity the shear foliation, then their structural relationships suggest normal faulting. The sub-horizontal quartz veins located in the sheared basalt suggest reverse movement along this shear zone.

Striations located on schistosity planes have an east trending shallow plunge, parallel to the measured intersection lineations, and the hinge measurements of folds in iron formation.

The consistency of structural measurements may suggest that the folding observed is related to the reverse motion on the shear zone located at the contact between the hanging wall basalt and the footwall rhyolite. Folding accompanying this reverse motion may have produced the folds observed in the iron formation and the other units.

Foliation measured in the felsic dykes is subparallel to the foliation measured in the basalt, but generally dips shallower, probably as a result of refraction.

The rhyolite is light gray to beige, characterized by 1 to 3 mm size blue quartz eyes which make up to 10% of the unit, and 20 to 30% cherty fragments which are elongated

parallel to the cleavage. Ash and lapilli sized cherty fragments contain iron- carbonate alteration in a sericitic matrix. Locally, the matrix is chlorite- altered. Thin beds of aphyric ash are intercalated with the lapilli tuff.

The rhyolite is moderately to strongly deformed proximal to the contact with the hanging wall basalt. Well defined cleavage planes exhibit east trending sub-horizontal striations. Near the contact with basalt, the rhyolite is host to several carbonatized felsic dykes. These dykes exhibit sharp contacts with the rhyolite, and a distinct foliation, that is not as strong as that observed in the rhyolite. The foliation in the dykes is parallel to the contacts. Joints are well developed in the fragmental rhyolite. Locally, shallow west-dipping, 2 cm- thick quartz-iron- carbonate-tourmaline veins occur.

A 30 to 60 cm- thick lens of massive sulphides in this area is hosted in the quartz-phyric rhyolite lapilli tuff, and is composed of well- banded fine- to medium- grained pyrite and sphalerite layers. The lens is folded, and south dipping on the west wall, but not present on the south part of the fold, the east wall, nor in the back.

North- dipping (45°), 2 m long, 10 cm quartz veins containing 2 to 3% feldspar and 2 to 3% disseminated pyrite, extend into the massive sulphide lens. These veins are in the hanging wall of the ore zone and locally occur in the ore zone. The quartz veins do not cut the ore.

A 60 cm- thick bed of graphitic pelite is in contact with the ore lens. This unit exhibits a tightly folded, synformal structure, shallowly plunging east. Rhyolite occurs in the core of the fold. All the rocks south of the massive sulphide lens are carbonatized and moderately deformed, and cross cut by iron- carbonate veinlets oriented parallel to the foliation.

Appendix A-viii: 600 LEVEL ORE PASS

This area was selected to analyse the style of folding in the mine. The approach was to establish the style of folding in the iron formation, and then try to test the application of this style to the ore, and to the entire mine. Overall, this area comprises of steep north and south dipping isoclinally folded iron formation intruded by several felsic dykes. Late faults cut folded iron formation, and parallel dyke contacts. The iron formation is composed of alternating beds of iron- carbonate and iron- silicate, with local iron sulphide laminations within the iron- carbonate beds.

Iron formation comprises of alternating 2.5 to 10 cm- thick beds of siderite and chlorite. Locally, siderite beds are up to 15 cm- thick, and boudinaged. Iron formation is weakly magnetic due to the presence of pyrrhotite laminations in the siderite beds.

Folded, and non folded felsic dykes 30 to 60 cm- thick intrude the iron formation. These dykes are typically observed in the mine to cross cut all the lithologic units. These felsic dykes are a rusty colour, fine- to medium- grained, carbonatized, and typically contain up to 20% chlorite clots oriented parallel to foliation. Intrusive contacts are sharp and locally correspond to fault planes.

Iron formation in this area of the mine forms tight to isoclinally folded east plunging beds (Figure 22 and Plate 13). These are truncated by a fault. Tight to isoclinal Z - shaped fold asymmetry is observed in plan view on the back. Folds are disharmonic and hinges and limbs are disruptive, reflecting the inherent competency differences of the bed compositions. Jointing occurs perpendicular to the hinges of these folds, a form as a result of stretching parallel to the bedding. One cm- thick subhorizontal quartz- siderite and chlorite bands occur in the limbs of the fold in an en echelon pattern. Subhorizontal striations on the fault plane has moved hanging wall up, suggesting reverse movement.

Axial planar schistosity is moderately to well developed in chlorite beds, sub parallel to bedding, but dipping more steeply.

Plate 13: Photograph of tight to isoclinal F1 folds in banded iron formation. Folded iron formation is truncated by faults. Cross section viewed to the west. Field of view is 2 meters.

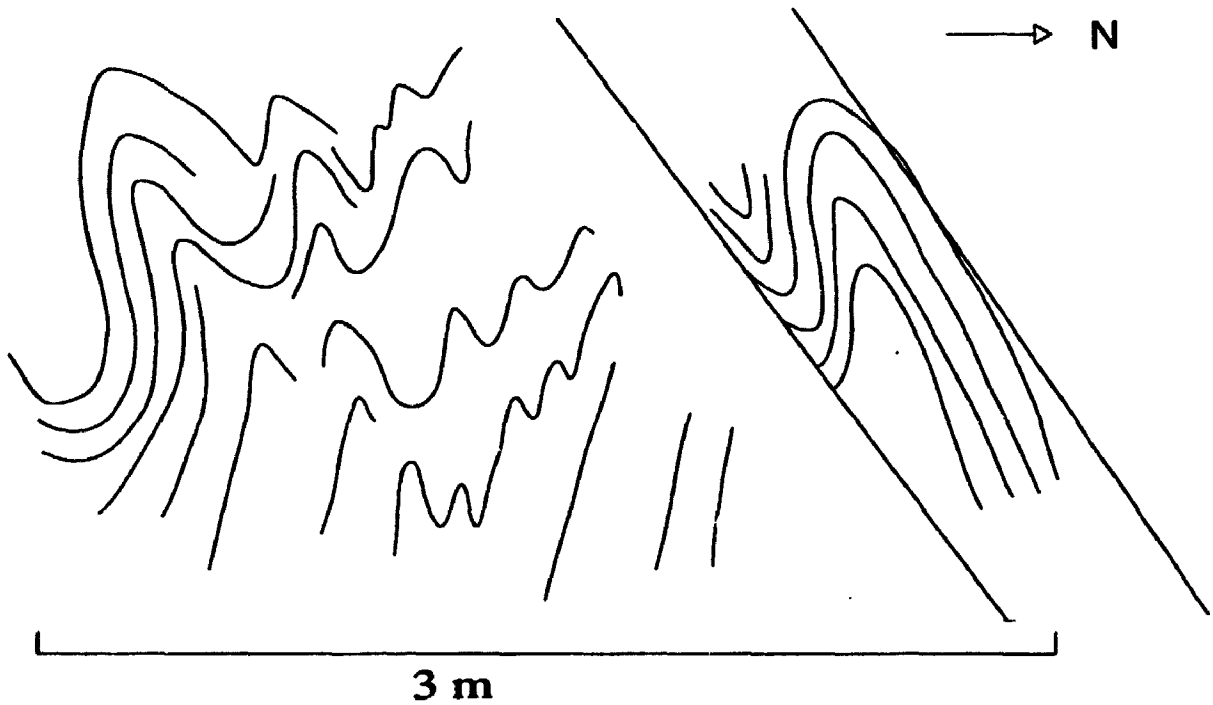

Figure 22: Sketch of Plate 13. Tight to isoclinal folds in banded iron formation.

Appendix A-ix: 600 LEVEL 1082 CROSSCUT

This area was mapped as a continuation of the iron formation mapped in the 600 level ore pass described above. Folded iron- carbonate and iron- silicate banded iron formation, quartz- phyric rhyolite intruded by a felsic dyke, and greywacke are present. All the lithologic units are folded; the iron formation is isoclinally folded, and the rhyolite, felsic dyke, and greywacke form a larger amplitude fold. The rock units all dip south; a north- dipping foliation is well defined in the rhyolite, and in the iron- silicate beds of the iron formation. The lithological units in this area dip in the opposite direction to those observed 33 m along strike, in the 600 level ore pass area, which are north- dipping. Applying the principals of vergence of asymmetric folds), to locate the major fold axial surfaces, combined with opposing dips of the lithologic units in these two adjacent areas, indicates that folding on a much larger scale than that observed in the iron formation exists in this area.

Rhyolite tuff is massive, gray, quartz- phyric, containing 1 to 2% blue quartz eyes. Sericite alteration is pervasive, and defines a steep north- dipping foliation. Locally, the foliation is very strong, observed as shear bands in thin section.

The contact between the rhyolite stratigraphically underlying the iron formation is sharp, and folded.

A felsic dyke intrudes the rhyolite at the contact between rhyolite and iron formation. The contact between the dyke and the rhyolite is irregular and discordant to the contact between rhyolite and iron formation, and on the back, this dyke forms a Z - shape asymmetric open fold, with an amplitude of 6.5 m.

Banded iron formation typical consists of banded siderite and chlorite- rich beds, with local veinlets of pyrrhotite and pyrite, oriented parallel to bedding. In this area, numerous east- plunging isoclinal folds (Plate 14) dip south and indicate northward vergence. In plan view, the iron formation and dyke is folded with S - shape folds with an

Plate 14: Isoclinal folds in banded iron formation. Folds plunge shallowly (25 to 35°) to the east. Cross section viewed to the west.

amplitude of 6.5 m. The beds lack a well defined axial cleavage. Locally, some subhorizontal quartz veinlets with traces of pyrite were observed cross cutting silicate beds of the iron formation at high angles (See sketch of quartz veins perpendicular to bedding confined to the silicate unit in the iron formation).

Appendix A-x: 1000 LEVEL CONVEYOR BELT

Folded iron formation is very well exposed in two areas on this level (Figure 23), and was mapped as a part of the study of the structural style of the mine, as well as to determine the stratigraphic continuity of the iron formation.

Several important observations were made in this area which helped to establish the structural style, and determine the possible origin of the observed folding.

The lithologic units observed in this area include oxide iron formation, greywacke, graphitic shale, rhyolite, and felsic dykes. All the lithologic units are folded, and exhibit north and south dipping bedding relationships.

Iron formation has an apparent thickness of 200 m and is characterized by magnetite- and pyrrhotite- bearing cherty beds, alternating with iron- silicate beds. Beds are 5 to 8 cm- thick. Magnetite occurs within the cherty bands as delicate laminations evenly spaced throughout the bed. Locally, pyrite - pyrrhotite veinlets occur in the iron-silicate beds parallel to bedding. Pyrrhotite is weakly magnetitic.

This area exhibits large scale folding of the iron formation. The fold is upright, shallowly plunging east, and has a minimum amplitude of 5 m, and a minimum wavelength of approximately 20 m (Figure 24). Locally the bedding in the iron formation is almost vertical, but its dip varies from south to north on opposite limbs of the fold nose. Smaller scale parasite folds occur on the limbs of the larger fold, and exhibit northward vergence in south dipping beds, and southward vergence in north- dipping beds. The iron formation beds exhibit typical M - shaped isoclinal folding in the nose of the fold. Isoclinal folding is

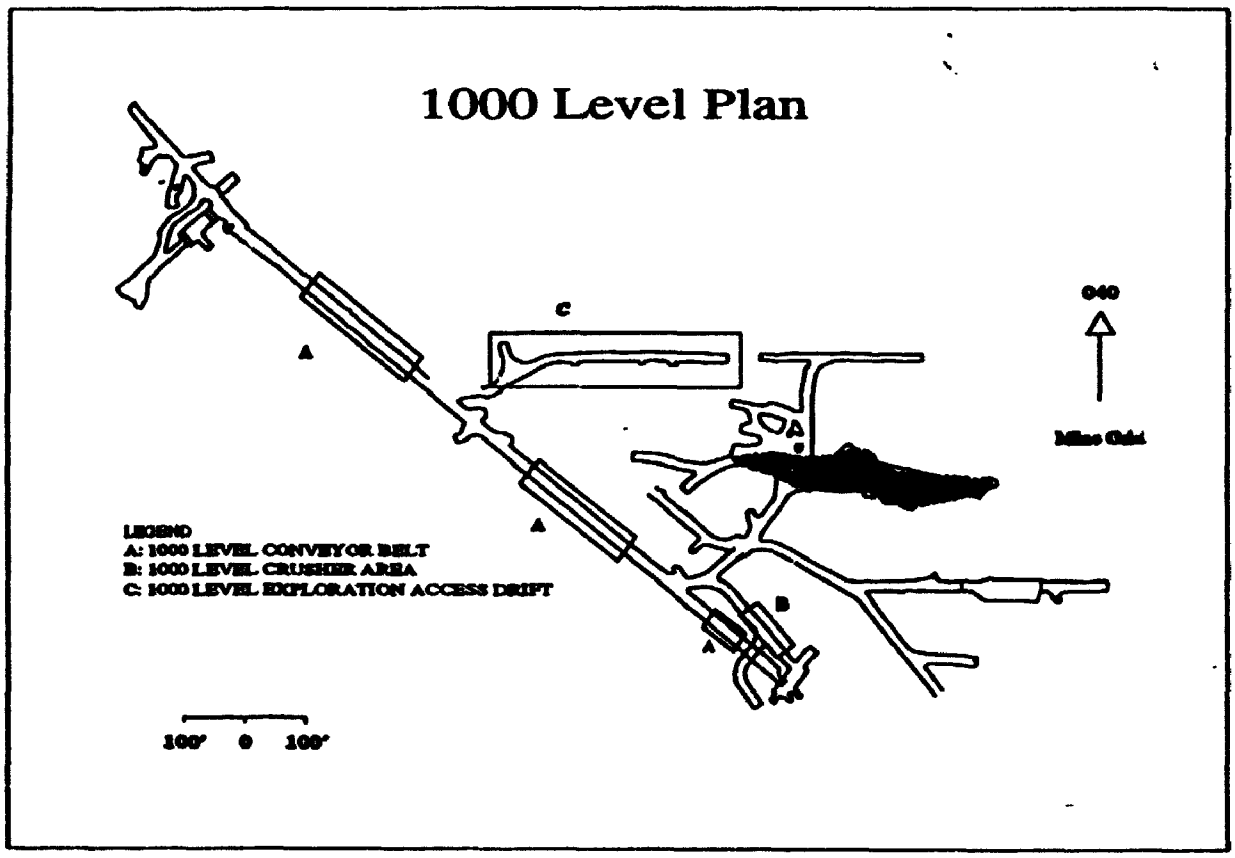

Figure 23: 1000 level plan map. Location map of areas of detailed mapping.

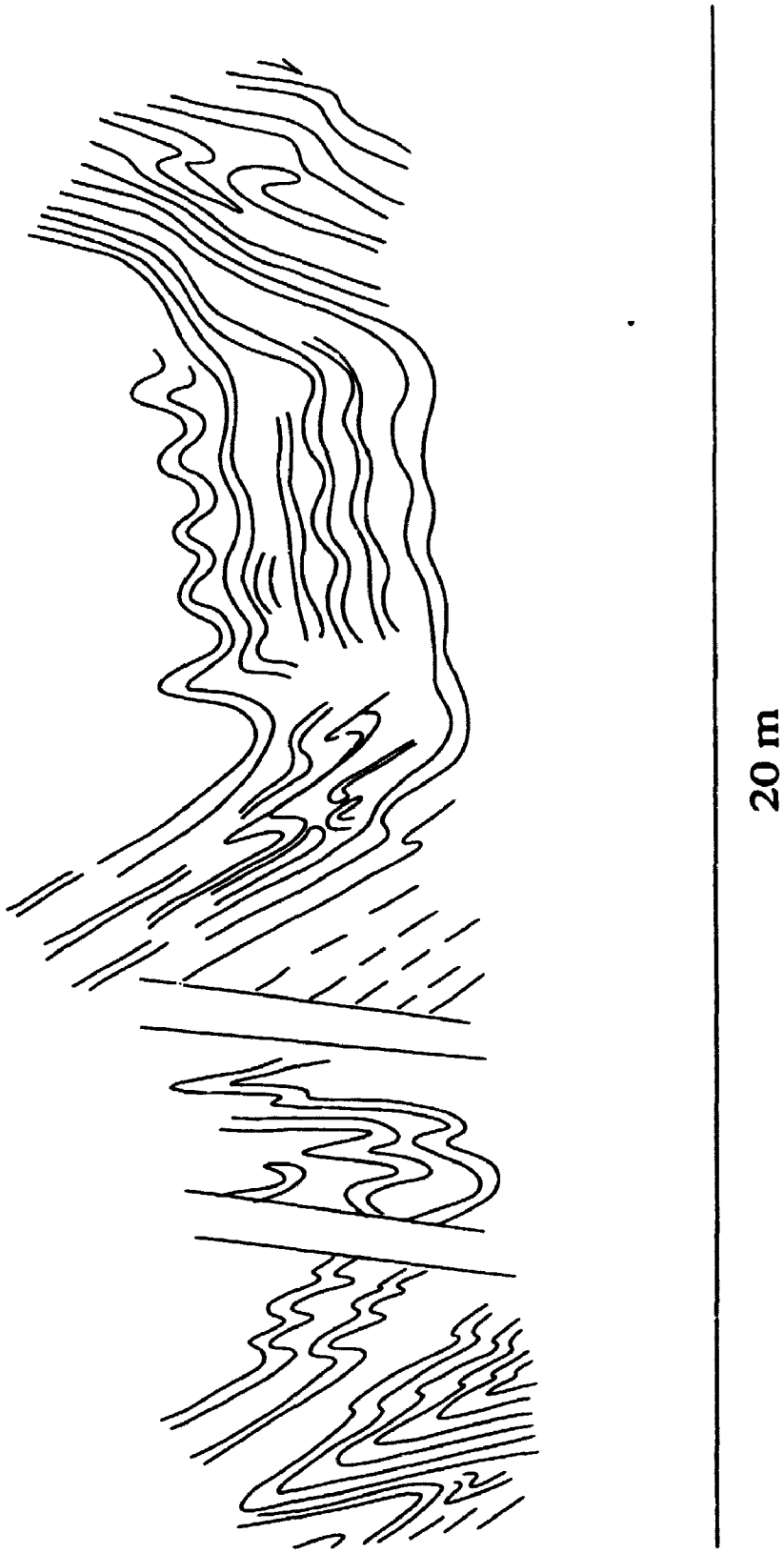

Figure 24: Large scale folding in the iron formation (looking down plunge). The minimum fold amplitude is 5 m and the minimum fold wavelength is approximately 20 m. Note the M- shaped folds in the nose of the larger fold. The northern limb of the fold is disrupted by two felsic dykes. Cross section viewed to the west.

also present at a much smaller scale; laminations of magnetite within the cherty beds are commonly isoclinally folded, particularly in the nose of the fold.

Rhyolite occurs stratigraphically above and below the iron formation in this area. Rhyolite is massive, light beige, and quartz- phyric. Locally, sericite and carbonate veinlets are abundant oriented parallel to bedding. Rhyolite is not strongly deformed, but does exhibits a weak foliation sub-parallel to bedding, and contains local 5 to 8 cm- thick pyrrhotite rich quartz veinlets parallel to the foliation.

Several 30 to 60 cm- thick north- dipping felsic dykes occur in the rhyolite, and at the contact between the rhyolite and the iron formation. Foliation in the dykes is parallel to, and shallower than the dyke contacts.

Locally, well defined quartz and pyrrhotite- filled fracture planes occur in the rhyolite. Striations on quartz-pyrrhotite veinlets plunge shallowly east. Locally, discrete shear zones in the rhyolite contain abundant sericite and pyrrhotite rich quartz veins oriented parallel to schistosity.

Several brittle faults occur in this area cross cutting the iron formation, indicating reverse movement, with dextral displacement of 30 cm as seen in plan view on the back of the drift. Fault breccia consists of quartz, feldspar, abundant sericite, plus trace pyrite. Striations on the fault plane plunge shallowly east.

A folded felsic dyke mapped on this level was of particular importance to the interpretation of folding of the lithological units including the iron formation. Fold morphology is a tight, inclined, plunging, Z type fold (Plate 11). No thickness variation occurs in the dyke. The dyke is broken, and thrust faulted onto itself, and then folded. Iron formation is squeezed in between the two stacked layers of dyke.

Appendix A-xi: 1000 LEVEL CRUSHER AREA

This area is located approximately 30 m north of the 1000 level conveyor belt area, and was mapped as a continuation of the iron formation in the down- plunge direction. Lithological units include iron- oxide iron formation, quartz- phyric rhyolite, and felsic dykes. Characteristics of the lithologies are similar to those observed in the conveyor belt area. Structural observations were of more significance, and are consistent in form with those throughout the mine.

Overall, this area comprises of north and south dipping isoclinally folded zone of iron formation intruded by felsic dykes. The isoclinally folded beds of iron formation are part of a larger fold envelope (Figure 25 and Plate 15). The latter is characterized by an upright fold plunging shallowly east. Folded and non folded felsic dykes cross cut the rhyolite and the iron formation.

Massive, quartz- phyric rhyolite tuff occurs stratigraphically above and below the iron formation. A strong axial planar cleavage is preserved in the iron formation and rhyolite tuff.

Tightly folded iron formation consists of 2.5 to 8 cm- thick iron- carbonate- rich cherty beds alternating with 2.5 cm- thick magnetite bands, and 2.5 to 8 cm- thick iron-silicate beds composed of chlorite. Locally, cherty beds are up to 15 cm- thick.

Iron formation is strongly deformed, for example, the cherty beds are disrupted, boudinaged, and fractured. Locally, isoclinally folded cherty beds exhibit a west- plunging fold pattern, which is opposite to the overall fold pattern of the mine which is east-plunging. (This may suggest more than one folding event occurred. Only two west plunging folds were observed throughout the mine. In the broader sense of the fold envelope, these west plunging folds occur in the hinge of a fold plunging east.)

The iron- silicate beds define the fold envelope, and striations on the bedding planes plunge east, parallel to the fold axes. In the hinge area of the fold envelope, tightly

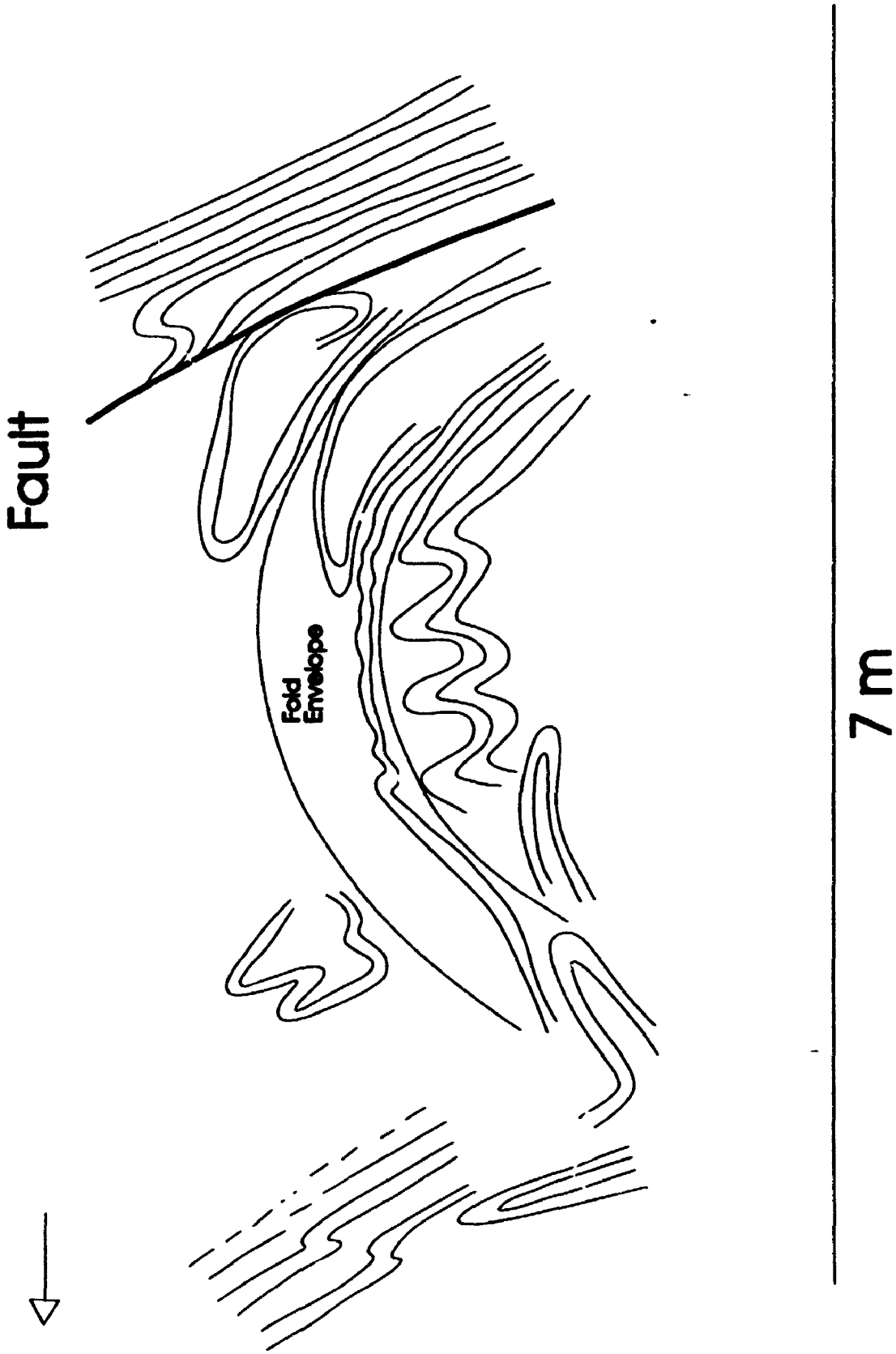

Figure 25: Variably folded beds of iron formation within a larger fold envelope. The fold envelope plunges east. Note the re- folded folds in the lower left corner, and a west plunging fold in the upper left corner. Plate 15 is a partial photograph of this fold envelop.

Plate 15: Photograph of fold envelop of beds of iron formation. Photograph compliments Figure 25. Cross section viewed to the east. Field of view is approximately 4 meters.

folded iron formation beds are ptygmatic. However, in the south dipping limb of the fold envelope, parasitic folds have an S - shape pattern with northward vergence.

South of the zone of folded iron formation, the iron formation is cross cut by a steep north- dipping quartz- filled brittle fault. Striations on the fault plane are sub horizontal, plunging shallowly east and west. The iron formation seems to be entrained by the fault, and indicates normal motion along the fault. No displacement is evident along the fault in the vertical plane, however, displacement in the horizontal direction is indeterminate.

Appendix A-xii: 1000 LEVEL EXPLORATION ACCESS DRIFT

This drift was selected to map the basalt and rhyolite, and the contact between the hanging wall basalt and the footwall rhyolite. Also, mapping a portion of this drift complements other areas mapped on this level because all the lithologic units were observed on this level.

Basalt is typically a green, fine- grained, amygdaloidal and schistose unit. Quartz-filled amygdules up to 4 cm in diameter, very rounded to ovoid are locally abundant in less deformed zones. Quartz and iron- carbonate veinlets, are pervasive in the strongly sheared basalt. The orientation of these veinlets is parallel to the foliation. The sheared basalt extends a minimum thickness of 30 m, from the contact with the footwall rhyolite. Schistosity strikes northwest, subparallel to bedding, and dips north more steeply than bedding.

Appendix A-xiii: 1260 SUB-LEVEL

This area (Figure 26) was mapped with the purpose of examining hypothesis 2; is the discontinuity of the ore lenses is the result of faulting; and have the ore lenses been displaced relative to one another?

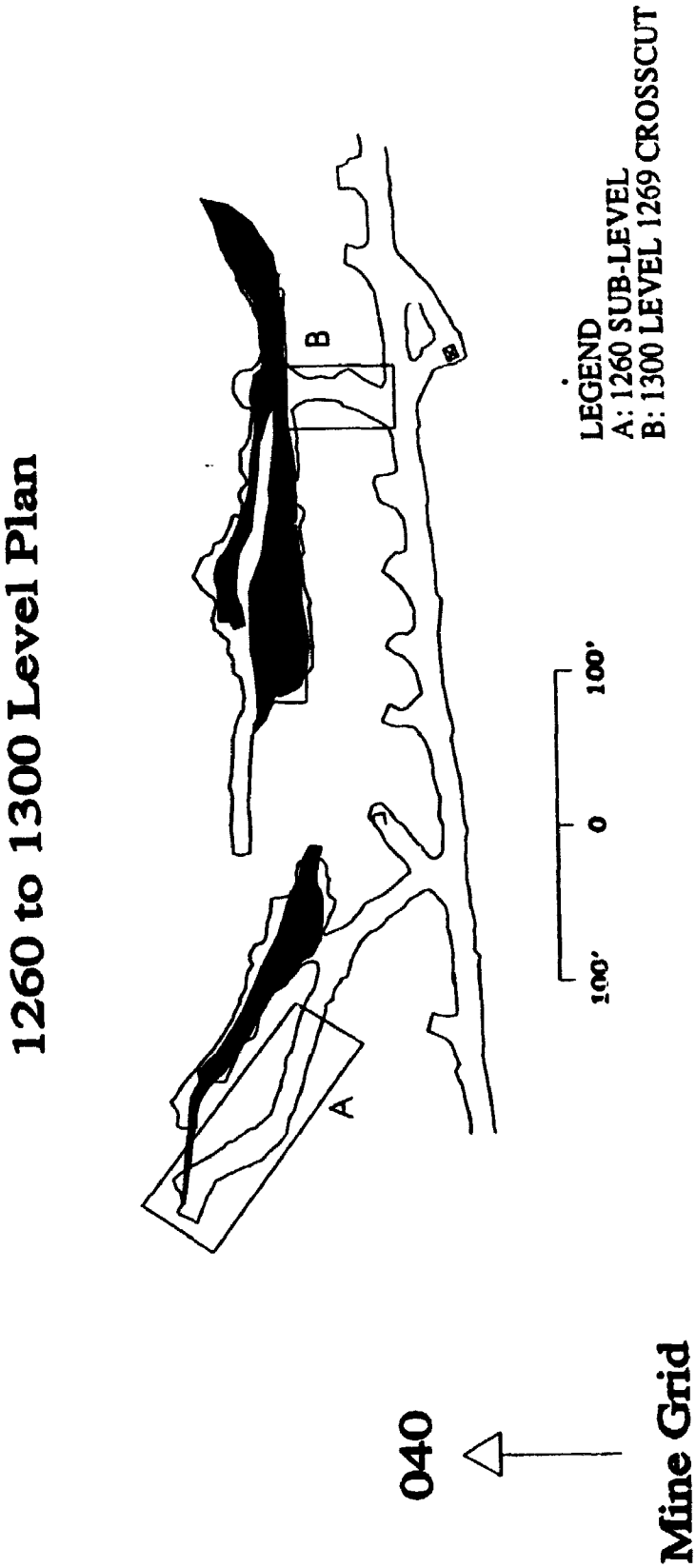

Figure 26: 1260 sub-level to 1300 level plan. Location map of areas of detailed mapping.

At the northern most end of this drift, massive sulphides occur on the east wall, but do not occur on the west wall (Figure 26). A shear zone occurs at the contact between the ore and the hanging wall rocks to the ore. The rock types observed in this area include rhyolite and massive sulphides. Massive sulphides are hosted in quartz- phyric fragmental rhyolite.

The ore zone is 1 m- thick, hosted in quartz- phyric fragmental rhyolite. The massive sulphides are deformed, folded, and occur only on the east wall of this drift. Massive sulphides comprise of equivalent proportions of coarse- grained sphalerite and pyrite. Two to 5 cm- thick bands of sulphides are discontinuous, wispy, and contorted.

Quartz- phyric fragmental rhyolite is light beige to light gray, and massive. Quartz phenocrysts are blue, 1 to 3 mm in size, and comprise 3 to 5% of the unit. Locally, quartz phenocrysts comprise 10 to 15% of the rock. Fragments are monolithic, subangular chert, and comprise 20 to 30% of the unit. Fragments vary in size from 1 to 5 cm, averaging 2 cm in diameter. Locally fragments are block size, up to 18 cm in diameter.

Several 30 to 80 cm- thick medium- grained felsic and intermediate dykes intrude the rhyolite. These dykes occur deep in the footwall rhyolite, approximately 50 m from the contact between the ore and the footwall rhyolite. The contacts between the rhyolite and the intrusions are sharp. The dykes are dipping steeply north, moderately foliated, folded, and show southward vergence (Figure 27).

The fold geometry is a steeply inclined, gently plunging, and tight fold. The dykes occur at a higher stratigraphic level on the west wall relative to the east wall which suggests an eastward plunge of the fold axis. Based on the variation of the stratigraphic level of the hinge of the fold on opposite walls, the plunge of the fold axis is estimated to be 20 to 30 degrees.

Locally, several white quartz veins cross cut the quartz- phyric fragmental rhyolite (Figure 28). These quartz veins are up to 3 m in length, and vary from 5 to 30 cm in

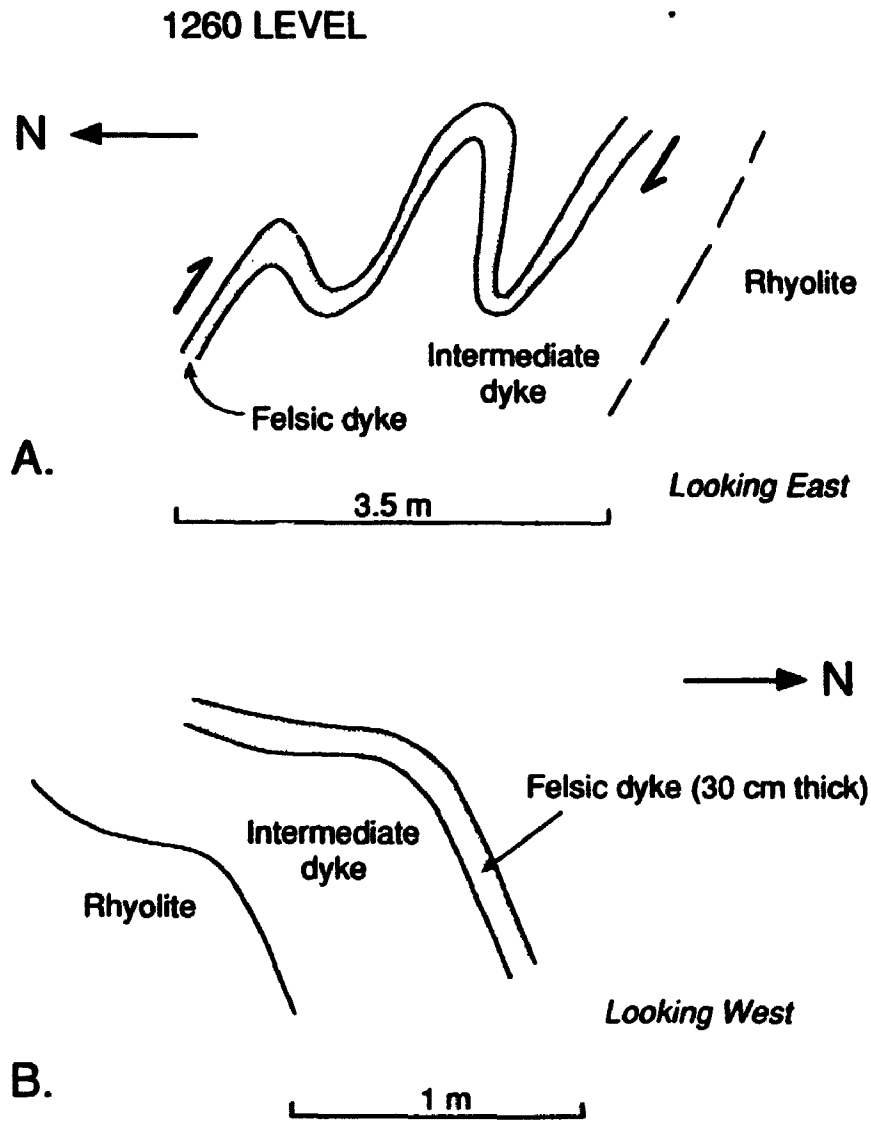

Figure 27: Folded felsic and intermediate dykes in the footwall rhyolite. A) looking east; tight to isoclinal folds show southward vergence, B) sketch of the same dykes on the opposite wall. The position of the dykes on the west wall are higher, therefore the plunge of the fold axes trends east.

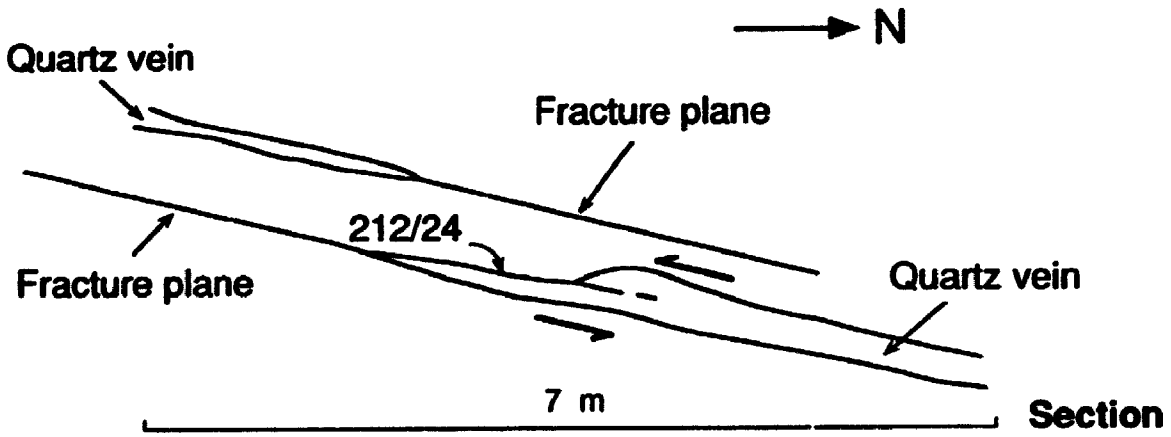

Figure 28: Sub- horizontal en echelon quartz veins in the footwall rhyolite.

width. They occur as en echelon subhorizontal west dipping veins spaced 60 to 90 cm apart. Along strike, these veins are represented by 1 mm- thick fractures filled with quartz and up to 5% pyrite. A dilation jog in the subhorizontal quartz vein suggests reverse motion. Numerous millimeter- thick fracture planes occur parallel to the subhorizontal quartz veins. Locally, subhorizontal veins are cross cut by subvertical veins (Figure 29). Displacement of the subhorizontal veins by the subvertical veins is 1 to 2 mm. A dilation jog suggests reverse motion of the subhorizontal quartz veins. An earlier generation of quartz veins cross cut by the subhorizontal quartz veins contain tourmaline and chlorite.

Throughout the entire drift, the rhyolite is pervasively altered to sericite. Proximal to the ore horizon, footwall quartz- phyric fragmental rhyolite exhibits sericite + chlorite + carbonate alteration zones, in a semi- conformable distribution.

The hanging wall rhyolite is pervasively chlorite- altered (in the shear zone), and has a mafic appearance. One to 2%, 2 mm euhedral pyrite occurs disseminated throughout.

In the entire mapped area, the quartz- phyric fragmental rhyolite has a very well defined moderate to strong cleavage. Fragments are elongate, oriented parallel to the cleavage. Proximal to the ore horizon, and in the hanging wall, blue quartz- phyric fragmental rhyolite is strongly deformed. Deeper in the footwall rhyolite, the cleavage is well defined and moderate. Sericite defines cleavage planes. Cleavage strikes northwest, and dips subvertically north and south. The north and south dipping subvertical foliation creates an impression of cross cutting relationships between two foliations. However, cleavage is controlled by the elongation of the cherty fragments (Figure 30). Cleavage is north- dipping except at the tips of the fragments where sericite wraps around the fragment.

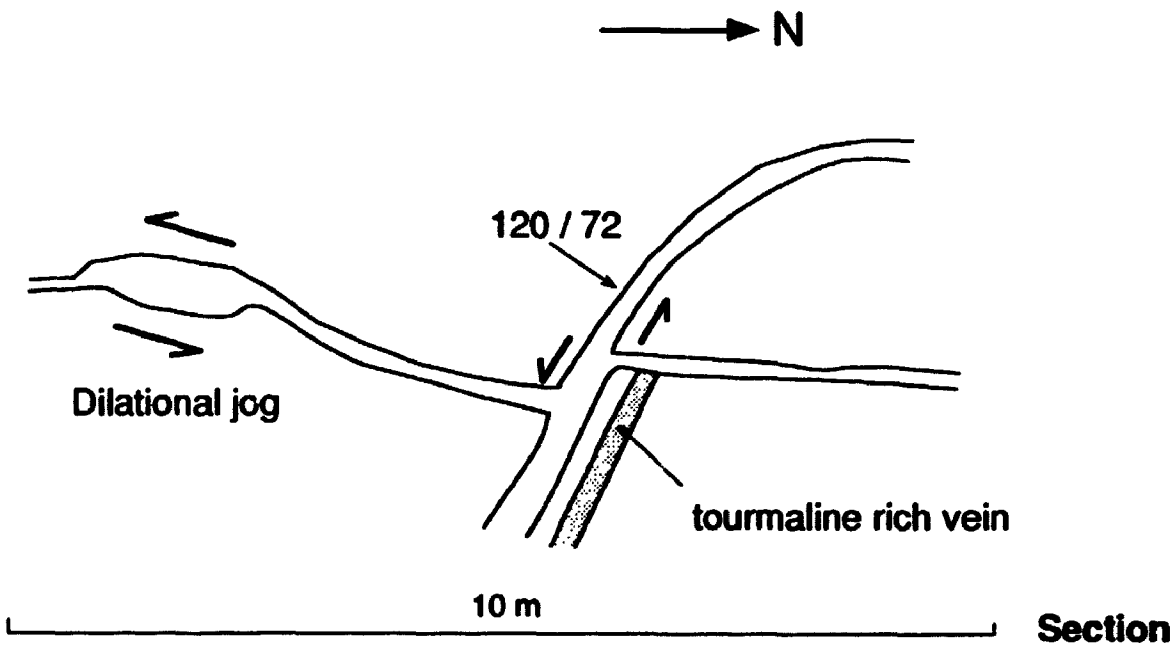

Figure 29: Sub-vertical quartz veins cross cutting the footwall rhyolite. Subvertical veins displace horizontal veins 1 to 2 mm. A dilation jog in the sub- horizontal vein suggests reverse motion.

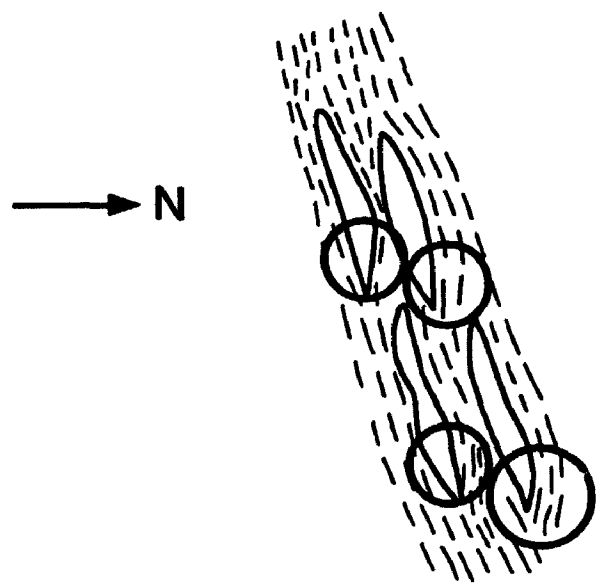

Figure 30: Sketch of north dipping cleavage with an apparent south dipping cleavage. The apparent south dipping cleavage is controlled by the elongation of fragments and wraps around the tips of the fragments.

The contact between the ore and the hanging wall rhyolite is marked by a steep north- dipping fault. The nature and characteristics of this fault varies over a strike length of 9 m. Figure 31 is a drift plan map illustrating the locations of the fault zone described below, and in Figure 32.

At the west end face of this drift (Figure 32A), the fault is characterized by a steep north- dipping brittle fault plane with associated fault breccia. The fault breccia is 30 to 45 cm wide, and consists of 30 to 40% fractured white quartz, 3 to 5% iron- carbonate, and 40% sulphides. Sulphides include pyrite and chalcopyrite, plus traces of sphalerite, tetrahedrite, and galena. Iron- carbonate and sulphides occur as fracture- fill material in the fractured quartz-breccia matrix.

On the east wall of the drift, the contact between the ore and the hanging wall to the ore is marked by a 3 m wide shear zone. Most of the strain is taken up in the hanging wall rhyolite which exhibits a very strong schistosity.

In section (Figure 32B), the relationship between the schistosity (S-plane) in the shear zone, and the sheared ore contact (C-plane) suggests reverse motion.

In longitudinal section, iron- carbonate- and sulphide- bearing en echelon sigmoidal quartz veins crosscuts the altered rhyolite, perpendicular to the long axis of the shear zone (Figure 32C, and Plate 16). Quartz veins are confined to the shear zone. They are 60 cm in length, 2.5 to 5 cm- thick, and spaced 30 to 60 cm apart. These veins comprise of 10 to 20% iron- carbonate, and 2 to 3% disseminated pyrite, chalcopyrite, sphalerite, and galena.

On the back, the fault plane is marked by a 1 to 2 cm- thick quartz-breccia zone, which crosscuts the shear zone (Figure 32D). The relationship between the shear zone and the fault plane suggests dextral movement.

Mineral lineations defined by sericite on schistosity planes in the shear zone plunge shallowly east.

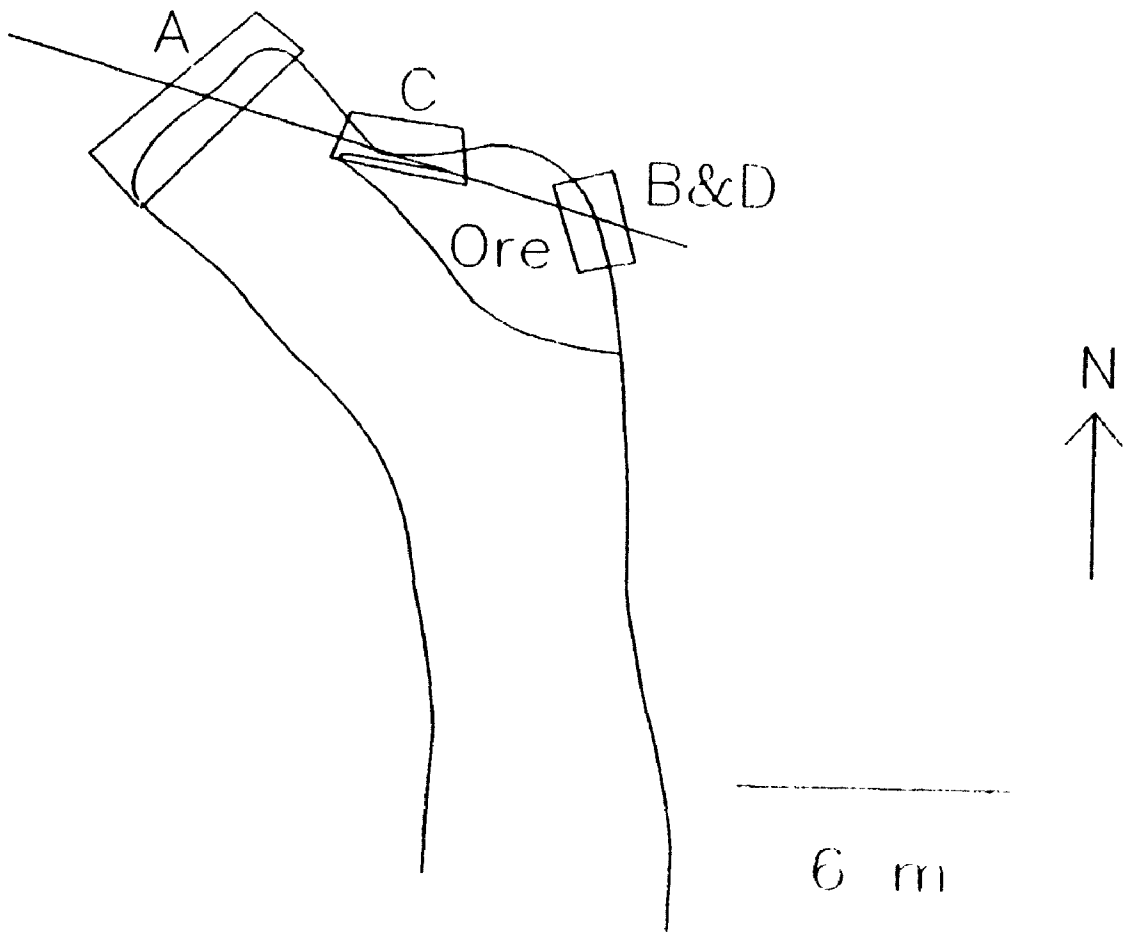

Figure 31: **Drift plan map with locations of detailed descriptions of the fault zone cross referenced with Figure 32A,B,C, and D.**

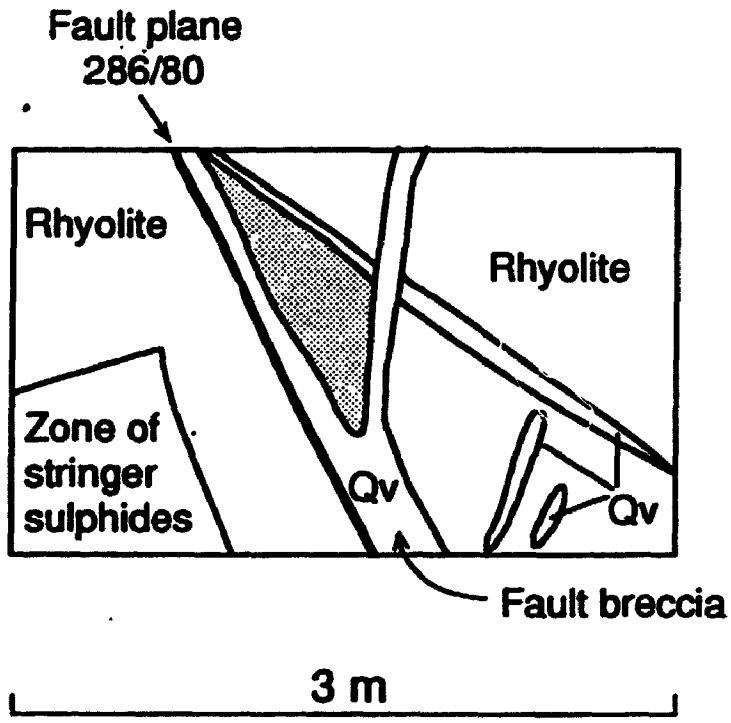

Figure 32A: Sketch of the face at the west end of the cross cut. the contact between the ore and hanging wall rhyolite is defined by a brittle fault.

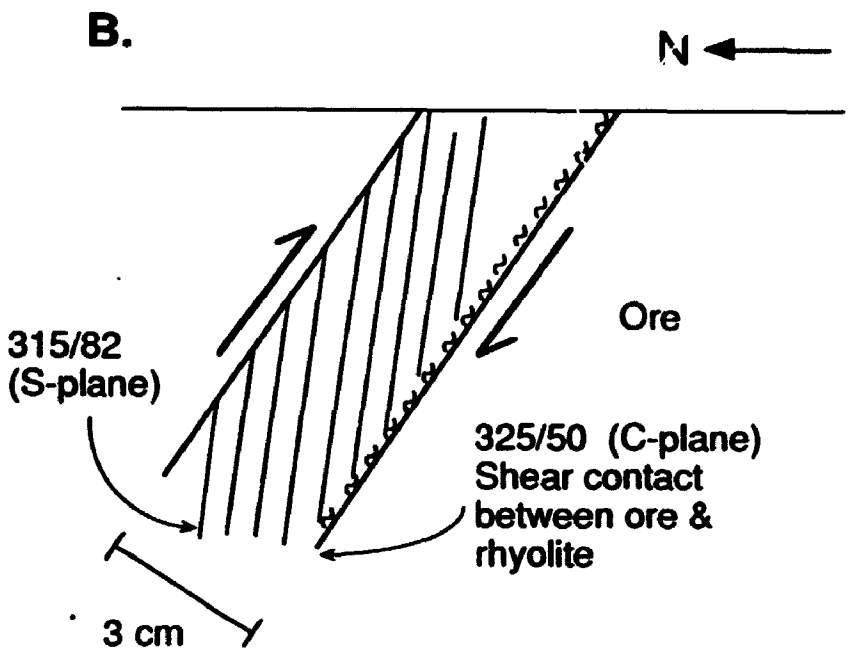

Figure 32B: Sketch of the shear zone at the contact between the ore and hanging wall rhyolite. East wall section of the shear zone shows the relationship between the ore contact and schistosity. This relationship suggests reverse motion.

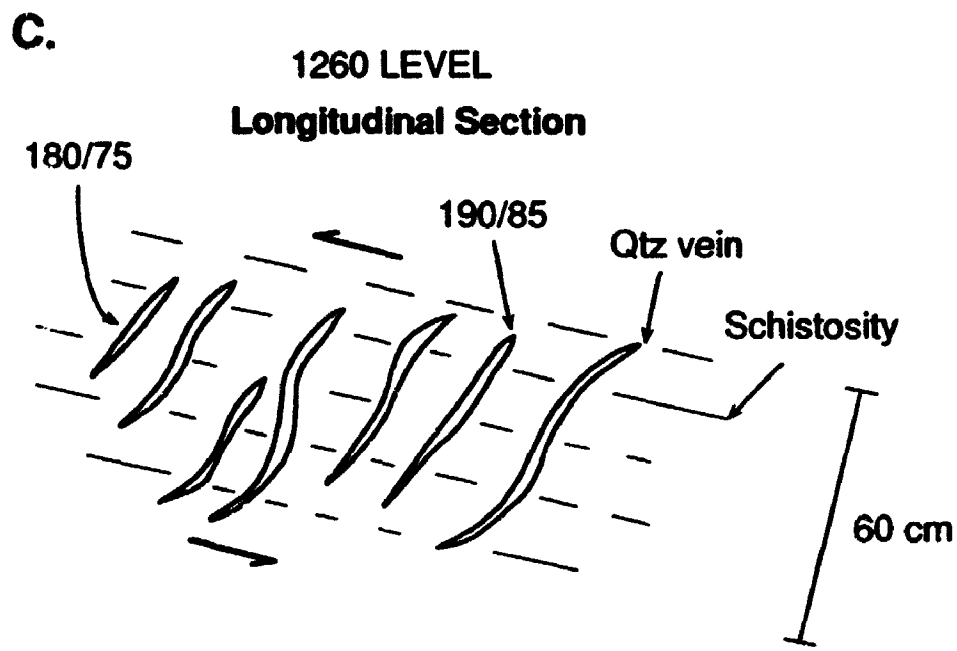

Figure 32C: Longitudinal section of shear zone with sigmoidal quartz veins perpendicular to the orientation of the shear zone.

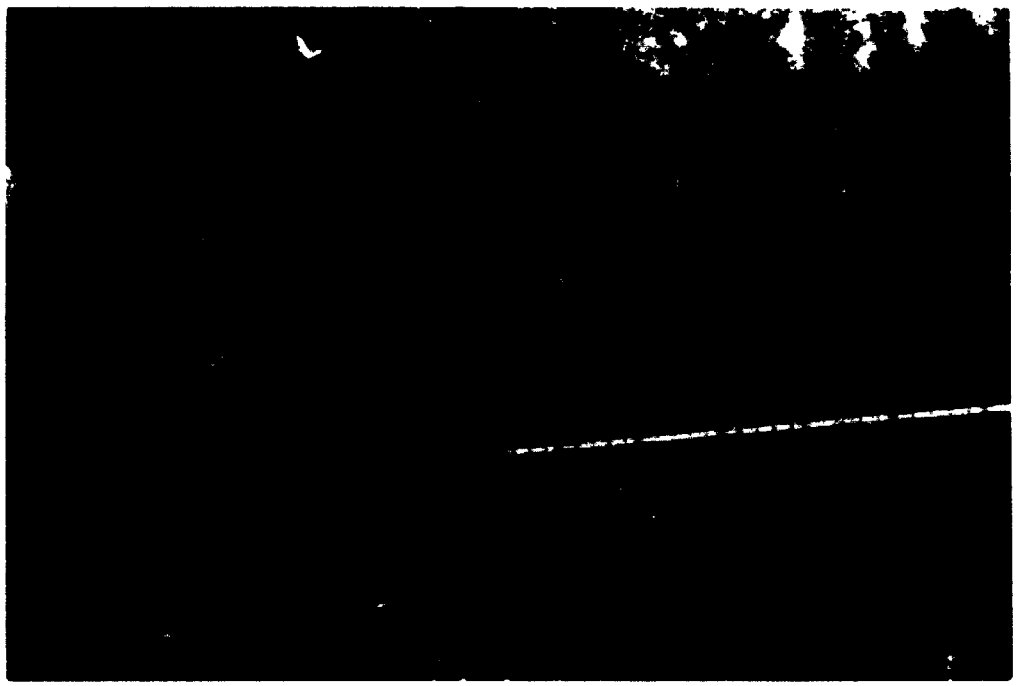

Plate 16: Sigmoidal quartz veins in sheared contact between the massive sulphides and the hanging wall rhyolite. Cross section viewed to the west. Field of view is 2 meters.

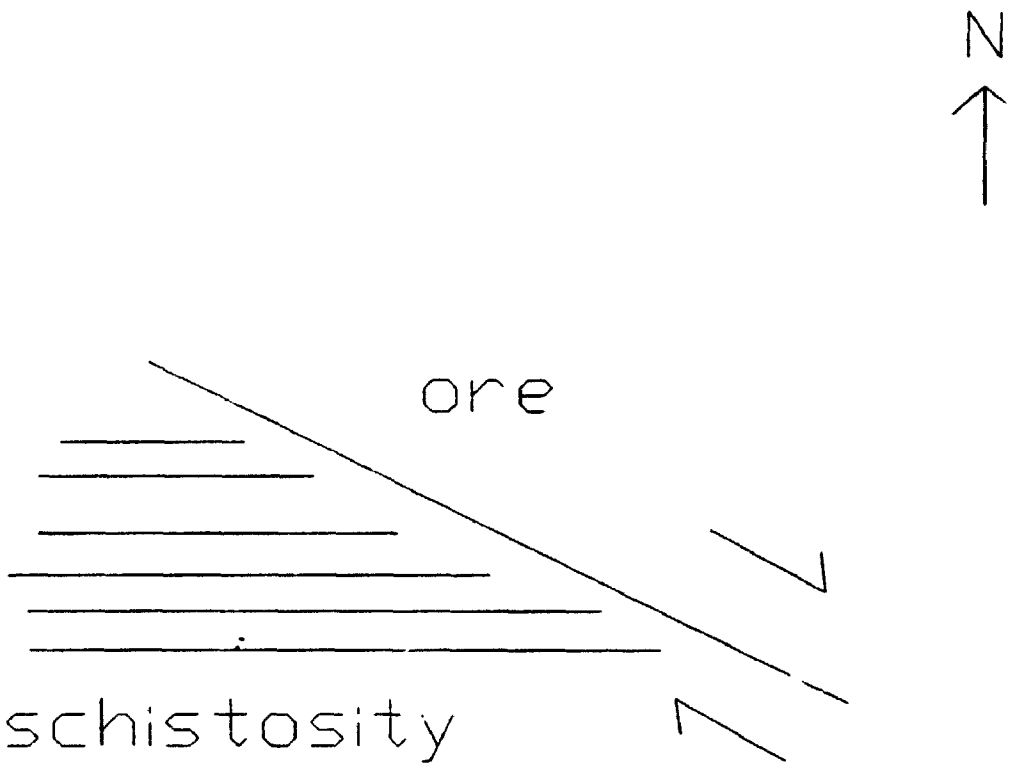

Figure 32D: Plan view sketch of the relationship of the faulted ore contact and schistosity in the hanging wall rhyolite. Relationship suggests dextral motion.

Based on the schistosity and sheared ore contact relationship, and the distribution pattern of the sigmoidal quartz veins in the shear, the motion along the fault zone is reverse dextral.

Appendix A-xiv: 1300-1269 CROSSCUT

This area was mapped for stratigraphic information of the immediate footwall rocks to the ore horizon. The drift extends from the stoped ore horizon through altered footwall rhyolitic rocks, but does not extend into the footwall sedimentary rocks (Figure 26, location B). Rock types observed in this area include massive sulphides, and interlayered rhyolitic quartz- phyric lapilli and ash flow tuffs.

Rhyolitic tuff consists of 5 to 10%, quartz- phyric, subrounded to subangular, cherty lapilli in a very fine- grained aphyric ash matrix. Fragments comprise 5 to 10% of the unit.

Ash beds are aphanitic, dark green to dark gray, and typically 30 to 60 cm- thick. Locally, 0.5 mm gray quartz phenocrysts comprise < 1% of the unit. Proximal to the ore lenses, ash beds contain blue quartz phenocrysts ranging from 1 to 2 mm in diameter and constitute 2 to 4% of the unit.

A bed of massive to semi massive fine- grained pyrrhotite, up to 4 m- thick, and an irregular shaped zone of coarse- grained massive sphalerite (Figure 33), up to 1 m- thick occurs below the main ore body, 10 and 15 m respectively. Both zones are north-dipping, and hosted in blue quartz- phyric rhyolite ash. The upper contacts between the massive sulphide lens and the rhyolite are very sharp, whereas, the lower contacts are very irregular and diffuse.

Footwall rocks to these massive sulphide lenses are pervasively altered to sericite and chlorite. Quartz and carbonate- filled microfractures, stringers, and veinlets, and patches are abundant, and locally, mineralized with 3% pyrrhotite and chalcopyrite.

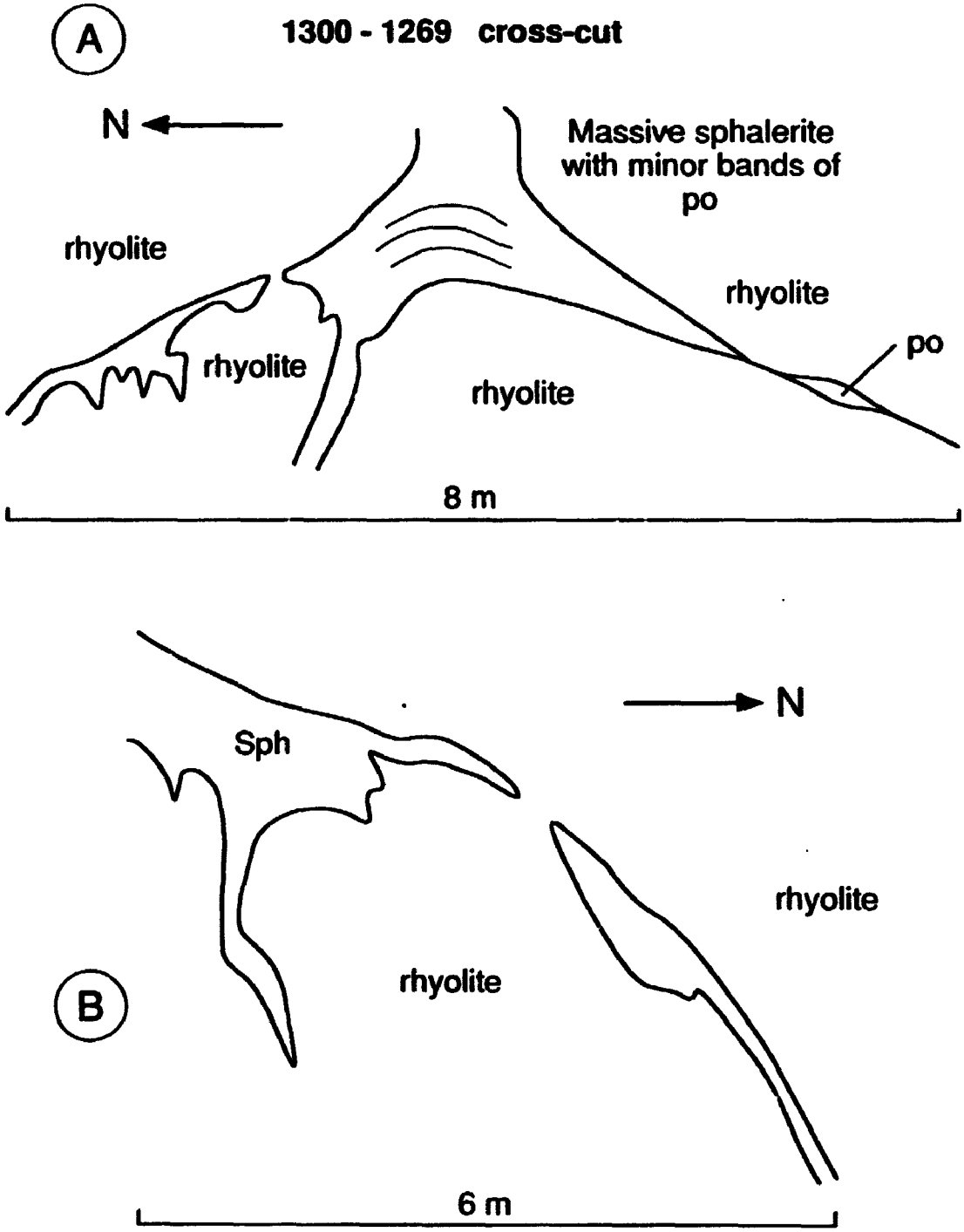

Figure 33: Irregular shaped zone of massive coarse- grained sphalerite footwall to the main lens. A. Looking east, and B. looking west.

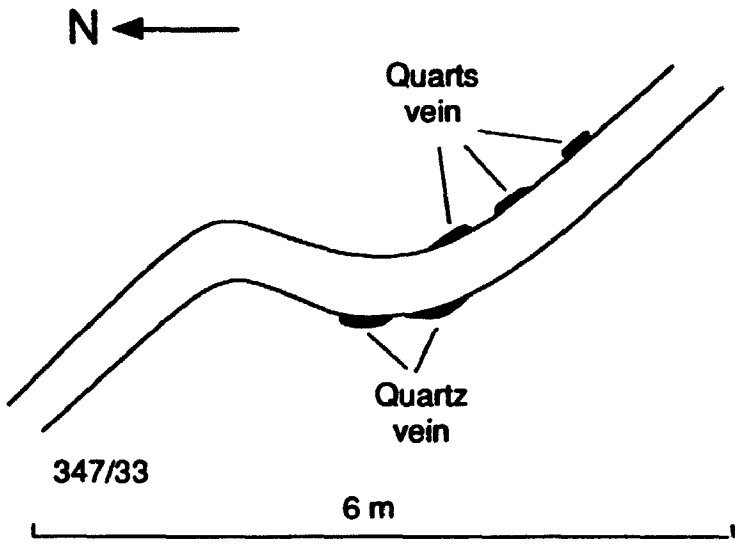

Figure 34: South- verging, north- dipping, shallowly plunging folded felsic dyke in the footwall rhyolite.

Two to 3 m below the main ore zone, rhyolite is cross cut by a 30 to 60 cm- thick, medium- grained, felsic dyke. This dyke is folded; both limbs and the axial plane are dipping shallowly north (Figure 34). The fold geometry is open, moderately inclined, and gently plunging. The plunge of the fold was not measurable, however, the higher stratigraphic level of the fold hinge on the west wall suggests an eastward trending shallow plunge.

The footwall rhyolite exhibits a weak northwest striking, steep north- dipping fabric defined by chlorite and sericite. Lapilli and quartz-carbonate stringers are oriented parallel to the foliation. Locally, rhyolite exhibits conchoidal fracture, probably related to silicification.

Ash beds are pervasively chlorite and sericite altered. Proximal to the main ore body, rhyolitic tuff is pervasively chlorite altered. Garnets are pervasive throughout the sequence. Garnets vary in size from 0.5 to 3 mm, and comprise 3 to 5% of the unit. Garnets are more abundant, comprising up to 10%, in the chloritic matrix of the lapilli tuff proximal to the ore zone, and in the chloritic ash beds deeper in the footwall. Locally, garnetiferous, chloritic ash contains 5% disseminated pyrrhotite, and minor quartz-carbonate stringers.

Appendix A-xv: 1480 LEVEL

This level is one of the few accessible places where massive banded sulphides are well exposed. The access drifts and open stopes provide a large areal exposure of the footwall rhyolite, massive sulphides, and hanging wall basalt. Structural observations on this level are of significance because the ore, footwall and hanging wall rocks are folded, and cleavage relationships pertinent to folding are evident. The geometric configuration of the massive sulphide, and associated units allow the determination of the structural style

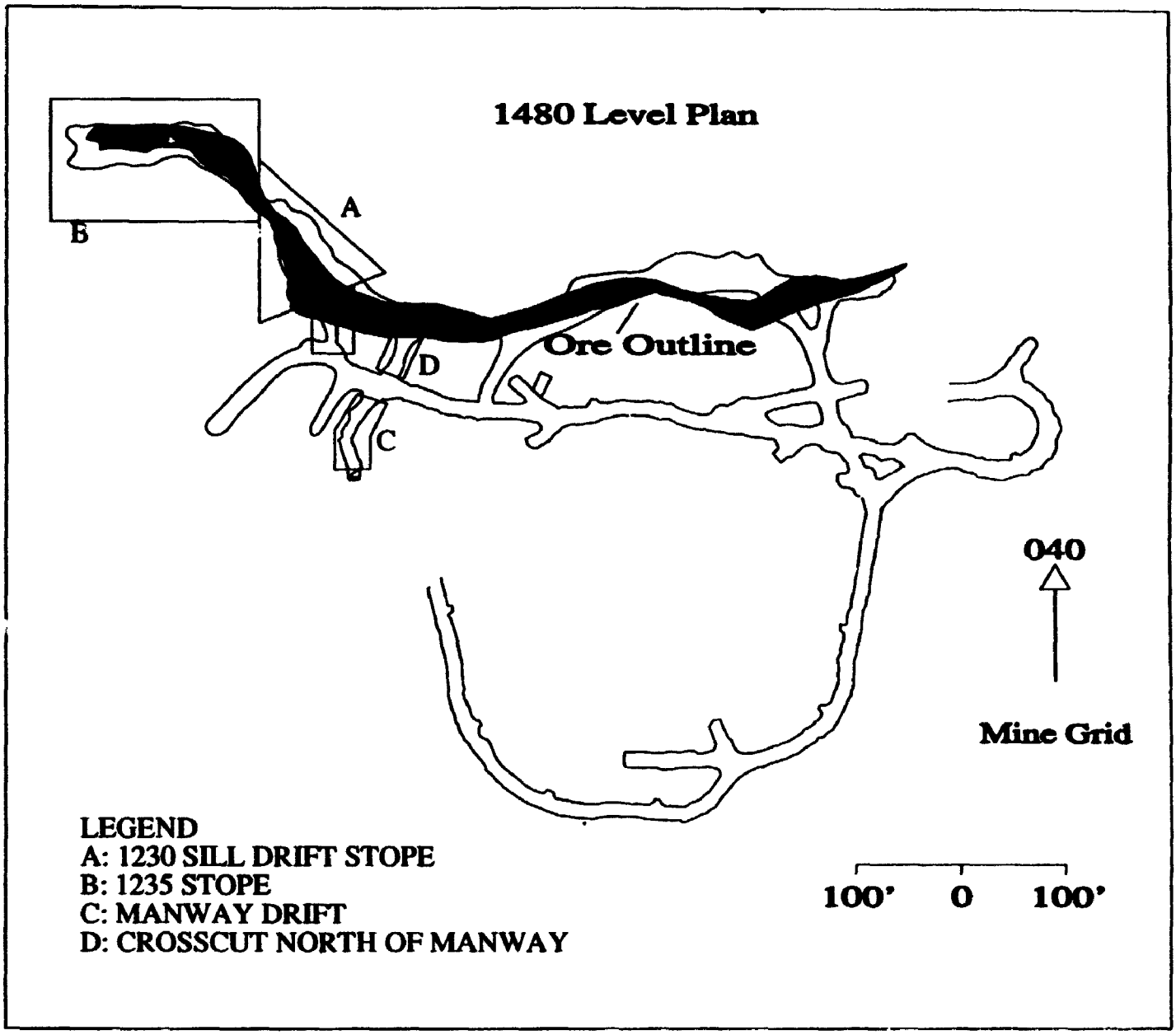

Figure 35: Location map of areas mapped in detail on the 1480 level.

of folding. Figure 35 is a location map of the areas described in detail in Appendix A-xvi to A-xx below.

Appendix A-xvi: 1480 LEVEL 1230 SILL DRIFT STOPE

The ore zone is hosted in quartz- phyric rhyolitic tuff. The ore varies in thickness from 1 to 3 m- thick, and comprises medium- grained pyrite and medium- to coarse-grained sphalerite. Locally, sphalerite- rich zones occur at the margins of the massive sulphide body, and pyrite forms the core. These sphalerite bands at the margins are commonly 30 to 45 cm- thick.

The contact between the massive sulphide horizon and the footwall quartz- phyric rhyolite tuff is commonly diffuse, or gradational. The contact between the ore and the hanging wall quartz- phyric rhyolite tuff is locally marked by a 15 cm- thick felsic dyke. The dyke is locally absent at the contact. Southward, the dyke is discordant, and the thickness increases up to 60 to 90 cm. Locally, the hanging wall is marked by quartz-breccia containing sulphides and fragments of host rock.

The dip of the massive sulphide horizon varies, from moderately north, to shallowly east, then moderately south. This variation in dip defines an open fold, with a wavelength of 15 m. The massive sulphide horizon is strongly deformed and exhibits discontinuous bands of pyrite and sphalerite. Sphalerite- rich zones occur at the margins of the massive sulphide horizon, along the limbs of the fold.

A well defined subvertical north- dipping cleavage occurs subperpendicular to bedding (Figure 36). The relationship between the subhorizontal bedding and the subvertical cleavage suggests this area is near the hinge of a fold. Striations measured on the bedding plane at the contact between the ore and the hanging wall plunge shallowly east.

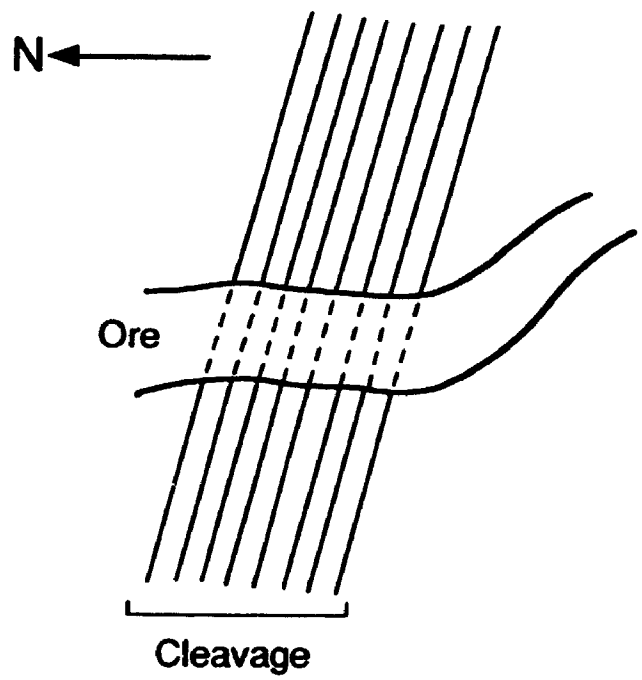

Figure 36: Sub- horizontal ore lens on the 1480 level. Bedding - cleavage relationship suggests proximity to the hinge of a fold.

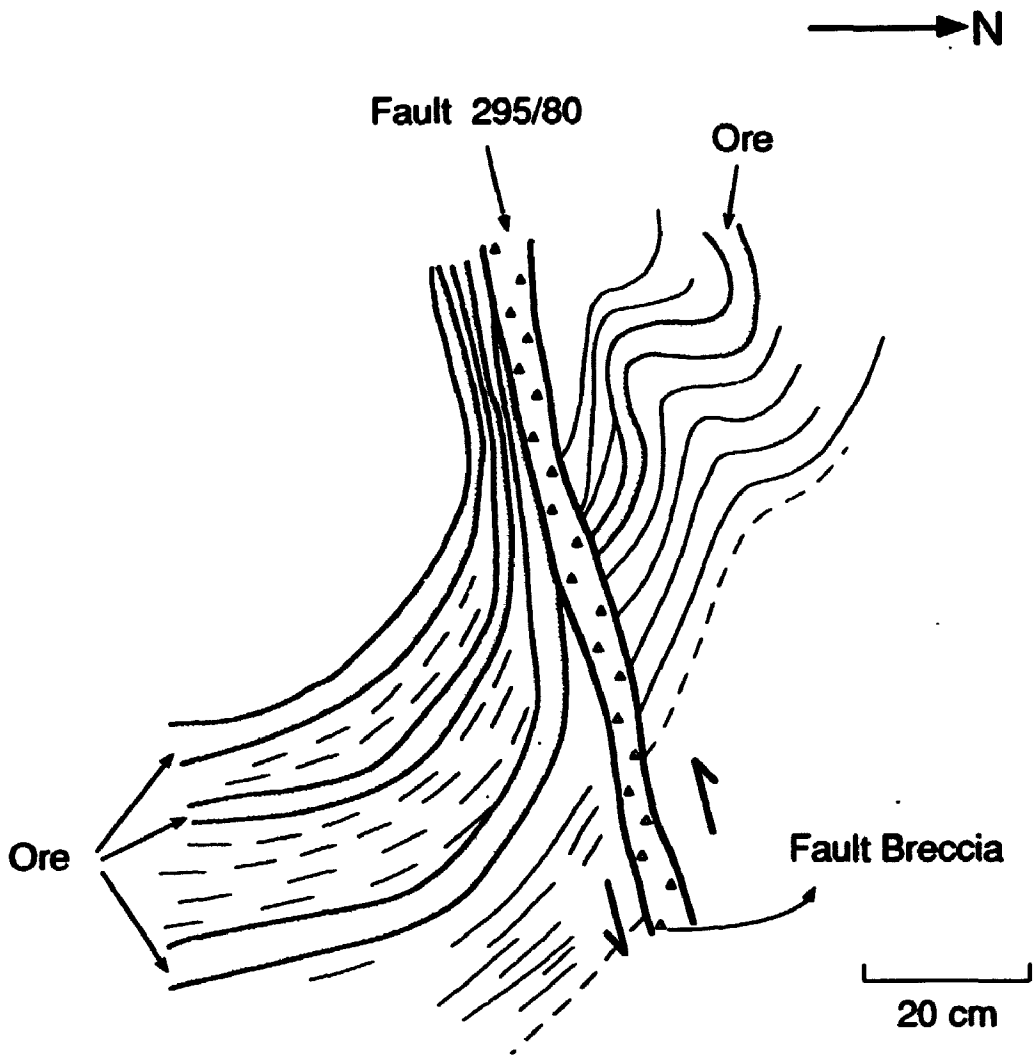

Figure 37: Sketch of massive sulphide bands hosted in quartz phyric rhyolite tuff displaced by a brittle fault. vertical displacement of the ore horizon is 30 to 40 cm. These brittle faults have no significant control on ore distribution.

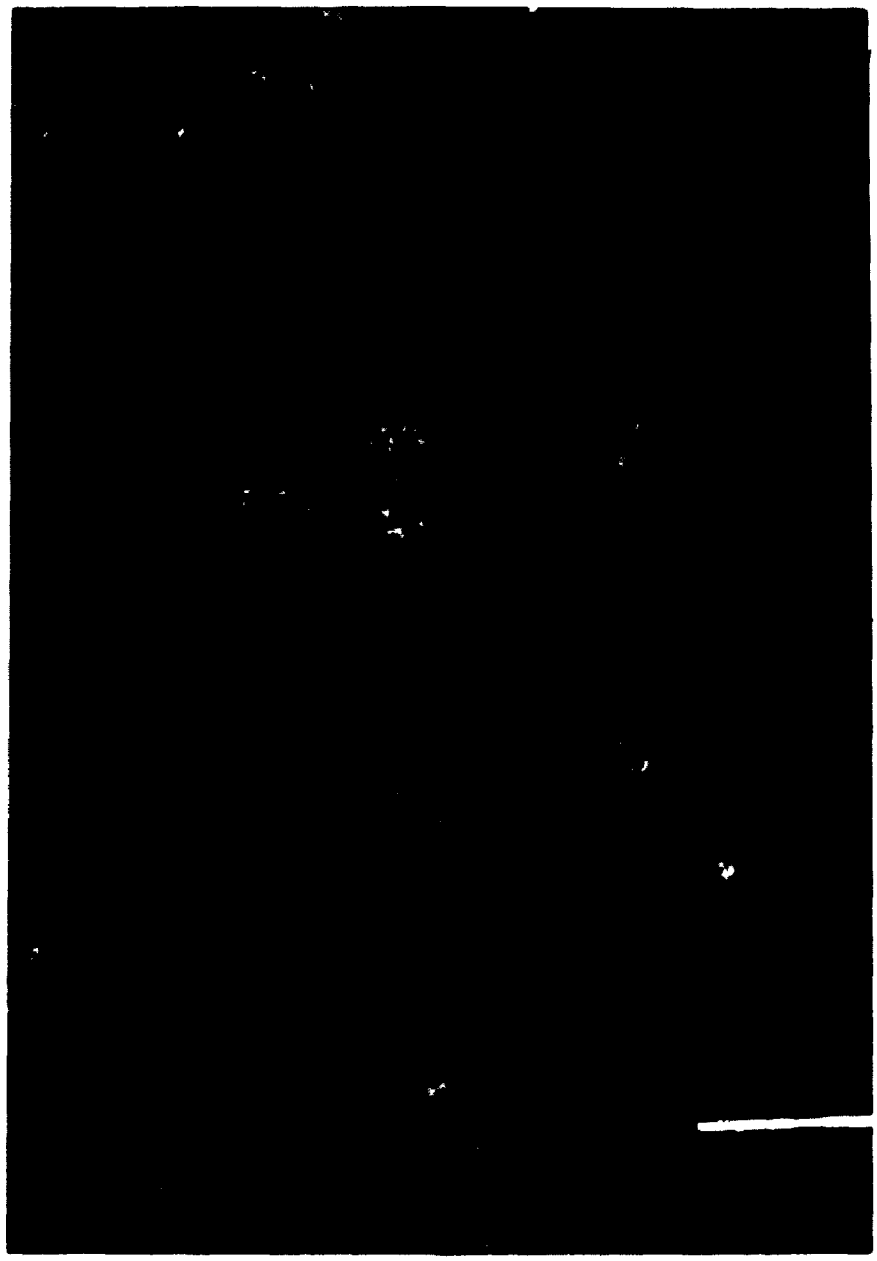

Plate 17: Photograph of the brittle fault sketched in Figure 37.

Appendix A-xvii: 1480 LEVEL 1230 SILL DRIFT / 1235 STOPE

At the entrance to the 1235 stope, quartz- phyric fragmental rhyolite forms the immediate footwall and hanging wall to the ore. Quartz eyes are typically blue and comprise up to 20% of the rock. Moving northerly and easterly from the sill drift into the stope, the hanging wall rock changes from quartz- phyric rhyolite to basalt. The contacts between the ore and the footwall and hanging wall rocks are well defined, shallow, and irregular.

A brittle fault zone cross cuts the ore and the footwall rocks. On the east wall, the fault zone is marked by a discrete 1 to 2 mm- thick planar discontinuity, whereas on the west wall, the fault is a 3 to 4 cm- wide zone comprised mainly of quartz, iron- carbonate, and sulphide fault breccia. The ore horizon is entrained on both sides of the fault, but no significant displacement (30 to 40 cm) occurs in the vertical plane. (Figure 37 and Plate 17). The localization of the ore on both sides of the fault, and the entrainment of the ore horizon suggests reverse movement. Striations were not observed on the fault plane.

Appendix A-xviii: 1480-1235 STOPE

Geological and structural relationships in this area are key to determining the structural style of the deposit. The geological section at 12200 E (Figure 9) indicates a flexure at the 1480 level. The 1480 - 1235 stope intersects this section and provides both plan and sectional views of the geology to complete the three dimensional picture.

At the west end face of the 1235 stope (Figure 38), the ore horizon is folded. Along section AB, the strike of bedding is parallel, but dip direction varies from south to north, to south, and then north again defining two synformal and antiformal structures (Figure 38B). The plunge of the fold axes is shallow (15°) trending east- southeast.

In this entire stope, the immediate footwall to the ore is characterized by a 30 to 60 cm- thick zone of banded cherty tuff, underlain by quartz- phyric fragmental rhyolite.

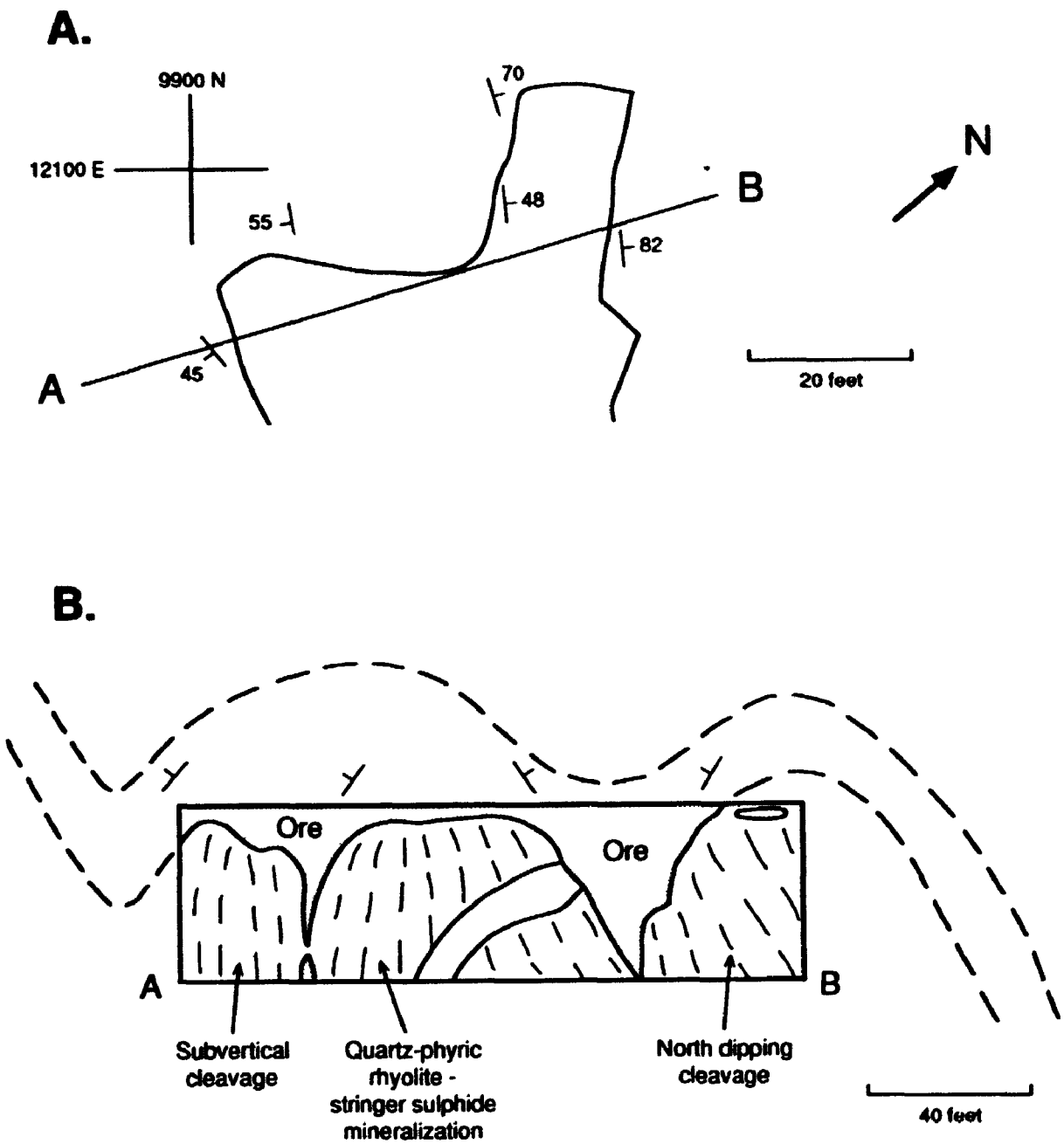

Figure 38: Sketch of section 12,200E on the 1480 level 1235 stope. A) Plan map of the west end face of 1480 level 1235 stope. This area intersects section 12,200E (Figure 9). B) Face sketch through section AB illustrating bedding relationships which define 2 antiformal and synformal structures.

This is atypical in comparison to other areas mapped in the mine; more commonly, blue quartz- phyric rhyolite tuff hosts the massive sulphides. In this area the banded tuff horizon typically contains 5 to 10% disseminated pyrite, and locally contains discontinuous veinlets of sphalerite parallel to bedding. The banded tuff is pervasively sericite- and carbonate- altered. The typical quartz- phyric fragmental rhyolite immediately underlies the tuff horizon. Quartz- phyric fragmental rhyolite footwall is composed of felsic fragments, 5 to 15 cm in diameter. Locally, large felsic fragments, varying from 60 cm to 1 m in diameter occur. Fragments are dark gray, supported by a white to light gray matrix.

Proximal to the ore, the matrix is pervasively chlorite altered, and contains 5 to 10%, 1 to 2 mm garnets, and up to 5% 1 to 2 mm euhedral pyrite. Fragments are iron-carbonate and sericite altered. Locally, chlorite stringers and sulphide veinlets occur, and garnets are more abundant, comprising up to 20% of the rock.

Rhyolite has a well developed schistosity oriented parallel to bedding in the tuffaceous horizon, and a strong cleavage oriented subperpendicular to bedding in the more massive and fractured underlying quartz- phyric fragmental rhyolite. Fragments and quartz-carbonate veinlets are oriented subparallel to foliation. The fragmental rhyolite is strongly jointed subparallel to the foliation.

Dark green, massive, aphyric basalt forms the hanging wall to the ore. Chlorite and carbonate alteration is pervasive.

A weak to moderate schistosity oriented subperpendicular to bedding occurs in the basalt up to 3 m from the contact with the host quartz- phyric rhyolite and ore.

In the entire area, the contacts between the ore and the footwall and hanging wall rocks are locally marked by a well defined quartz-breccia. These breccias are strongly fractured, and contain iron- carbonate and pyrite in the fractures. These breccias are discontinuous (Plate 12), and locally, up to 60 cm- thick. No movement or displacement

seems to have occurred associated with these quartz-breccia faults, other than very local dilation at the contacts.

Appendix A-xix: 1480 MANWAY DRIFT

This area was briefly examined as part of the overall walk through of the mine. The rock type observed in this area is a monotonous rhyolite, intruded by felsic dykes.

The rhyolite is massive, aphyric, and light gray to beige. At the entrance to this drift, a 2 m- wide zone of shallow south dipping (120/33) alteration bands occur. These bands vary from 2.5 to 9 cm- thick, and are defined by black chlorite rich bands alternating with gray-silica-carbonate rich bands.

At the manway, two parallel felsic dykes cross cut the rhyolite (Figure 39). These dykes are folded, and exhibit a well defined southward vergence. One dyke is uniformly 10 to 15 cm- thick, whereas the other dyke is 60 cm- thick in the limbs, and structurally thickened to 3 m- thick in the nose of the fold.

Appendix A-xx: 1480 LEVEL - CROSS CUT NORTH OF MANWAY DRIFT

This cross cut shows the footwall contact with the ore. All the units are dipping north, showing southward vergence. Quartz- phyric rhyolite contains quartz- phyric fragments. Fragments are subrounded to angular, 5 to 15 cm in diameter, and locally up to 1 m in diameter. Fragments are slightly darker than the matrix. Rhyolite exhibits a moderate foliation defined by an evenly spaced cleavage. The entire drift is well jointed. Bedding is difficult to define in the rhyolite fragmental unit because the fragments are poorly defined, and gradation of the fragment sizes was not observed.

A north- dipping, 30 to 45 cm- thick, fine- grained, felsic dyke is cross cuts the rhyolite. On the west wall, the felsic dyke is coarser- grained, and up to 1 m- thick. This dyke is discontinuous, and isoclinally folded, with both limbs dipping north. Folds in this

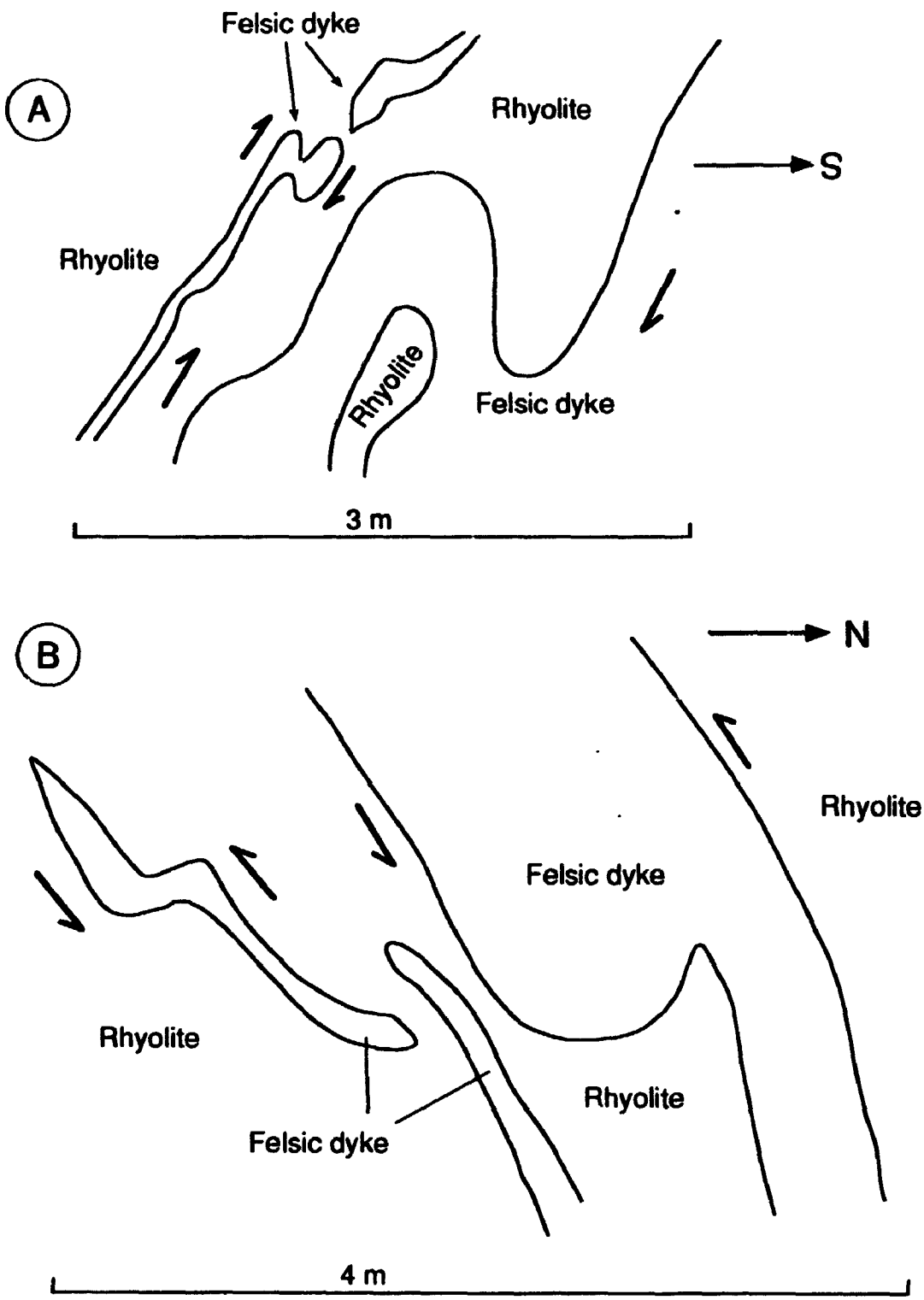

Figure 39: Folded felsic dykes illustrating southward vergence, structural thickening in the hinge, and attenuated boudinaged fold limbs. A) looking east; B) looking west.

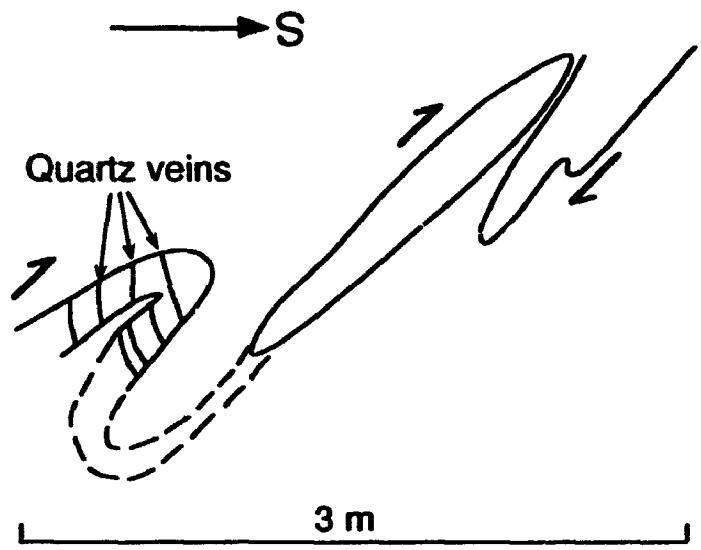

Figure 40: Isoclinally folded felsic dyke cross cuts the footwall rhyolite. Typically, north dipping limbs of the fold show southward vergence.

north- dipping dyke have southward vergence (Figure 40). A strong foliation occurs in the dyke parallel to the intrusive contact. Pyrite mineralized quartz veins occur at the dyke contact, and within the dyke. Locally, pyrite- filled fractures comprise up to 25% of the quartz veins.

Stratigraphically up section there is a noticeable increase in the amount of deformation in the fragmental rhyolite. The fragments are strongly elongated parallel to the foliation. Numerous small- scale quartz-carbonate veinlets occur parallel to the foliation. Proximal to the ore, the matrix of the fragmental rhyolite is pervasively chloritized and contains 5 to 10%, 1 to 2 mm garnets. The fragments are carbonatized and sericitized. Up to 5%, 1 to 2 mm euhedral pyrite occurs in the matrix and the fragments.

A 2 mm- wide discrete brittle fault, filled by quartz, cross cuts the rhyolite. Slickensides formed in the quartz-infill to the fault plunge shallowly east, and the direction of motion is oblique dextral.

The contact between the ore and the footwall in this area is shallow and irregular, locally marked by a well defined 15 to 20 cm- thick quartz-breccia. The quartz-fault breccia contains calcite and ferroan dolomite, plus 5 to 15% pyrite, and trace galena. Carbonate and pyrite are related spatially. Striations along this quartz-breccia plunge east. No displacement was observed along this fault breccia.

The ore zone comprises dominantly of pyrite. However, at the contact with the quartz-breccia, the ore is extremely rich in sphalerite. A 15 cm- thick massive sphalerite band occurs at the base of the massive sulphide horizon, in contact with the quartz-fault breccia.

Appendix A-xxi: 1480 TO 1580 RAMP

This area was mapped for stratigraphic and structural information of the middle section of the mine. The area (Figure 41) is comprised of footwall sedimentary rocks, including banded iron formation interbedded with graphite shale, quartzose pelite, and beds of massive pyrrhotite and pyrite. The sedimentary rocks are folded, and the structural data obtained provide additional information for the deformation history of the mine area.

There are no correlative units between the east and west walls along the southern part of the ramp, because this area transects a longitudinal section, parallel to the strike of the strata. Where the ramp changes direction, cross sections of the sedimentary strata were observed.

Banded iron formation on this level is compositionally different from that observed on other levels. Banded iron formation here is composed of 10 to 30 cm- thick black and gray chert beds containing 3 to 10 mm- thick laminations of magnetite. Two and a half to 15 cm- thick chlorite and argillite beds alternate with the chert beds.

Further up section, beds of magnetite alternate with beds of chert and siderite. The beds are of uniform thickness, averaging 1 to 2 cm- thick.

Medium- grained pink, white, and gray quartzose pelite beds are intercalated with the iron formation. One to 2 cm- thick pink and gray beds alternate producing a colour banding. The pink beds are feldspathic containing up to 10% pink feldspar. The pelites contain 4 to 5%, 1 to 5 mm pyrrhotite nodules, and 2 to 3% chlorite flakes, 1 to 3 mm- in width. Locally, quartzose pelite is cross cut by 1 cm- thick, contorted and folded pyrite and pyrrhotite veinlets. Several 30 to 60 cm- thick beds of massive pyrrhotite and pyrite are intercalated with the quartzose pelite.

Fine- grained graphitic pelite and quartzose pelite beds (described below in Appendix A-xxii: 1580 ramp and level intersection) occur overlying the iron formation. Locally, laminations of graphitic shale are intercalated with the quartzose pelite.

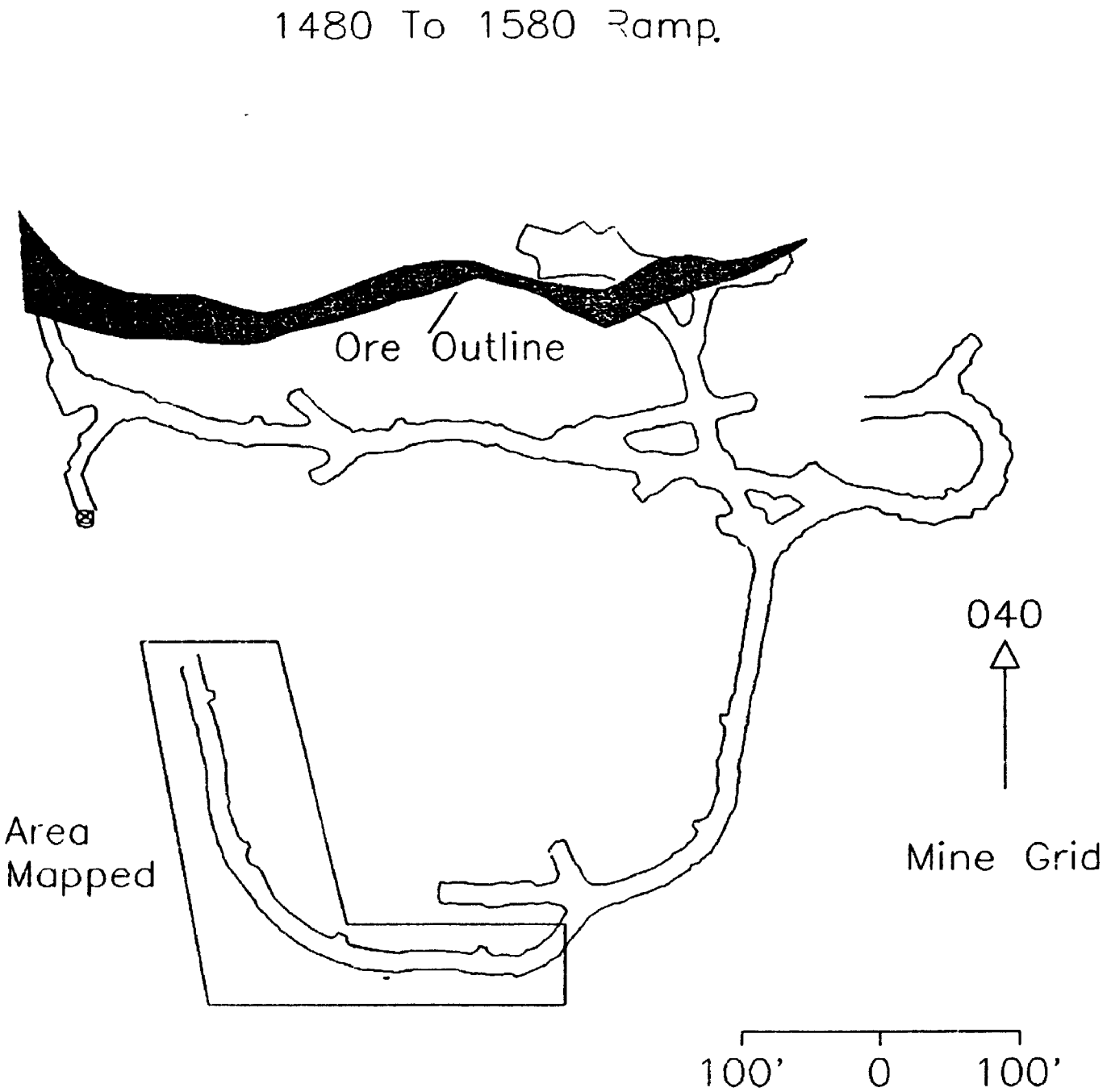

Figure 41: Area mapped along the ramp from 1480 level to 1580 level. This areas is entirely within the sequence of footwall sedimentary rocks.

Several intermediate dykes intrude the sedimentary rocks. These dykes are light brown to light rust in colour, medium- grained, and contain 25 to 30% amphibole phenocryst pseudomorphs, altered to chlorite, in a quartz and feldspar matrix. The matrix is pervasively carbonate- altered. Five to 10%, 1 to 3 mm- thick quartz and carbonate veinlets within the dykes are oriented parallel to the intrusive contacts, producing a banded appearance.

The sedimentary rocks are structurally massive, homogeneous, and lacking a defined cleavage. Locally, a weak foliation is observed in quartzose pelites defined by chlorite and sericite. Bedding is parallel to the foliation.

Throughout this entire area, the banded iron formation is folded. All the banded iron formation beds follow continuously. Class 1a and 1c parallel open folds are the most common type of fold observed in the chert beds in the iron formation, and class 2 similar folds are common in the iron- silicate beds of the iron formation Figure 42). The axial plane of those folds is not always parallel from one fold to another, some folds are reclined and some are inclined (Figure 43). Typically, beds of iron formation whereas pelite beds are tightly folded (Figure 44). Beds may be broken along the limbs of a fold, or at the hinge of a fold. Evidence of small scale refolding was not observed, in contrast to the folding observed on the 1000 level.

A subvertical brittle fault cross cuts the quartzose pelite (Figure 45). Striations on this fracture plane plunge shallowly west. Slickensides of quartz on the fault plane plunge 32° west, and indicate sinistral movement. Subhorizontal quartz-filled tension fractures occur on both sides of the fault. These quartz veins are 2.5 to 8 cm- thick, 2 m long, and minor calcite. Normal offset of the quartz veins is 2 to 3 cm.

A steep, north- dipping, 20 to 30 cm- thick shear zone cross cuts beds of iron contain formation, and an intermediate dyke (Figure 46). A 5 to 15 cm- thick quartz and iron- carbonate vein occurs within the shear zone. The dip of the shear foliation within the

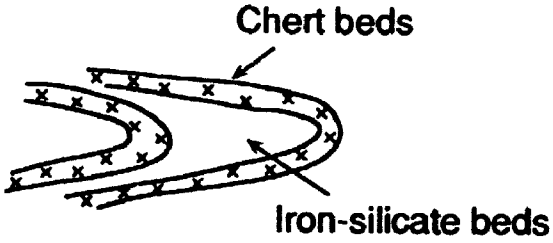

Figure 42: Typical type of folds in the banded iron formation. Parallel type folds in chert beds and similar type folds in iron- silicate beds.

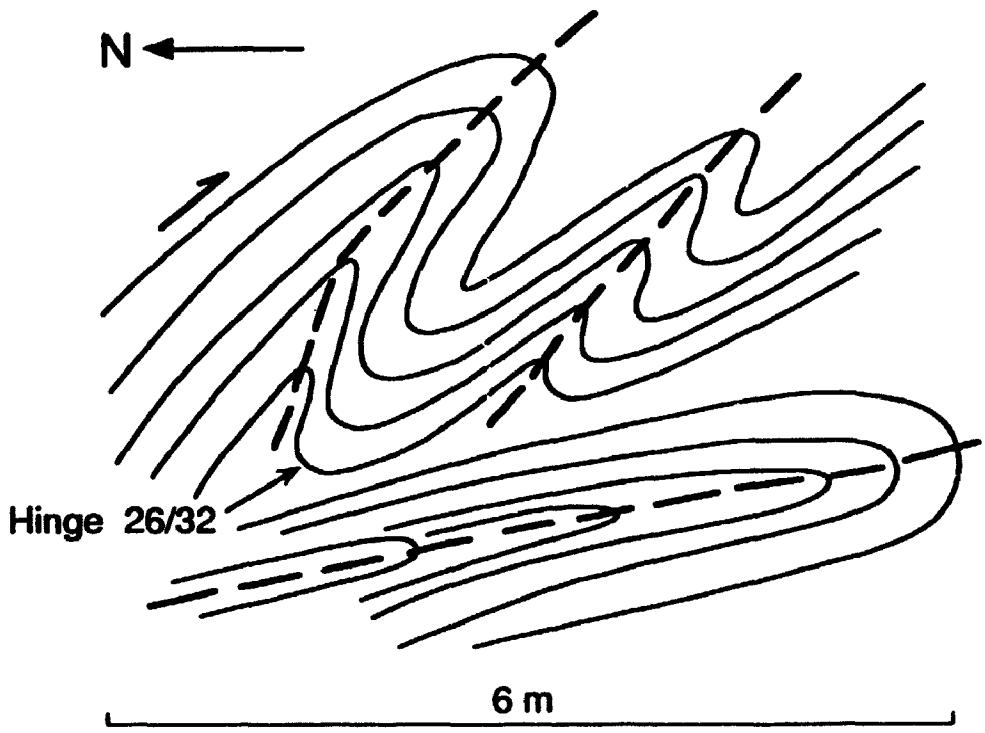

Figure 43: Parallel and similar type folds in banded iron formation. the axial plane of the folds is not always parallel. Some folds are reclined.

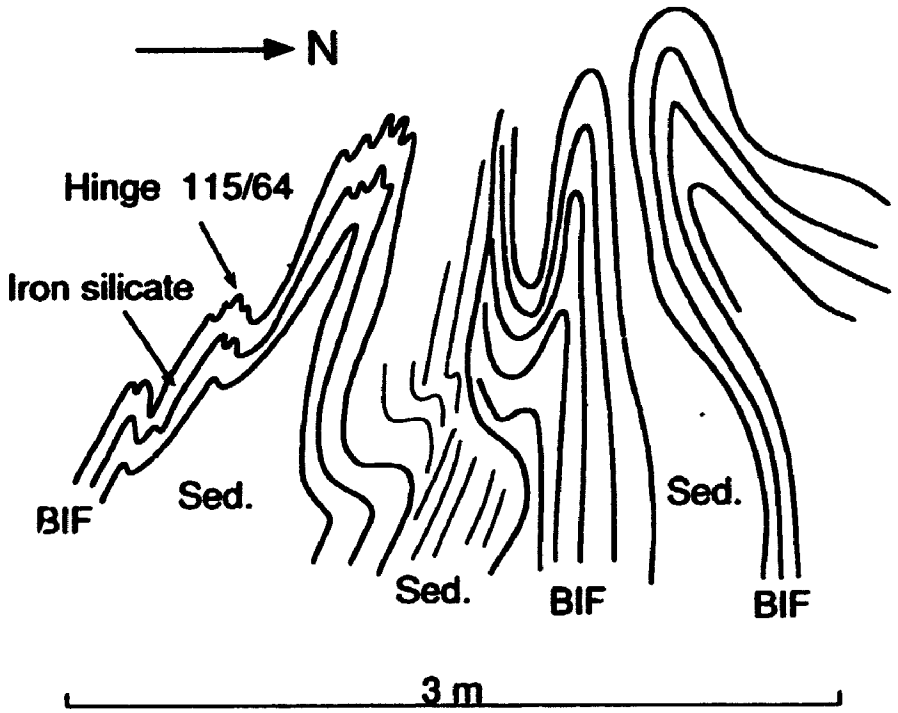

Figure 44: Isoclinally folded banded iron formation intercalated with tightly folded sedimentary rocks. Bedding is traced using silicate and cherty beds in the iron formation.

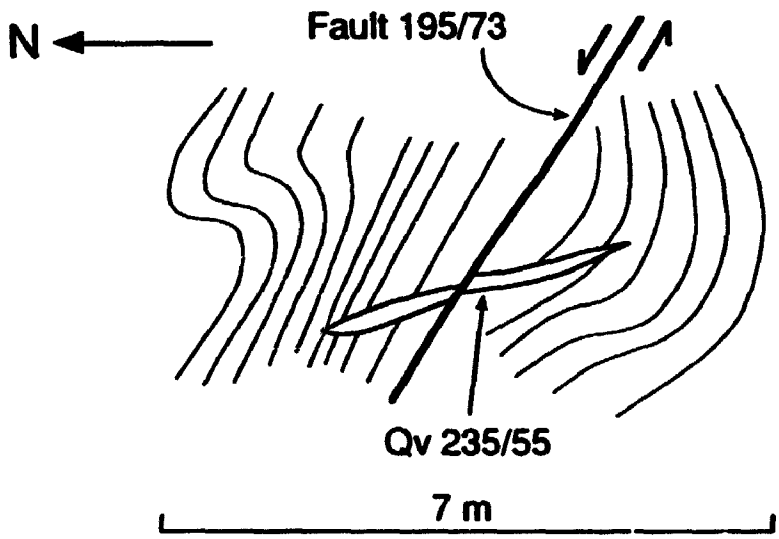

Figure 45: Bedded quartzose pelite truncated by a normal sinistral brittle fault.

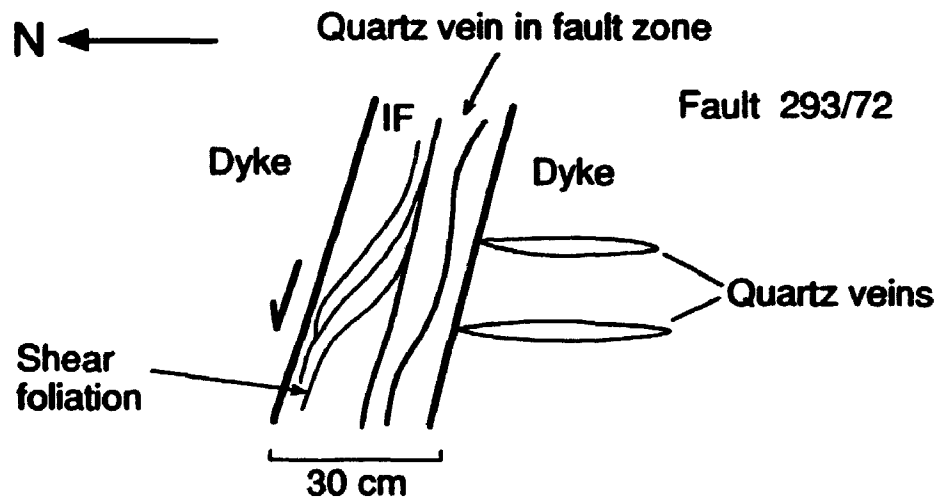

Figure 46: Shear zone in iron formation and intermediate dyke. Sigmoidal schistosity in the shear zone at a shallower angle than the shear boundaries suggest normal movement.

shear zone boundaries is shallower than the dip of the shear zone boundaries, suggesting normal movement of the fault. Striations were not observed on schistosity planes or the fault plane. Subhorizontal quartz veins in the dyke in the structural footwall south of the fault, suggest vertical movement.

Locally, rods of magnetite define a lineation; striations on magnetite bedding planes in the iron formation plunge 30 ^{o} towards the east. These lineations are oriented parallel to the fold axis of the mesoscopic folds in the iron formation. Slickensides suggest dextral movement parallel to the fold axis.

A north- dipping 1 to 2 mm- thick brittle fault cuts the iron formation. The fault is splayed, and the fault surface is characterized by brown to black fault gouge clays. Well defined striations and slickensides on the fault plane plunge shallowly east, and steps indicate sinistral movement. Between the splayed fault boundaries, the iron formation is pervasively carbonate and sericite altered.

Several 1 to 2 mm- thick brittle faults were observed cross cutting the graphitic shales. These faults are filled with quartz and carbonate.

Jointing occurs in the graphitic shales, oriented perpendicular to bedding.

Appendix A-xxii: 1580 RAMP AND LEVEL INTERSECTION

This area is important, as it shows the relationships between the rhyolite and the underlying sedimentary rocks. The lithological units in this area include massive, poorly bedded graphitic pelite and quartzose pelite, which form the top of the sequence of sedimentary rocks, conformably overlain by quartz- phyric rhyolite. Locally, beds of quartz- phyric rhyolite are intercalated with the sedimentary rocks. Figure 47 is a location map indicating the area mapped. This section describes area A on the map. The quartz-phyric rhyolite is described in Appendix xxii below.

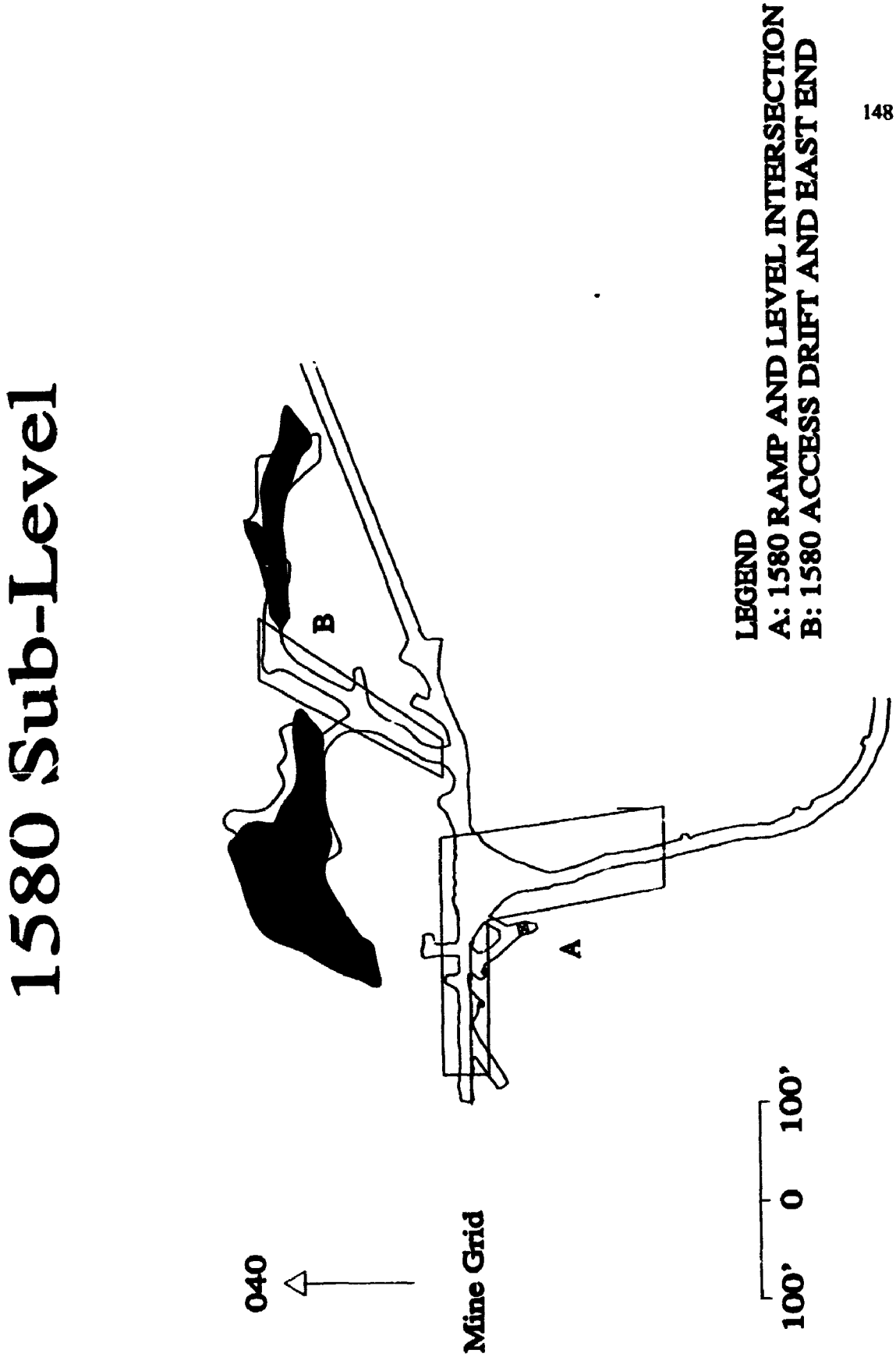

Figure 47: Location of the area mapped in detail on the 1580 sub-level.

Graphitic shale is dark gray to black, very brittle, and exhibits conchoidal fractures. One to 5 mm size, ovoid pyrrhotite blebs comprises 5 to 8% of the unit. These blebs are evenly distributed throughout the unit. The long axes of these blebs are oriented subparallel to the foliation. Millimeter- scale stringers and fractures oriented subparallel to the foliation are composed of pyrrhotite.

The quartzose pelite is massive, pale yellow to light beige, comprised of moderately sorted, subrounded to subangular, silt to sand size quartz grains and minor feldspar grains. Clastic grains are well packed and comprise 80% of the unit. In thin section, quartz grains are clear, and feldspar grains are frosted due to alteration to mica. The matrix comprises of clay- size quartz, sericite, and biotite. Chlorite is locally present, associated with biotite. The unit is pervasively carbonate- altered.

The contact between graphitic pelite, and the overlying quartz- phyric rhyolite was observed in one location. At this location, no apparent structural disruption along this contact was evident.

A 30 to 60 cm- thick shear zone oriented parallel to bedding (295/81) cross cuts the graphitic shale. A discrete 1 to 2 mm- thick north- dipping brittle fault cross cuts the quartzose pelite. Coarse- grained quartz grains up to 6 mm in diameter fill the fault plane. Both the fault and shear zone are oriented subparallel to bedding.

Appendix A-xxiii: 1580 LEVEL ACCESS DRIFT AND EAST END

The following area was mapped as a continuation of the stratigraphic information from the footwall sedimentary rocks in the ramp, to the footwall rhyolitic rocks. The area mapped is indicated as area B on Figure 47.

This area comprises of footwall rhyolitic ash and quartzose breccia. Graphitic pelite beds underlie the footwall rhyolite (described in Appendix A-xxii).

Rhyolite ash is light gray, massive, quartz- phyric, and sugary textured. One to 2 mm size quartz eyes make up 10% of the rock. Locally, rhyolite contains 5% disseminated pyrite. A 15 cm- thick, north- dipping lens of massive sphalerite and pyrite, plus minor pyrrhotite occurs in the quartz- phyric rhyolite. This sulphide lens is approximately 30 m into the footwall stratigraphically below the main ore body. At the contact between rhyolite ash and the underlying graphitic pelites, the ash is bedded.

Quartzose breccia overlies the rhyolite ash, and comprises of angular, white quartz fragments. Fragments vary from 2 to 10 cm- in diameter, supported in a dark green to black, fine- grained chloritic matrix.

The contact between rhyolitic ash and the overlying quartzose breccia is very diffuse, marked by a 10 m wide deformation zone. A 30 cm- thick felsic dyke occurs in the rhyolite ash within this shear zone. Within the shear zone, both rhyolite ash and quartzose breccia are garnetiferous. Garnets comprise up to 10% and vary in size from 1 mm to 3 mm. Sericite alteration is pervasive, and defines the foliation in the shear zone.

The entire area exhibits a strong, steep, north- dipping penetrative fabric. Fragments in the quartzose breccia are oriented parallel to the foliation.

Appendix A-xxiv: 1640 LEVEL WEST SILL

All the areas mapped on this level expose massive sulphide lenses and footwall rocks (Figure 48). The footwall rocks include quartz- phyric rhyolite ash and lapilli tuff. The footwall rocks are pervasively altered to chlorite, sericite, and garnet, with local carbonate alteration. Pyrrhotite stringers and microfractures are abundant in the immediate footwall to the ore. The entire area exhibits a very strong foliation. The ore lens observed in this drift is folded.

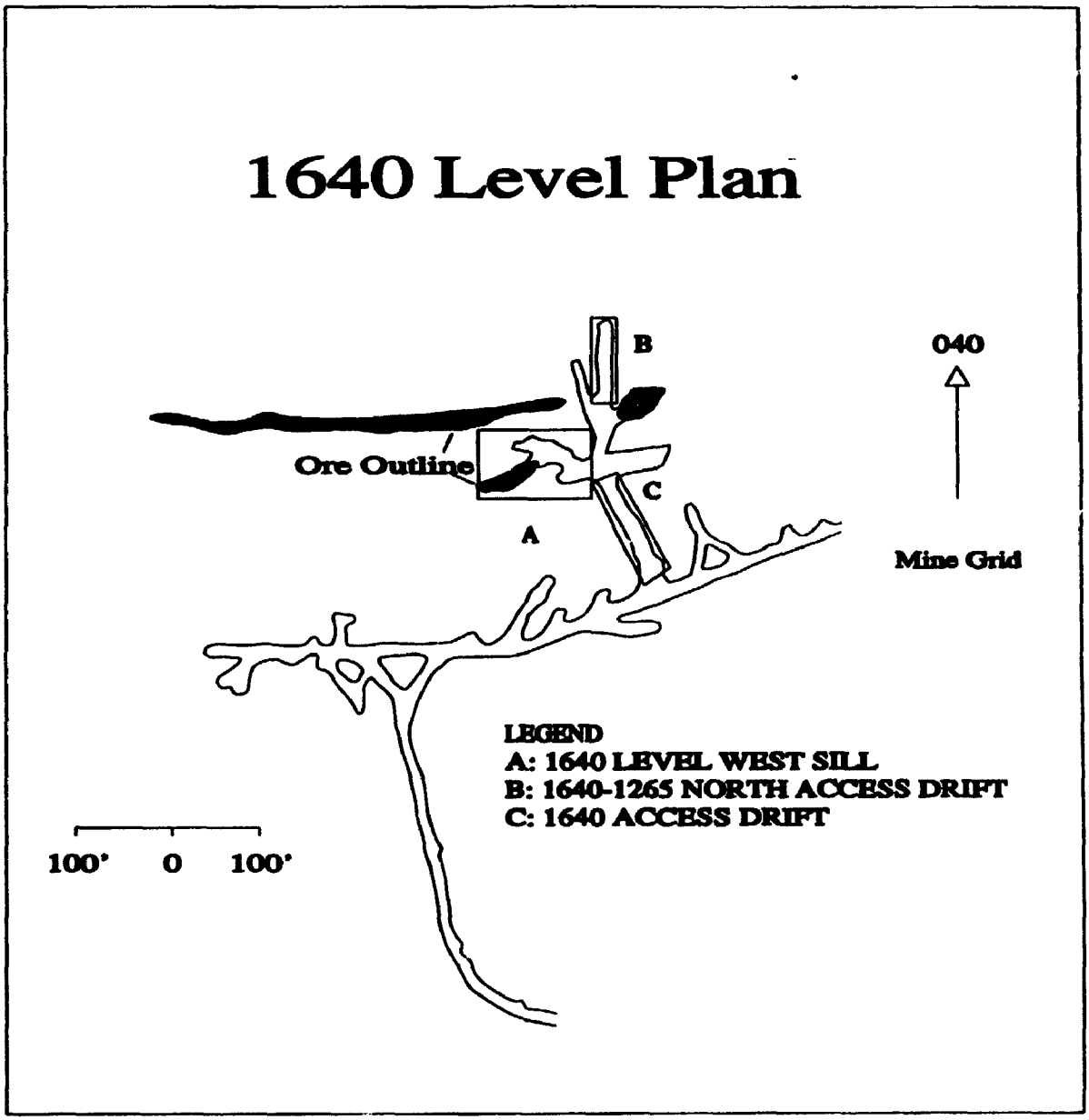

Figure 48: Location map of areas mapped in detail on the 1640 level.

Rhyolite is a medium gray to beige lapilli tuff. Milky white lapilli comprise 10 to 15% of the unit, in a quartz- phyric ash matrix. Locally, fragments are block size and contain blue quartz phenocrysts. In the ash matrix, quartz phenocrysts are gray and blue, translucent, average 1 mm in diameter, and comprise 1 to 2% of the rock. The immediate footwall to the ore horizon is ash. Quartz phenocrysts are blue, up to 2 mm in diameter and comprise 8 to 10% of the rock.

The footwall rhyolite is intruded by several north- dipping feisic and intermediate dykes.

Massive sulphides in most of the area is located in the back of the drift. The massive sulphide lens as a whole is comprised of discontinuous and smeared bands of medium- grained pyrite and sphalerite. These bands are oriented subparallel to the bedding. Sphalerite bands are more abundant at the outer margins of the massive sulphide horizon, and pyrite bands are more abundant in the core of the lens. Locally, 60 to 90 cm-blocks of altered rhyolite are caught up in the massive sulphide horizon. Sulphide bearing quartz breccias are common along the ore contacts. Eastward in the drift, the massive sulphide lens is exposed on a west facing wall. The lens is subhorizontal and dipping shallowly east.

Quartz- phyric rhyolite ash in the immediate footwall to ore is pervasively altered to chlorite, sericite and garnet. Locally, porphyroblasts of calcite up to 1 cm- in diameter are abundant in garnetiferous zones immediately below the massive sulphide lens. Carbonate occurs as single subhedral to euhedral rhombs, is evenly distributed, and locally, occurs as patches of aggregates. Locally, rhyolite is bleached in silicification zones. Stringers and microfractures of quartz + carbonate + pyrrhotite, and quartz + pyrite + chalcopyrite are common, comprising 3 to 5% of the footwall rhyolite.

Almandine garnets are pervasive in this area. Garnets are 3 to 5 mm in diameter, locally up to 1 cm in diameter and comprise 1 to 3% of the rock. Garnets are commonly

more abundant in chlorite altered zones, and in the immediate footwall rhyolite to the ore, comprising 10 to 15% of the rock.

The rocks in the entire area exhibit a strong penetrative foliation striking northwest, and dipping steeply north. The massive sulphide horizon and the contacts with the host rocks are highly strained. Quartz-breccia units are particularly common in these high strain zones. Cherty fragments in the rhyolite host rock are oriented subparallel to the foliation, and have aspect ratios which vary from 3:1 to 6:1. Sericite and chlorite define the foliation. Locally, patchy sericite and chlorite alteration is oriented subparallel to the foliation, and produces an apparent fragmental texture.

A gentle east plunging parasitic fold occurs on the south limb of the massive sulphide horizon. The fold axis trends east and plunges 20 to 30 degrees. The fold is tight to isoclinal in the west end of the drift. Eastward towards the main drift, the fold is more open.

Appendix A-xxv: 1640 - 1265 NORTH ACCESS DRIFT

The dominant rock type observed in this drift is heterolithic quartzose breccia. This breccia overlies the quartz- phyric ash described in the 1640 west sill. Beds of aphyric and quartz- phyric ash and lapilli tuff are intercalated within the breccia. Intercalations of ash are more abundant near the upper contact of the breccia.

The breccia is composed of angular fragments of varying composition, in an aphanitic dark green to black matrix. Fragments comprise 30 to 50% of the unit. The types of fragments observed include; white chert, iron sulphide, chlorite, and quartz-phyric rhyolite. Blue and gray quartz phenocrysts occur in the matrix, and in some cherty fragments. The matrix is chloritic, graphitic, and contains up to 10% chloritoid. Locally the matrix is garnetiferous. The composition of the matrix suggests a sedimentary origin for this rock type. However, quartz eyes in the matrix may suggest a volcanic origin.

Beds of quartz- phyric rhyolite ash and lapilli tuff intercalated with the breccia comprise of 3 to 4% blue quartz phenocrysts. Cherty lapilli comprise 5 to 10% of the unit. The ash matrix is pervasively chlorite and sericite altered. The contacts between the ash and lapilli tuff beds and the heterolithic breccia are gradational.

Petrographically, the matrix of the heterolithic breccia is comprised of interlocking quartz, plagioclase, and sericite. Felsic lithic and cherty fragments are distinguished from the matrix by the finer- grain size of recrystallized quartz, and pervasive sericite alteration of the fragments. Quartz phenocrysts vary from 0.5 to 2 mm in diameter, and comprise 1% of the unit. Commonly, quartz phenocrysts are fractured, and fractures are infilled with fine- grained polygonized quartz.

Ten percent of 0.5 to 2 mm chloritoid porphyroblasts occur in the matrix. Chloritoid is randomly oriented, evenly distributed, and locally in clusters. Texturally, chloritoid grains are twinned and skeletal. Some chloritoid grains are intergrown with polygonized quartz.

Calcite occurs in veins and microfractures. Proximal to the ore, this unit is pervasively chlorite and carbonate altered.

A very strong schistosity is developed in the unit, defined by sericite and chlorite in the matrix. The intensity of deformation is exhibited by the rotation of some quartz phenocrysts, and the schistosity wraps around these grains.

Appendix A-xxvi: 1640 ACCESS DRIFT

This drift extends from the 1640 west sill to the main haulage drift. This drift cross cuts the deeper footwall rocks, but does not extend into the footwall sedimentary rocks.

The entire drift comprises of aphyric rhyolite ash, and locally quartz- phyric rhyolite ash to lapilli tuff. The rocks are aphyric except where local quartz eyes and lapilli

are observed. The quartz phenocrysts are blue, 0.5 to 1 mm in diameter, and comprise less than 1% of the rock.

Aphyric rhyolite ash is medium gray, massive to weakly foliated. Fractures and joints are evenly spaced 1 to 2 m apart, producing an overall blocky appearance. Conchoidal fracturing is common, suggesting the unit is very siliceous. The only variation observed in this section is the presence or absence of quartz eyes and lapilli. Contacts between the aphyric ash and phyric lapilli tuff are very diffuse, and bedding planes are indistinguishable.

Alteration in this area is very weak. Irregular patches of sericite alteration, and chlorite alteration were observed. Less than 1% disseminated pyrite, and less than 1%, 1 to 3 mm garnets occur sporadically throughout the unit.

Appendix A-xxvii: 1720 SUB - LEVEL

This area was mapped to examine the relationship between the massive sulphides in this drift and the ore body, 100 m to the east (Figure 49). The rock types observed include massive sulphides and the typical quartz- phyric rhyolitic lapilli tuff.

Several massive sulphide lenses up to 1 m- thick, and comprise of fine- to medium-grained pyrrhotite and pyrite. Pyrrhotite and pyrite stringer zones are commonly associated lateral to, and/or in the footwall to, the massive sulphide lens. One of the lenses observed exhibits a geometric configuration resembling an "M" shape, typical in the hinge area of a fold (Figure 50).

A 20 cm- thick, medium- grained intermediate dyke cross cuts the rhyolite, and occurs in contact with a massive pyrrhotite lens at the west end face. The dyke is tightly to isoclinally folded, and broken in the hinge area (Figure 51). The dips of the limbs and the axial plane are steep, oriented subparallel to bedding, and to the penetrative fabric.

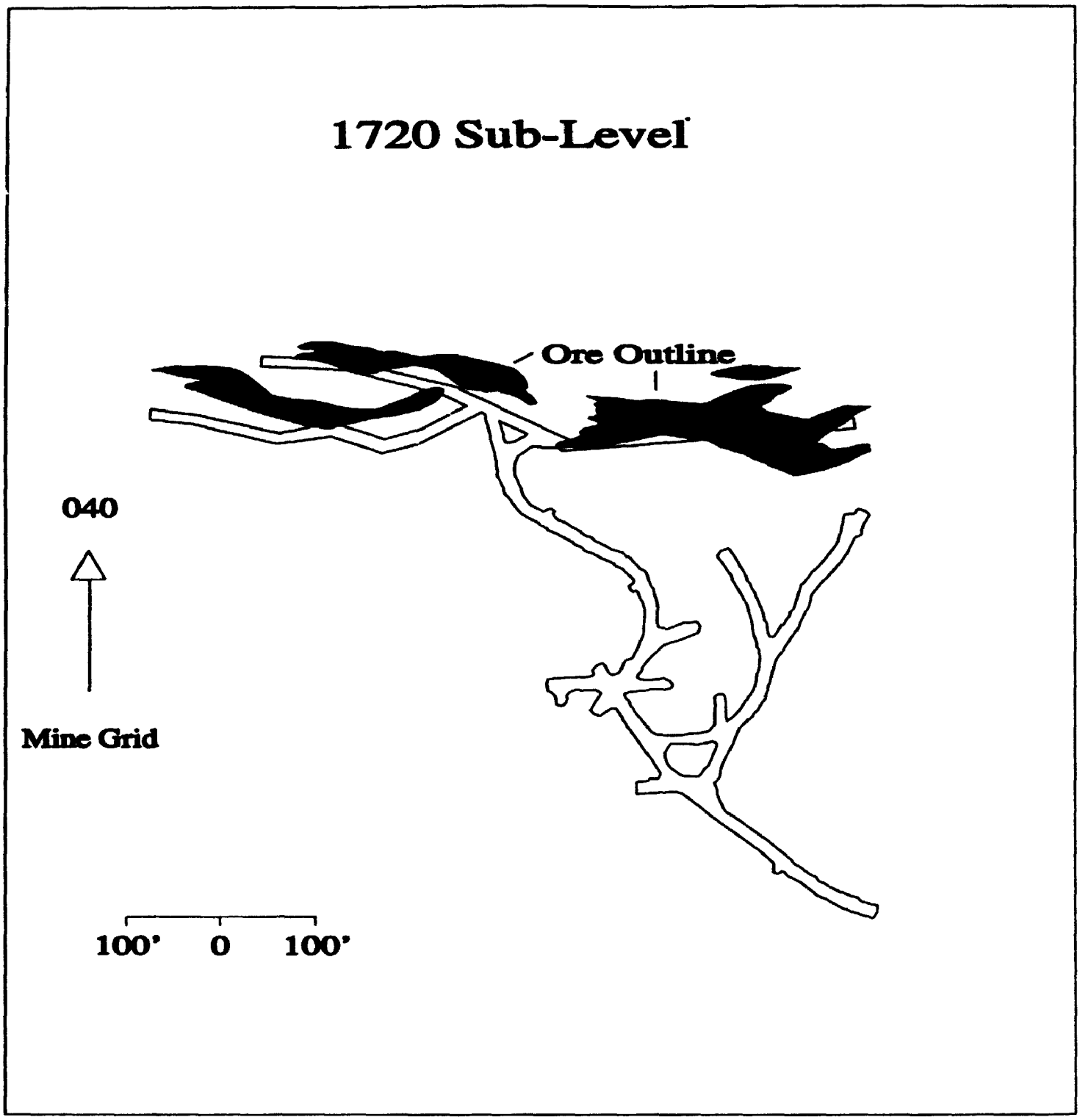

Figure 49: Location map of detailed mapping on the 1720 sub-level.

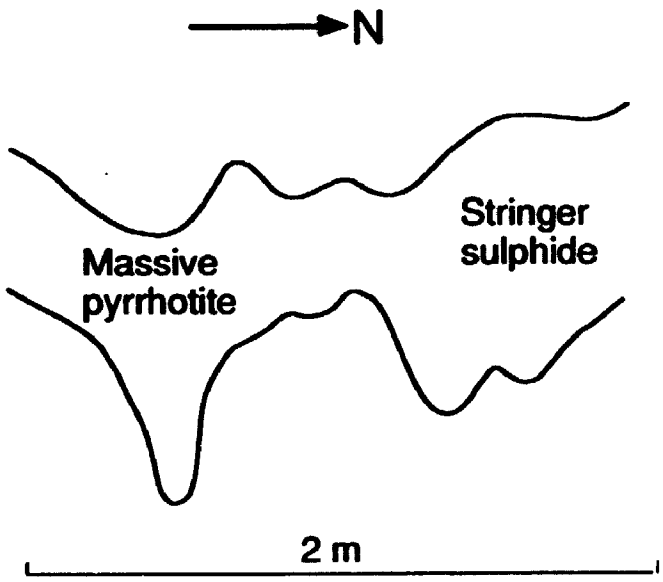

Figure 50: Massive sulphides exhibiting "M-shaped" folding typical in fold hinges.

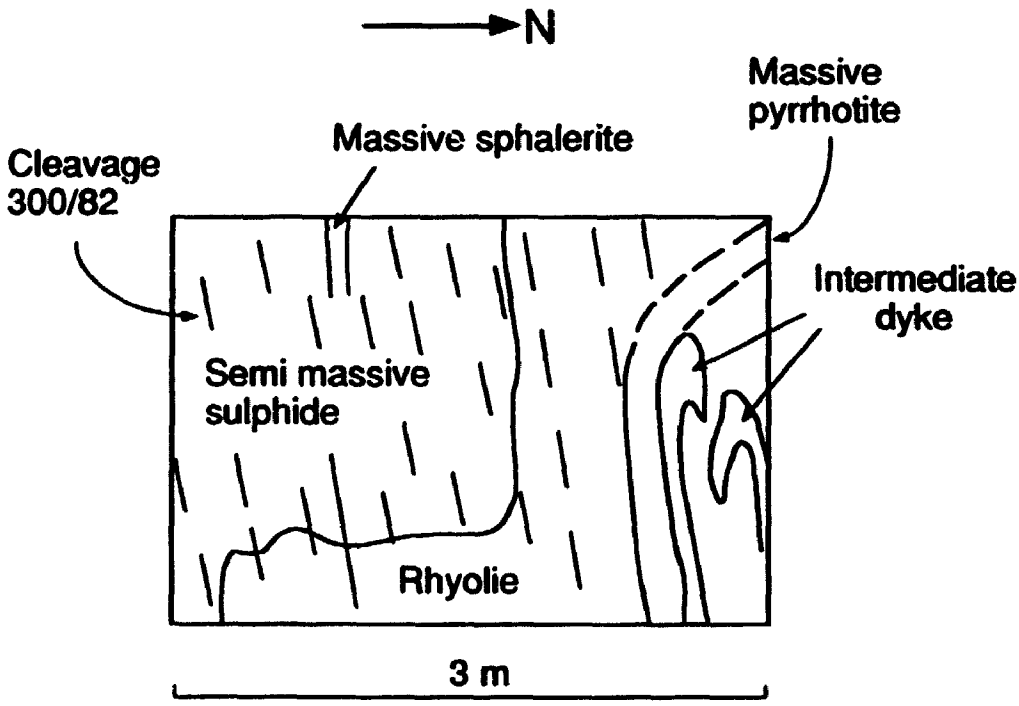

Figure 51: West end face of the 1720 sub-level north drift. Note the isoclinally folded and broken intermediate dyke. the dip of the fold limbs is sub- parallel to the axial planar cleavage of the dyke and the open fold of the rhyolite and massive sulphides.

Numerous subhorizontal quartz veins occur in the rhyolite along the drift. Locally, the veins occur in an en echelon pattern. Veins are 1 to 2 m long, and 2.5 to 20 cm- thick. They comprise of white quartz, 2% carbonate, 2% pyrite, and locally trace galena. Carbonate and sulphides occur as fracture infilling in the quartz.

Throughout the entire drift, rhyolite and massive sulphides are strongly deformed by a northwest striking, steep, north- dipping cleavage. The long axes of both sulphide stringers and elongate cherty lapilli, are oriented parallel to the foliation. Shearing occurs at the contacts between massive sulphide lenses and rhyolite.

The area is moderately jointed and fractured. Joints and fracture planes are oriented parallel to cleavage.

Lineations along cleavage planes are defined by sericite, and plunge shallowly east. Locally, quartz slickensides and striations on fracture planes also plunge shallowly east, and indicate both reverse (oblique) sinistral and dextral motion.

Appendix A-xxviii: 1800 LEVEL

This level has the most laterally extensive drift in the mine, which extends from the shaft, due east 1300 meters (4000 feet) (Figure 52). This tracked level is the main tramming horizon where locomotives move the ore.

This level was briefly examined to document structural observations, and similarities and/or differences of the lithological units, at a lower level in the mine.

Quartz- phyric rhyolitic ash is intercalated with banded iron formation and graphitic pelite. The rhyolite is composed of < 1%, 0.5 to 1 mm gray quartz phenocrysts.

Graphitic pelite is fractured containing iron- carbonate filled fractures up to 3 cm-thick. Locally, the graphitic beds are schistose.

Banded iron formation on this level is compositionally similar to that observed on the 600 and 1000 levels (600 level ore pass, and 1000 level conveyor belt). Banded iron

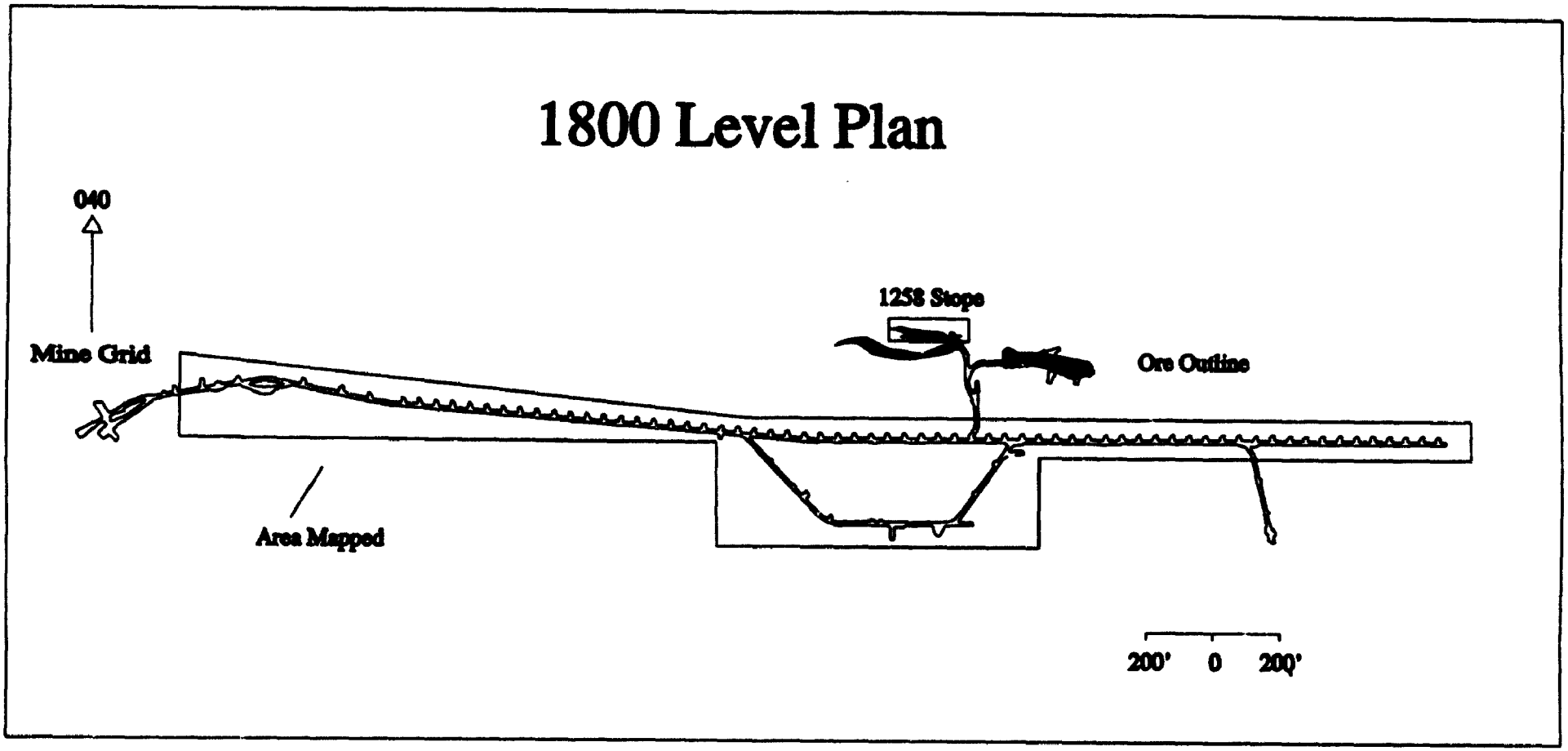

Figure 52: 1800 level plan.

formation is comprised of beds of chert, iron- silicate, iron- carbonate, +/- iron- oxide. Beds average 5 to 8 cm- thick. Locally, 2.5 to 5 cm- thick magnetitic beds are intercalated with cherty beds containing laminations of magnetite.

Along the entire length of this level, banded iron formation strikes northwest, and dips steeply north and south. Locally, banded iron formation is isoclinally folded with fold wavelengths up to 6.5 m. Fold hinges plunge east 20 to 30 degrees.

In the 1800-1258 north stope, heterolithic quartzose breccia was observed in the immediate footwall to the ore. This quartzose breccia was also observed in the footwall to the ore on 1580 and 1640 levels, and in the footwall and hanging wall to the ore on 1700 level.

Appendix A-xxix: 2600 LEVEL EAST END

The 2600 level is the lowest level extensively developed in the mine workings (Figure 53). This level was mapped for stratigraphic information, and to complete the overall geology of the mine from surface to depth. The rocks observed include quartz-feldspar- phyric felsic flows and flow top breccia, overlain by sedimentary rocks including iron formation, and sulphide breccia.

The sedimentary rocks are 400 m in apparent thickness, and are composed of greywacke interbedded with graphitic pelite, iron formation, and beds of massive pyrrhotite. Iron formation and brecciated iron formation are intercalated with graphitic pelite. Lenses of massive pyrrhotite (up to 30 cm- thick), and sulphide breccia (pyrrhotite) are intercalated with iron formation.

The sedimentary rocks generally consist of coarse- to fine- grained greywacke beds with slaty tops. Normal grading was observed in one place that suggests tops are to the north. Local black chert horizons of a cm scale are common and show weak banding or bedding.

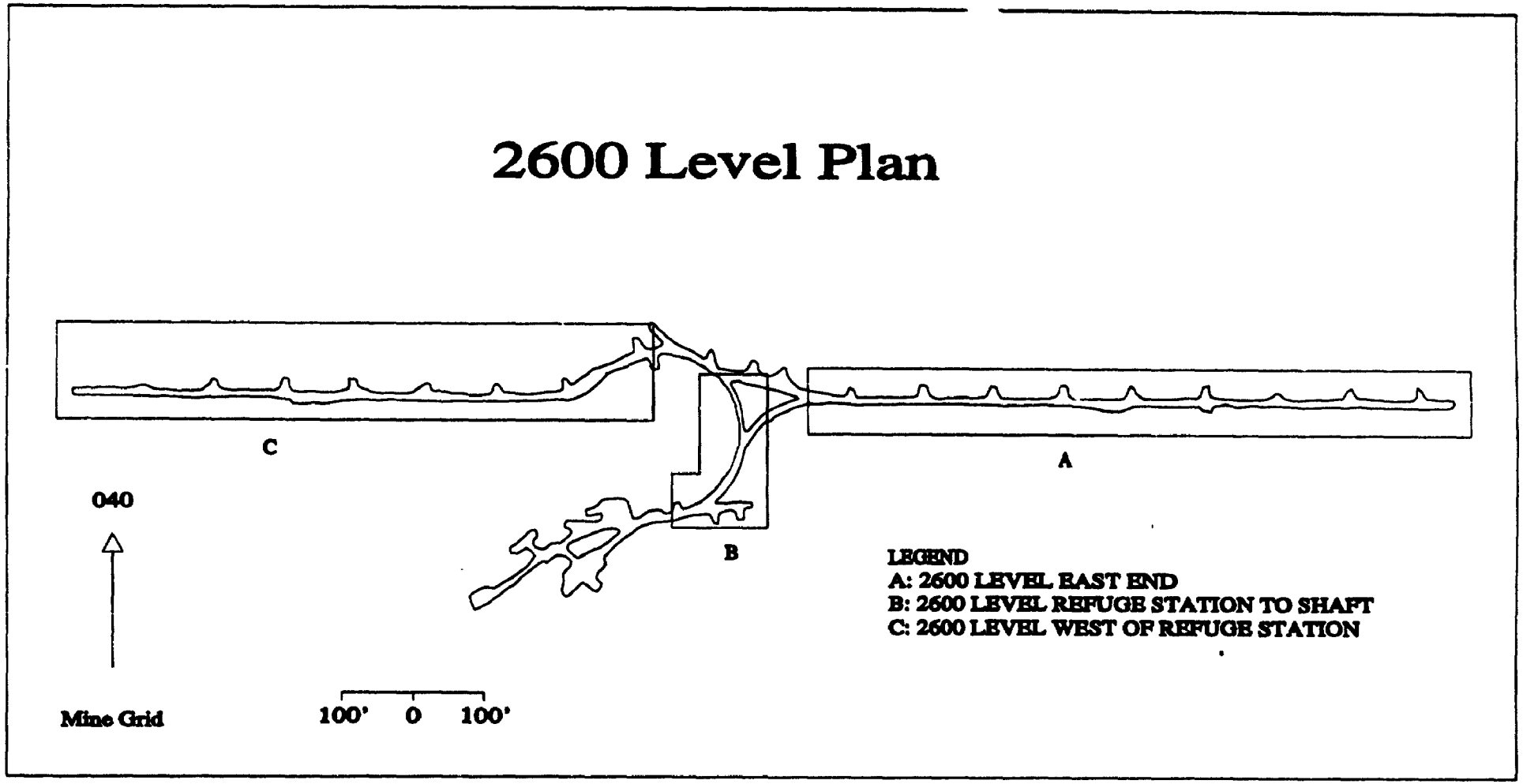

Figure 53: Level map of the 2600 level. This is the lowest level developed in the mine. Drill core data indicate sulphide mineralization occurs 2000 feet east of the eastern edge of the map.

Locally, up to 2 m- thick beds of fine- grained, black graphitic pelite are intercalated with medium- grained wacke beds. These black beds are generally cherty, and contain ovoid, centimeter scale blebs of pyrrhotite. Other beds are medium- grained and have a salt and pepper appearance due to a light coloured detrital component set in a matrix of chlorite.

Ten centimeter to 2 m- wide zones of banded iron formation occur at the base of the sedimentary sequence, and are intercalated with wacke and pelite. Banded iron formation comprises of intercalated beds of chert, iron- silicate (chlorite), and iron- oxide (magnetite). Locally, beds of iron sulphide are intercalated with iron- silicate and iron-oxide iron formation. A common pattern of compositional banding in the iron formation is illustrated in Figure 54. Banding is well defined in the western zone and moderately to poorly defined in the eastern zone due to tectonic disruption. Beds vary from 0.5 to 5 cm-thick. Locally, chert beds are up to 10 cm- thick, and contain laminations of magnetite.

Iron- silicate beds are dark green, chloritic and contain 1 to 3%, 1 to 3 mm garnets. Locally, minor 5 mm- thick pyrrhotite beds occur in iron- silicate iron formation.

Locally, iron formation is brecciated. Zones of brecciated iron formation up to 10 m- thick are intercalated with banded iron formation and sedimentary rocks. Angular and lensoid fragments of white chert with magnetite laminations and iron sulphide occur in a dark green, weakly magnetic matrix.

Locally iron formation is isoclinally folded. Fold hinges plunge shallowly east-southeast. Fold amplitudes are up to 3 m. Asymmetric Z- shaped folds occur on the back.

Greywacke and iron- silicate beds of the iron formation are moderately to pervasively altered. Garnets are common, associated with the chlorite, and comprise 1 to 2% of the rock. Garnets vary from 2 to 5 mm and locally up to 1 cm in size. In the

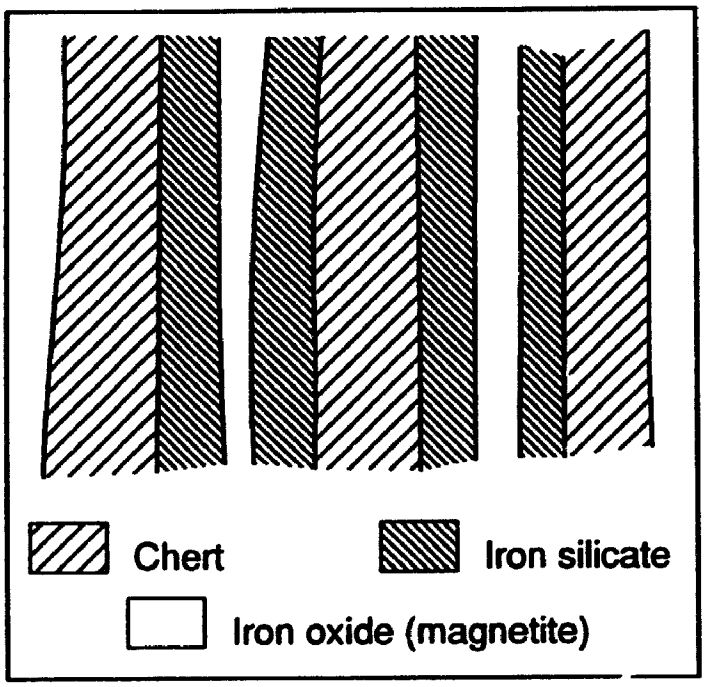

Figure 54: Banded iron formation on the 2600 level. The symmetric compositional banding of the iron formation is a reflection of isoclinal folds.

brecciated iron formation, cherty fragments are weakly carbonatized, and iron- silicate clasts are green chlorite.

Quartz-feldspar phyric felsic volcanic rocks underlie the iron formation. The contact between the quartz- feldspar- phyric felsic volcanic rock and the oxide iron formation is defined by a mafic dyke. The contacts between the dyke, felsic volcanic strata, and iron formation are sharp, and dip subvertically to the north.

The quartz- feldspar- phyric felsic volcanic unit is light to medium gray, massive, fine- grained, has a grainy texture, and contains ash to block size fragments. Blue quartz eyes are 1 to 2 mm in diameter, and comprise 2% of the rock. Locally, quartz eyes may comprise up to 30%, and feldspar up to 60% of the unit. Locally, ripped up portions of cherty iron formation occur as inclusions within this unit. This suggests that the iron formation overlies the quartz- feldspar- porphyry, and is not structurally juxtaposed. An 8 to 10 cm- thick quartz- feldspar- phyric dyke, compositionally and texturally similar to the felsic volcanic rocks, cross cuts the graphitic pelite and iron formation.

Monolithic, subrounded to subangular quartz and feldspar phyric cherty fragments up to 15 cm in diameter occur near the top contact of the quartz- feldspar- phyric felsic flow (flow top breccia). Locally, these fragments have chloritic rims.

Within this unit, several 1 to 3 cm- thick, quartz-tourmaline veins occur. Massive tourmaline generally occurs at the margins of the quartz veins, but also occurs disseminated throughout the vein. Locally, several quartz-tourmaline veins are offset by subhorizontal fractures.

A shallow dipping mafic dyke crosscuts the felsic flow. This particular dyke contains ladder quartz veins. Ladder veins are evenly spaced 60 cm apart contain quartz, chlorite +/- garnet plus pyrrhotite.

The quartz- feldspar- phyric felsic flow is pervasively altered to sericite and chlorite. Alteration produces a banded appearance. Locally, alteration bands are very

distinct pale green, medium green, pink, and/or purple. Sericite and chlorite is abundant particularly along cleavage planes. Locally, the rock contains up to 3% disseminated and patchy zones of iron sulphide.

The metamorphic mineral assemblage consists of sericite, quartz, chlorite, +/- biotite. Cherty bands are common, chlorite alteration is locally intense, and biotite occurs locally with chlorite. Sericite, chlorite and biotite occur aligned parallel to the foliation, and as irregular fracture filling mineral in quartz-- tourmaline veins. Tabular white feldspar laths are partially or completed altered to sericite and carbonate. Fragments are preferentially altered to sericite.

A strong, penetrative fabric striking northwest, and dipping steeply to the north is observed throughout the area. Deformation increases towards the east, as observed by the disruption in bedding of the iron formation.

Locally, shear foliation in the feldspar phyric unit is defined by pyrrhotite stringers and vein quartz-breccia fragments, which are elongate parallel to foliation and to the pyrrhotite stringers. Also, locally, chlorite defines a mineral lineation on shear foliation planes.

A 16 m- wide shear zone contains a 3 m- wide quartz vein with randomly oriented fractures containing chlorite, and sulphides. Carbonate veins cross cut the quartz vein, and are oriented perpendicular to the quartz veining. Carbonate veins up to 15 cm- thick also occurs at the margin of the quartz veining.

Several 2 to 3 m- wide shear zones occur in the quartz-feldspar phyric felsic flow. Alteration bands of chlorite and sericite, and the long axis of fragments are oriented parallel to the shear foliation.

Appendix A-xxx: 2600 LEVEL CROSSCUT FROM REFUGE STATION TO SHAFT

This area represents a short cross section through the footwall sedimentary rocks. The drift comprises of monotonous, massive, medium- grained, medium to dark gray greywacke intercalated with silicate iron formation. Locally, greywacke is cross cut by abundant, randomly oriented, pyrrhotite- bearing quartz-carbonate veins.

Several 30 cm- thick zones of weakly magnetic iron formation are intercalated with greywacke. This iron formation is composed of iron- silicate beds alternating with pyrrhotite- bearing chert beds.

A 6.5 m wide shear zone occurs in the greywacke. Within this shear zone, mineral assemblages include calcite, chlorite, garnet, pyrrhotite, and pyrite. Garnets are 2 to 3 mm and comprise up to 5% of the unit.

Appendix A-xxxi: 2600 WEST OF REFUGE STATION

This area is composed dominantly of massive greywacke, overlain by rhyolitic ash flows. Sedimentary rocks are greywacke and contain 1% angular clasts of quartz. Local sedimentary units of breccia occur within the massive greywacke. Clasts of chert are angular, fractured, and commonly broken. Locally, fragments are altered to iron-carbonate. The matrix is pelitic, composed mainly of quartz and chlorite.

The rhyolitic ash flow is massive and comprises of 1 to 2%, 1 mm gray quartz phenocrysts in a quartz, feldspar, and sericite matrix.

At the western most end of this level (9300 E), a 5 m- thick mafic dyke intrudes felsic volcanic rocks. The dyke is massive, brittle and weathers to rusty orange.

Appendix B: Major and minor mineral components determined by X-Ray Diffraction

(X-Ray Diffraction patterns on file at the Geological Survey of Canada)

Uppercase: Major minerals

Lowercase: Minor and trace minerals

Sample Number	Lithology	Mineral Assemblage
89-FRK-027	rhyolite ash	QUARTZ + chlorite + mica gp + Na- feldspar + calcite + dolomite
89-FRK-028	rhyolite ash	QUARTZ + chlorite + dolomite + Na- feldspar + calcite + mica gp
89-FRK-029	rhyolite	QUARTZ + CHLORITE + Na- feldspar + mica gp + dolomite + calcite
89-FRK-030	quartz- phyric rhyolite	QUARTZ + NA- FELDSPAR + chlorite + mica gp
89-FRK-031	graphitic pelite	QUARTZ + NA- FELDSPAR + chlorite + mica gp
89-FRK-032	rhyolite ash	QUARTZ + NA- FELDSPAR + chlorite + mica gp
89-FRK-033	rhyolite ash	QUARTZ + NA- FELDSPAr + chlorite + mica gp
89-FRK-035	graphitic pelite	QUARTZ + Na- feldspar + chlorite + mica gp
89-FRK-036	quartz- phyric rhyolite	QUARTZ + Na- feldspar + chlorite + mica gp
89-FRK-050	graphitic pelite	QUARTZ + Na-feldspar + chlorite
89-FRK-051	quartzose pelite	QUARTZ + Na- feldspar + mica gp + chlorite
89-FRK-053	rhyolite ash	QUARTZ + NA-FELDSPAR + chlorite + mica gp

89-FRK-056	graphitic pelite	QUARTZ + CHLORITE + mica gp + dolomite + Na- feldspar + calcite
89-FRK-059	rhyolite tuff	QUARTZ + NA- FELDSPAR + CHLORITE + mica gp + calcite
89-FRK-060	rhyolite ash	QUARTZ + NA- FELDSPAR + chlorite + mica gp
89-FRK-061	graphitic pelite	QUARTZ + Na- feldspar + chlorite + calcite + mica gp
89-FRK-062	rhyolite ash	QUAR[illegible] + NA- FELDSPAR + chlorite + mica gp
89-FRK-063	rhyolite ash	QUA[illegible] NA- FELDSPAR + chlorite + mica gp
89-FRK-064	rhyolite ash	QUARTZ + [illegible]HLORITE + Na- feldspar + mica gp + calcite
89-FRK-067	rhyolite	QUARTZ + NA- FELDSPAR + chlorite + mica gp + calcite
89-FRK-076	rhyolite ash	QUARTZ + NA- FELDSPAR + MICA GP + calcite + chlorite
89-FRK-077	greywacke	QUARTZ + NA- FELDSPAR + chlorite + mica gp + calcite
89-FRK-087	quartzose pelite	QUARTZ + NA- FELDSPAR + chlorite + mica gp
89-FRK-088	greywacke	QUARTZ + CHLORITE + mica gp + calcite + Na- feldspar
89-FRK-101	greywacke	QUARTZ + NA-FELDSPAR + MICA GP + chlorite
89-FRK-102	greywacke	QUARTZ + CHLORITE + MICA GP + Na- feldspar
89-FRK-104	greywacke	QUARTZ + NA-FELDSPAR + chlorite + mica gp + calcite
89-FRK-105	greywacke	QUARTZ + CHLORITE + Na - feldspar + mica gp + calcite
89-FRK-1800-01		QUARTZ + CHLORITE + Na- feldspar + mica gp + calcite + dolomite
89-FRK-1800-02		QUARTZ + NA- FELDSPAR + chlorite + mica gp + calcite
89-FRK-1800-03		QUARTZ + CHLORITE + Na- feldspar + mica gp + calcite
89-FRK-1800-04		QUARTZ + NA- FELDSPAR + chlorite + mica gp + calcite
89-FRK-1800-05		QUARTZ + chlorite + Na- feldspar + pyrrhotite + siderite + mica gp
89-FRK-1800-06		QUARTZ + NA- FELDSPAR + chlorite + mica gp

89-FRK-1800-07		QUARTZ + Na- feldspar + chlorite + calcite + mica gp
89-FRK-1800-08		QUARTZ + Na- feldspar + chlorite + calcite + mica gp
89-FRK-1800-09		QUARTZ + Na- feldspar + chlorite + mica gp + calcite
89-FRK-1800-10		QUARTZ + NA- FELDSPAR + mica gp + chlorite
89-FRK-1800-12		QUARTZ + NA- FELDSPAR + chlorite + mica gp
89-FRK-1800-13		QUARTZ + Na- feldspar + mica gp + chlorite
89-FRK-1800-14		QUARTZ + NA- FELDSPAR + mica gp + chlorite
89-FRK-204	feldspar- phyric rhyolite	QUARTZ + NA- FELDSPAR + mica gp + chlorite
89-FRK-211	feldspar- phyric rhyolite	QUARTZ + MICA GP + Na- feldspar + chlorite
89-FRK-213	quartzose pelite	QUARTZ + CHLORITE + Na- feldspar + mica gp + calcite
89-FRK-215	quartzose pelite	QUARTZ + Na- feldspar + chlorite + mica gp + calcite
89-FRK-216	graphitic pelite	QUARTZ + CHLORITE + MICA GP + Na- feldspar + calcite
89-FRK-233	greywacke	QUARTZ + CHLORITE + Na- feldspar + mica gp + calcite
89-FRK-245	pelite	QUARTZ + Na- feldspar + chlorite + mica gp + calcite + dolomite + pyrrhotite
89-FRK-261	quartzose pelite	QUARTZ + NA- FELDSPAR + mica gp + calcite + chlorite
89-FRK-303	heterolithic fragmental	QUARTZ + CHLORITE + amphibole + dolomite

END

20-07-94

FIN